



Measurements of vector-boson scattering with the ATLAS experiment

Deep Inelastic Scattering (DIS) 2024
Grenoble

9th April 2024

Antonio Giannini
on behalf of the ATLAS collaboration

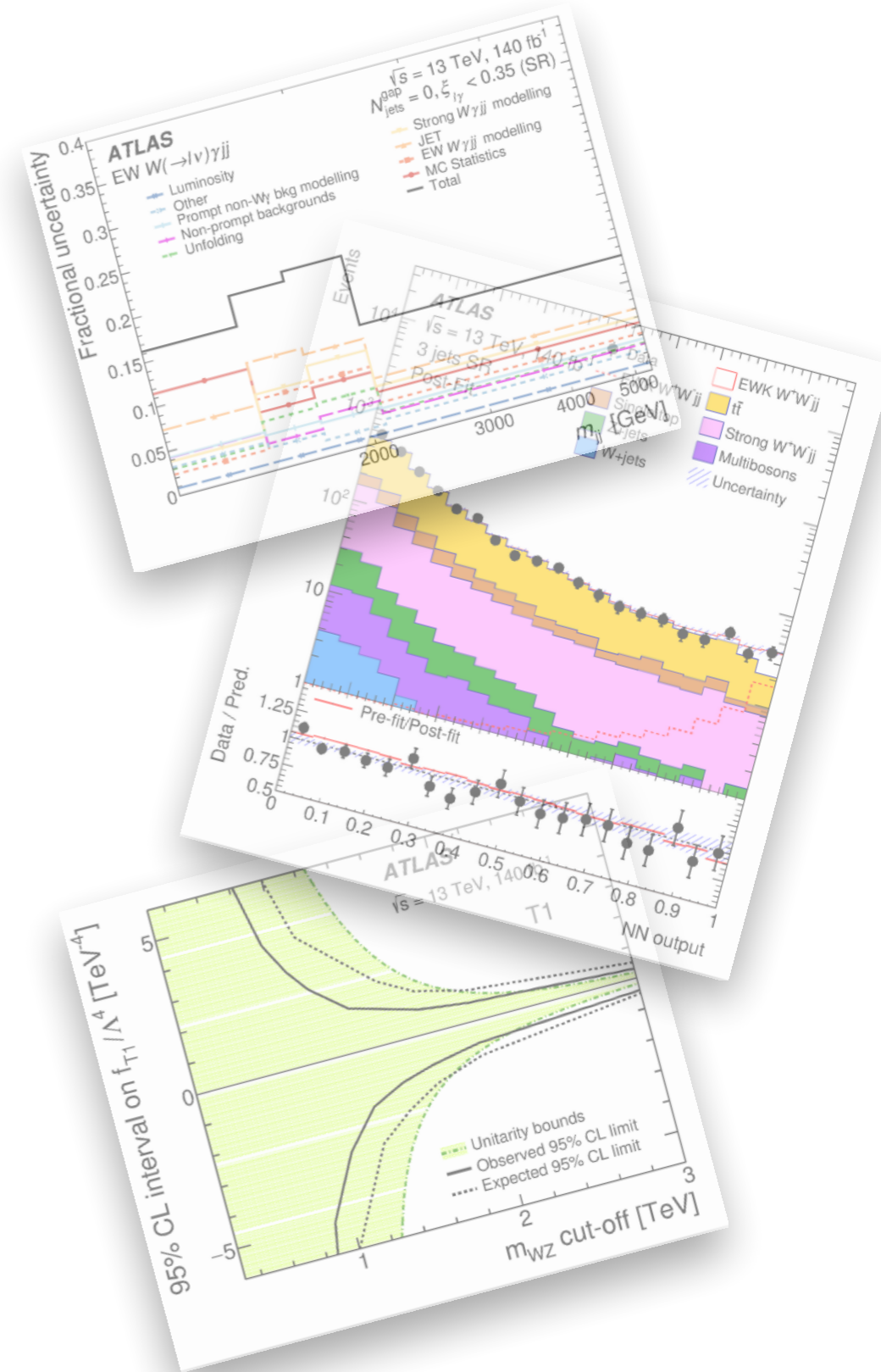


Outline

- **Measurements of Vector Boson**

- **Scattering with the ATLAS experiment**

- Introduction
- Summary of ATLAS results
- Results' highlights
- Final states
 - ▶ $W(l\nu)\gamma + jj$
 - ▶ opposite-sign $W(l\nu)W(l\nu) + jj$
 - ▶ $W(l\nu)Z(l\ell) + jj$
- **Wrap-up**





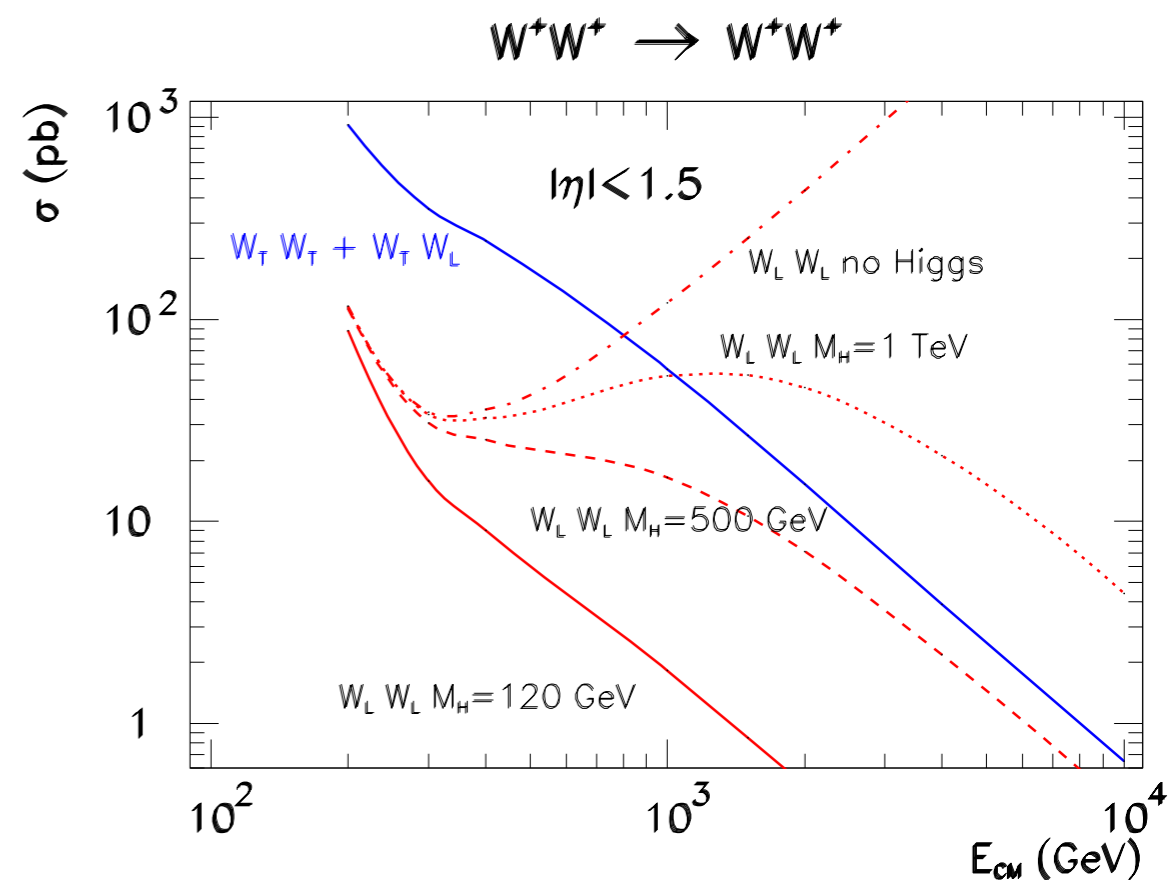
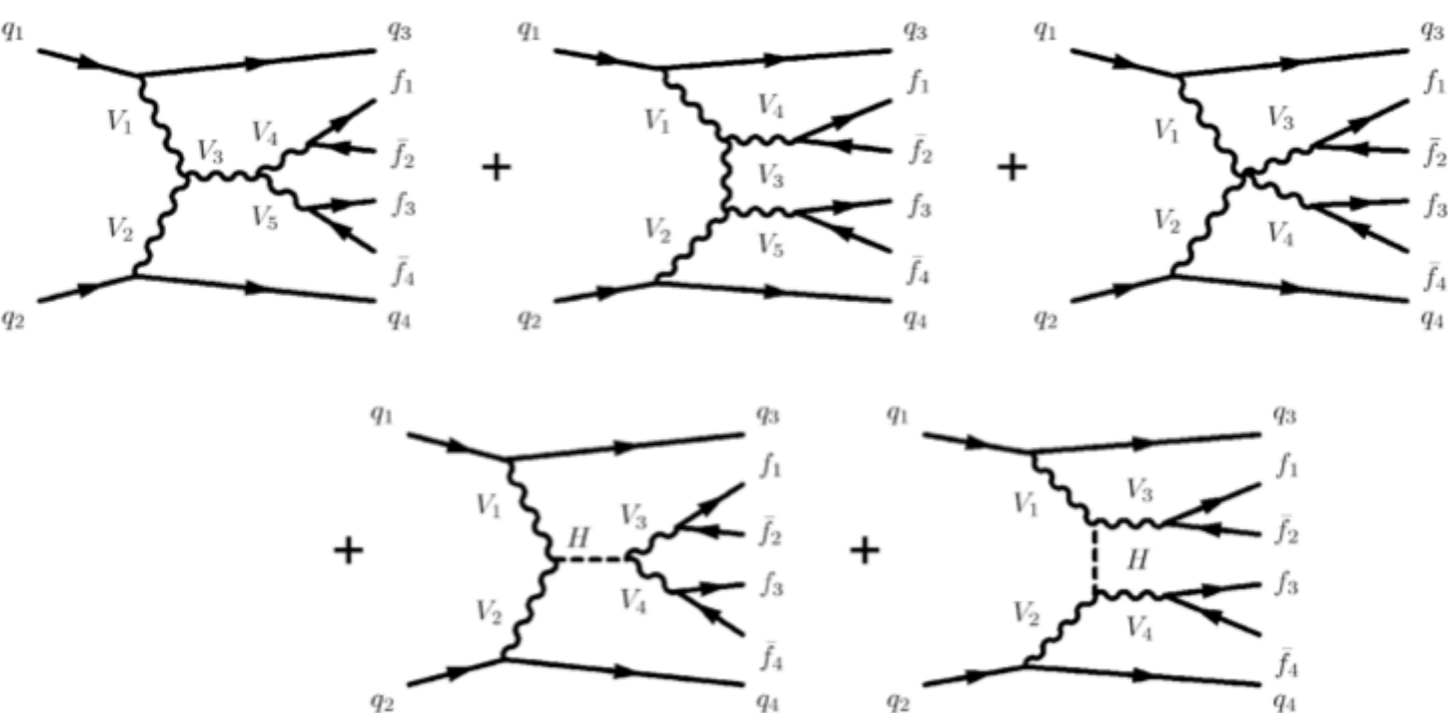
Introduction: why VBS?

- **Diboson physics has been a crucial test of the SM**

- ▶ experimental constraints in many diboson channels
- ▶ still huge interest in probing higher ranges

- **Vector Boson Scattering (VBS)**

- ▶ probe the Electroweak Symmetry Breaking
- ▶ sensitive to New Physics



[arxiv.1412.8367](https://arxiv.org/abs/1412.8367)



Experimental perspective

VBS experimental signature

- Energetic and forward jets

- ▶ large rapidity separation, $\Delta\eta_{jj}$

- ▶ large invariant mass, M_{jj}

- Centrality

- ▶ low hadronic activity in the central region (color singlet exchange)

- Key discrimination for EWK $VV+jj$ and VBS components

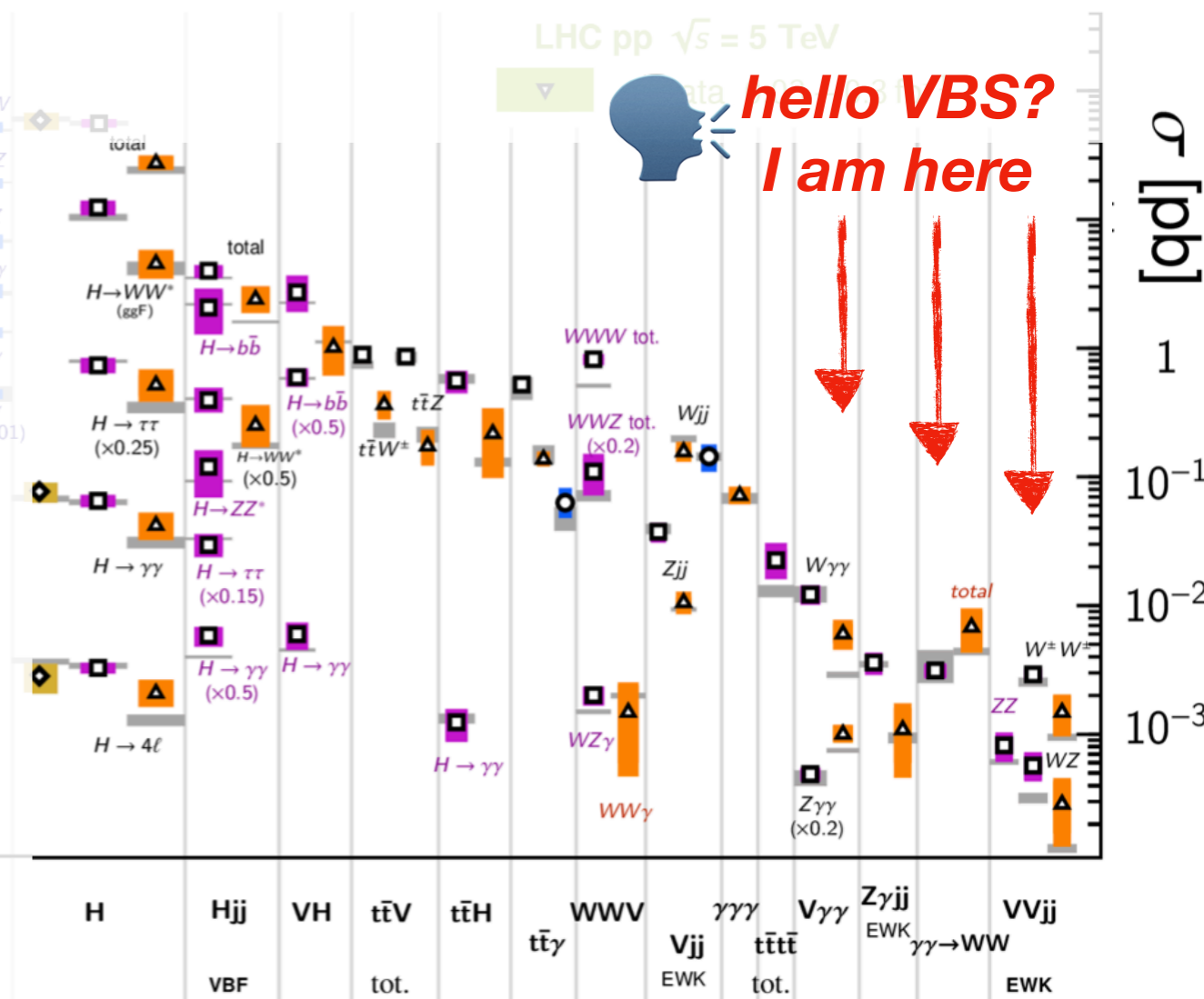
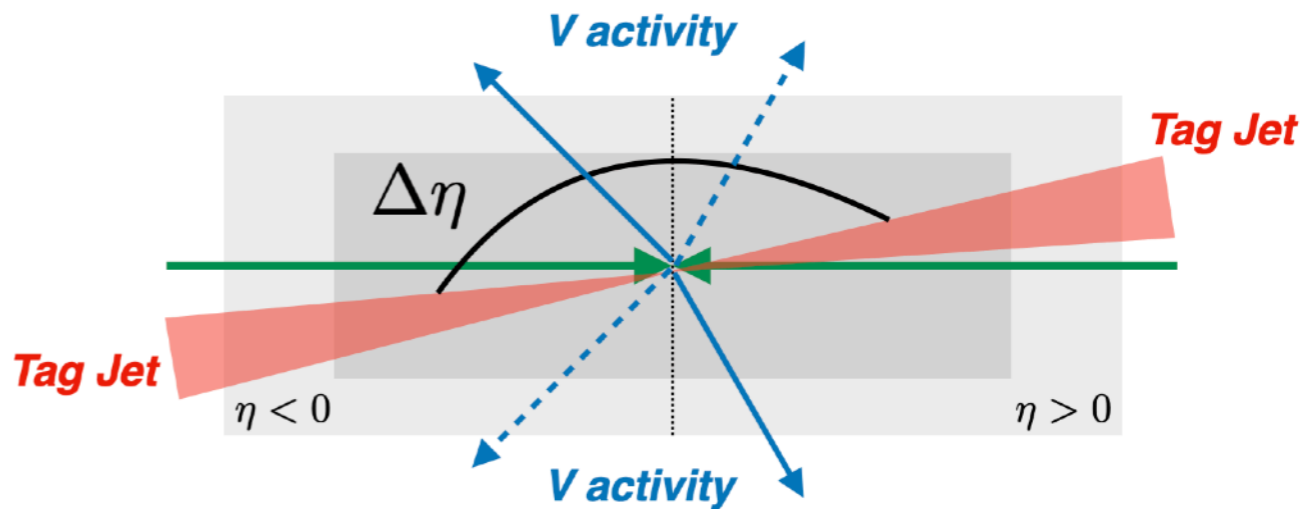
VBS experimental challenges

- Rare process and large variety of background processes

- Forward jets identification

- VBS can NOT be directly extracted to due gauge invariance \rightarrow EWK $VV+jj$ in VBS-enhanced phase space

- Interference with QCD $VV+jj$ production

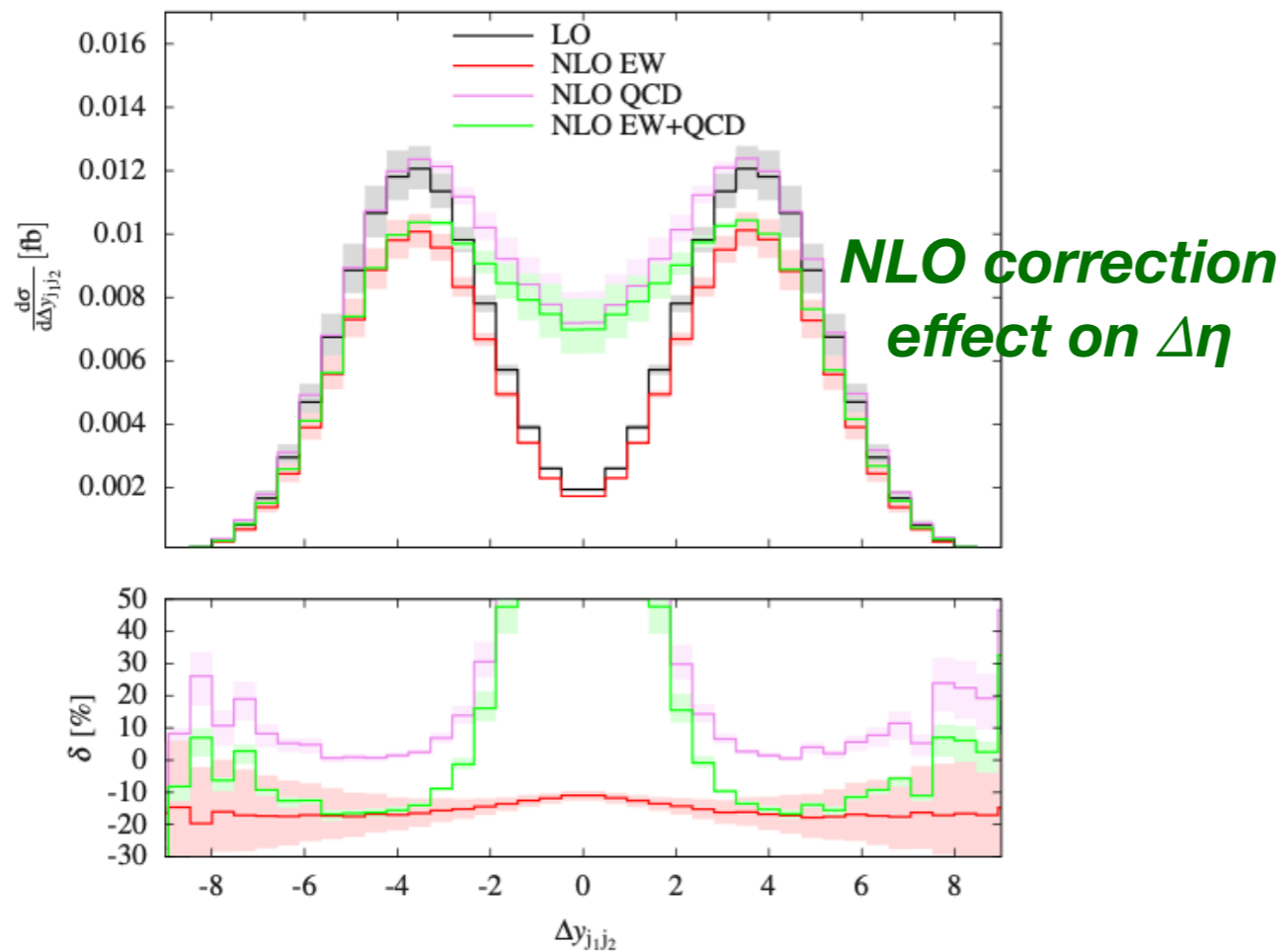




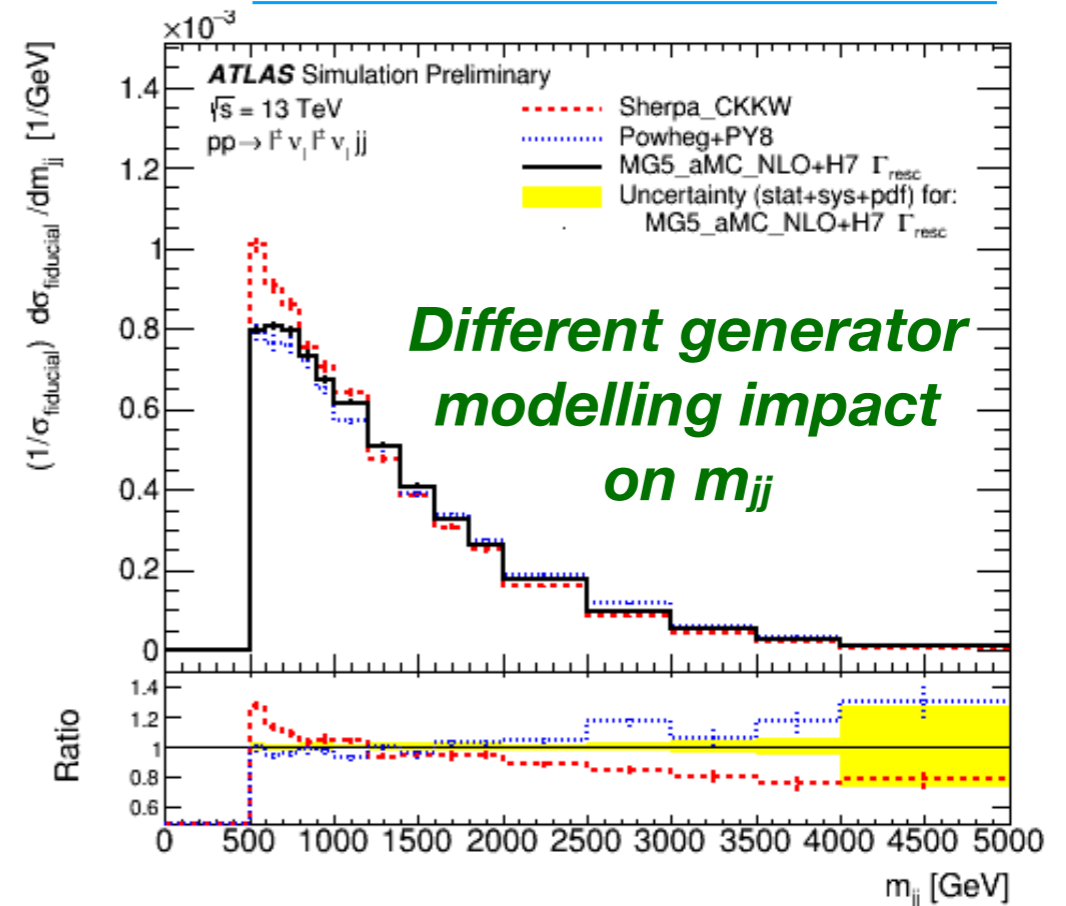
Theoretical challenges

- **Precise theory predictions to constraint QCD and EWK VV+jj productions**
 - ▶ generations can not distinguish between VBS and no-VBS components
 - ▶ non-VBS components: VV and t-X diagrams
- **Understand experimental data with theory predictions**
 - ▶ high-order corrections impact the phase space
 - ▶ modelling description plays a leading role in this phase space

[arxiv.2009.00411](https://arxiv.org/abs/2009.00411)






[ATL-PHYS-PUB-2019-004](https://arxiv.org/abs/1904.00404)





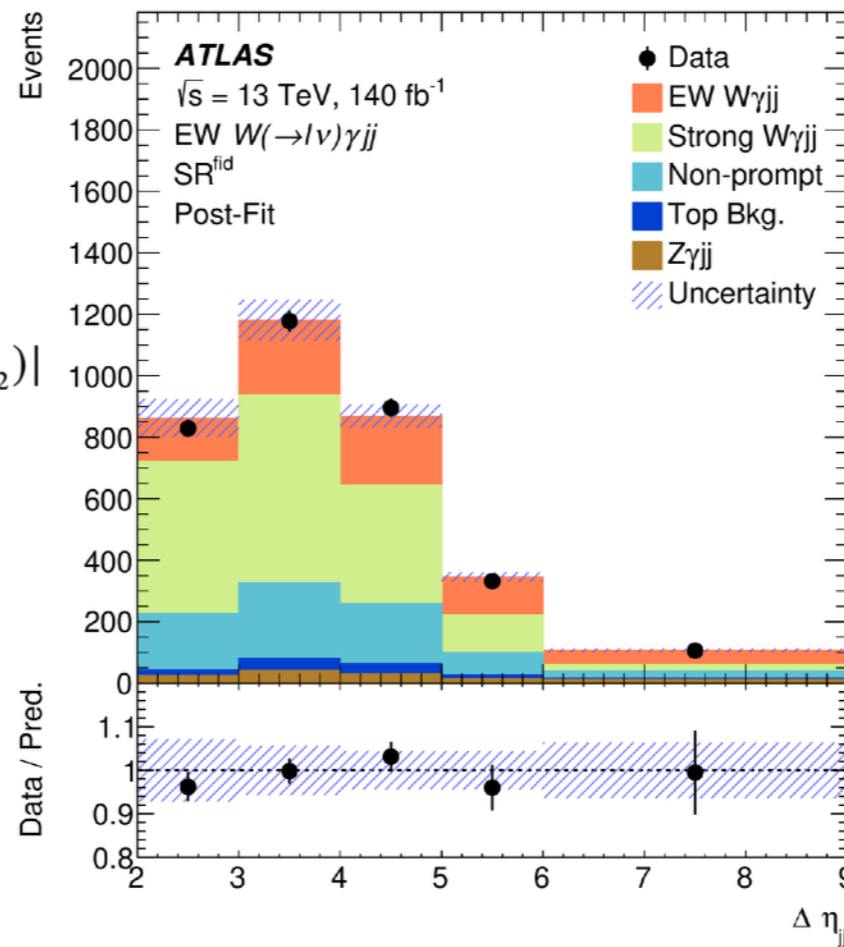
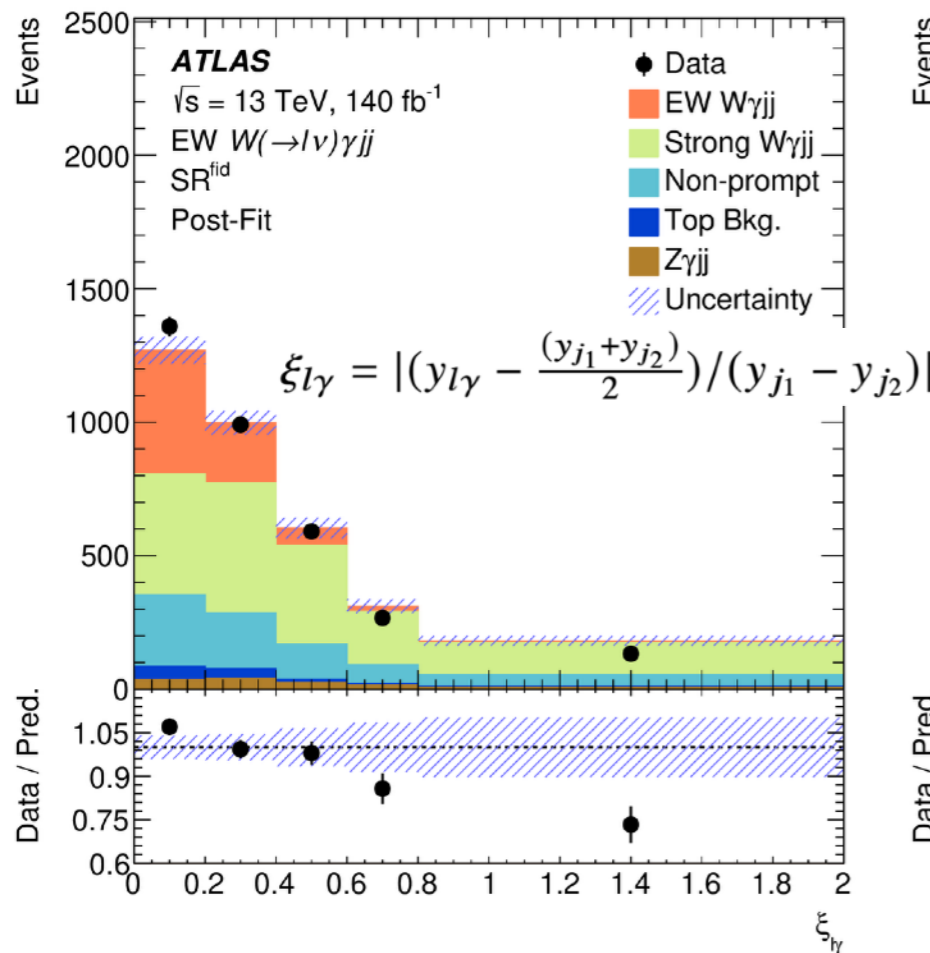
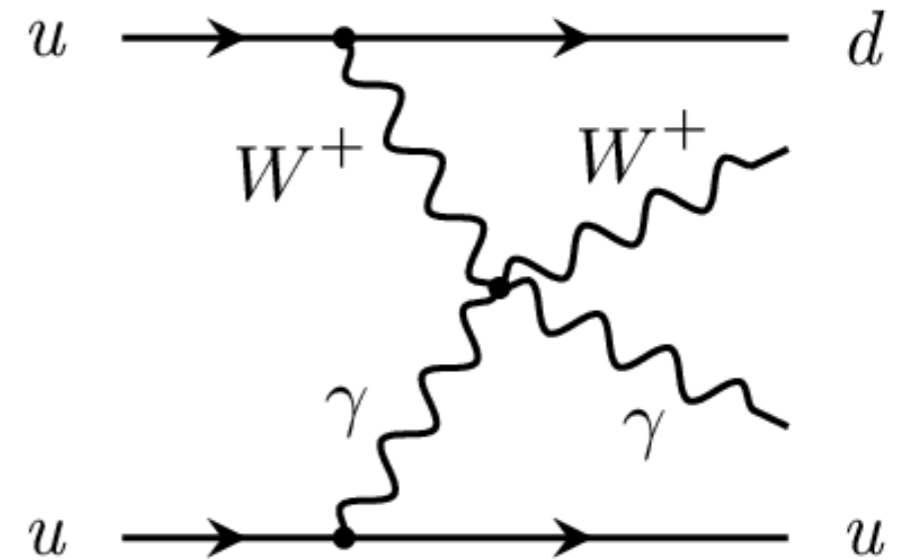
ATLAS results in a nutshell

Channel	Final state	Dataset	ATLAS paper
W⁺W⁻ + jj	 $e\nu\mu\nu + jj$	139/fb	Submitted to JHEP
	$l\nu l\nu + jj$	140/fb	Submitted to JHEP
W[±]W[±] + jj	 $l\nu ll + jj$	140/fb	Submitted to JHEP
	$4l + jj$	140/fb	JHEP 01 (2024) 004
WZ + jj	$2l2\nu + jj$	139/fb	Nature Phys. 19 (2023) 237
	$\nu\nu qq/l\nu qq/llqq + jj$	35/fb	Phys. Rev. D 100 (2019) 032007
ZZ + jj	 $l\nu\gamma + jj$	140/fb	Submitted to EPJC
	$ll\gamma + jj$	140/fb	Phys. Lett. B 846 (2023) 138222
VV + jj semi-leptonic	$\nu\nu\gamma + jj$	139/fb	JHEP 06 (2023) 082
	$e\nu\mu\nu + X$	139/fb	Phys. Lett. B 816 (2021) 136190



$W\gamma + jj$ production

- **W and γ associated final state**
 - ▶ clean signal topology
 - ▶ both electron and muon channels explored
- **Typical VBS-enhanced phase space selection**
- **Source of background processes**
 - ▶ irreducible: QCD $W\gamma + jj$ production
 - ▶ others: non-prompt, top, fakes

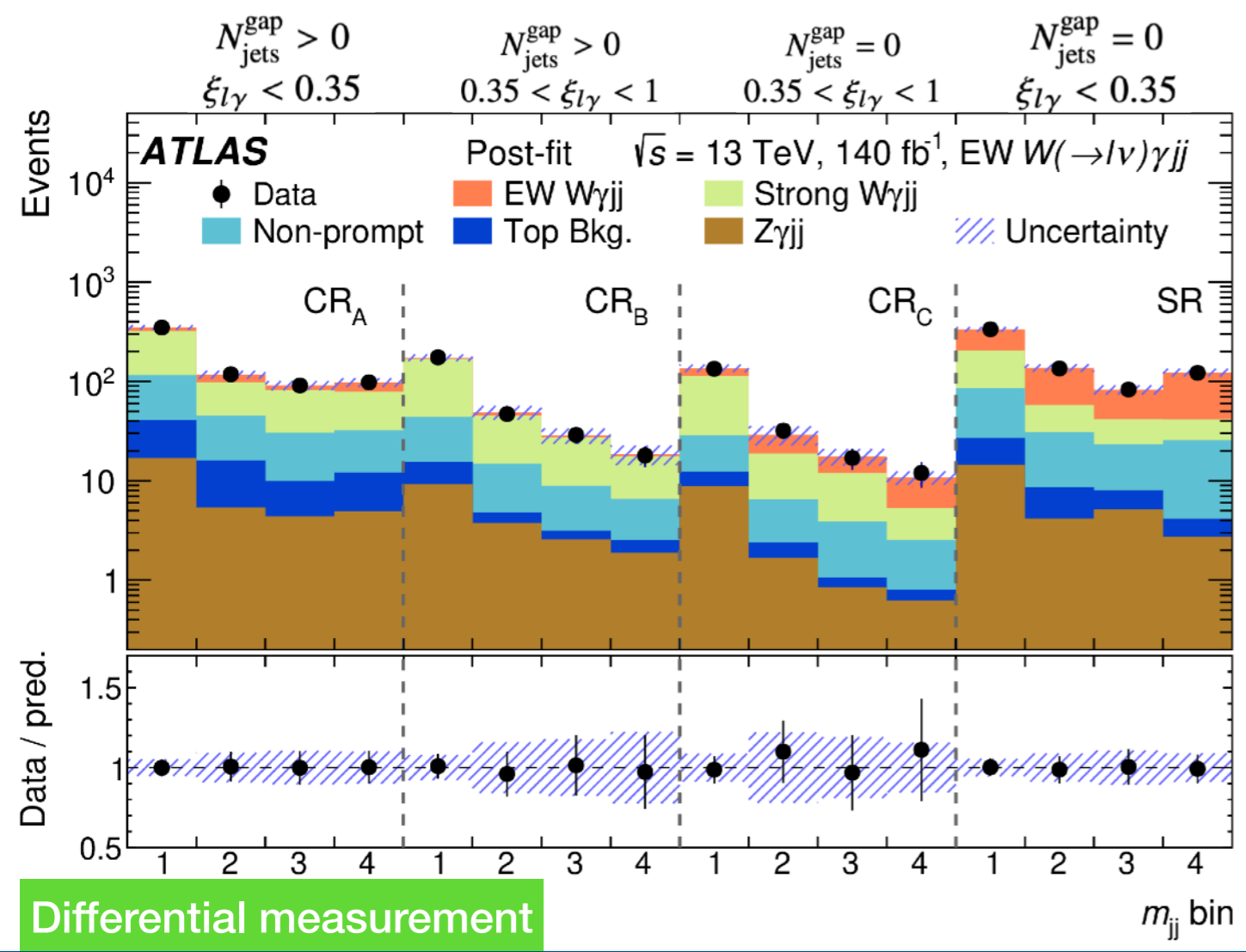


**Good separation power
for the EWK signal
against the other SM
processes for relevant
kinematics**



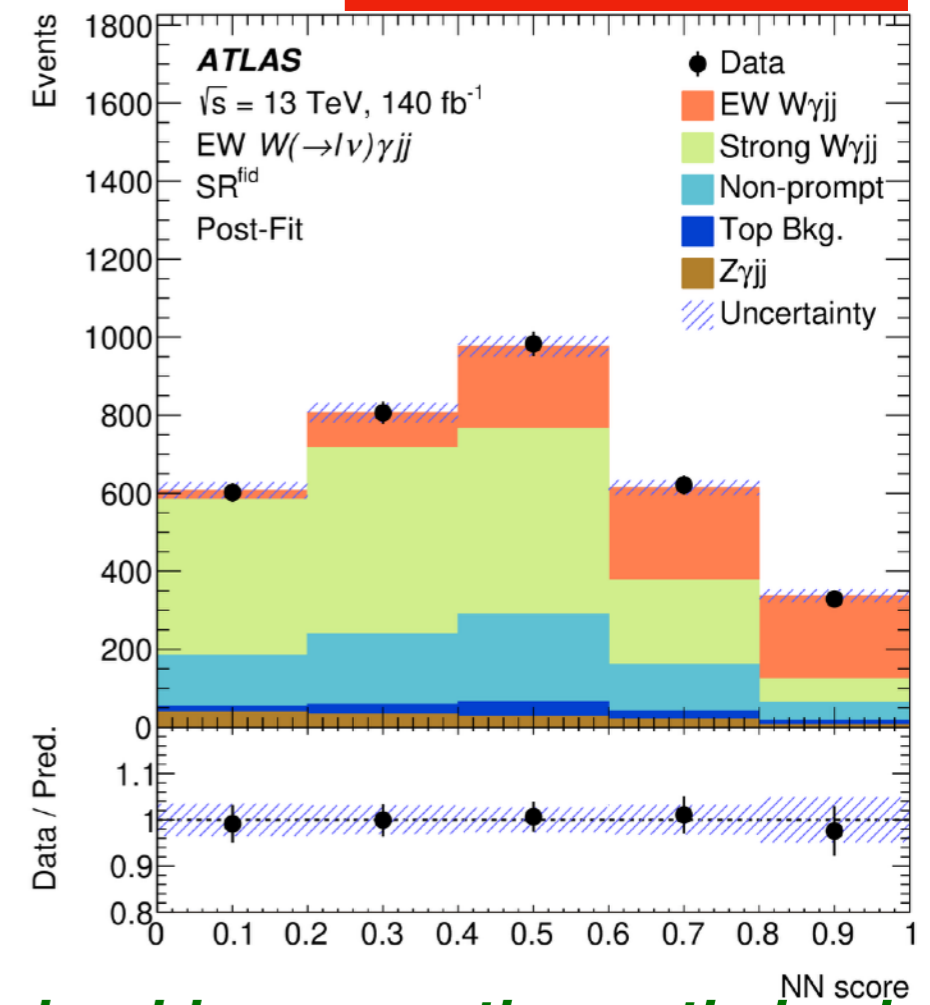
How to: CRs and ML

- Events are **categorised in Signal Region (SR) and Control Regions (CRs)**
 - ▶ constraint the main background, QCD $W\gamma+jj$
- **Inclusive measurement:**
 - ▶ SR^{fid}: $N_{\text{jets}^{\text{gap}}} = 0$, CR^{fid}: $N_{\text{jets}^{\text{gap}}} > 0$
- **Differential measurement:**
 - ▶ SR + 3 CRs based on $N_{\text{jets}^{\text{gap}}}$ and $l\gamma$ -centrality

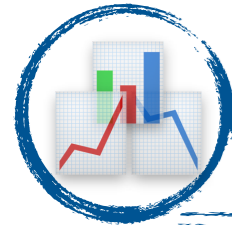


Differential measurement

Inclusive measurement



- **Signal vs bkg separation optimised using Machine Learning (ML)**
 - ▶ DNN with 13 kinematic variables
 - ▶ training in the SR phase space
- **Observation of the EWK $W\gamma+jj$**
 - ▶ 6.3σ , $\mu = 1.5 \pm 0.5$
 - ▶ $\sigma_{\text{EWK}} = 13.2 \pm 2.5 \text{ fb}$



Goal: differential measurement

- Differential measurement performed in high m_{jj} (> 1 TeV) phase space
- **Fiducial definition at particle level defined to mimic the reco level selection**

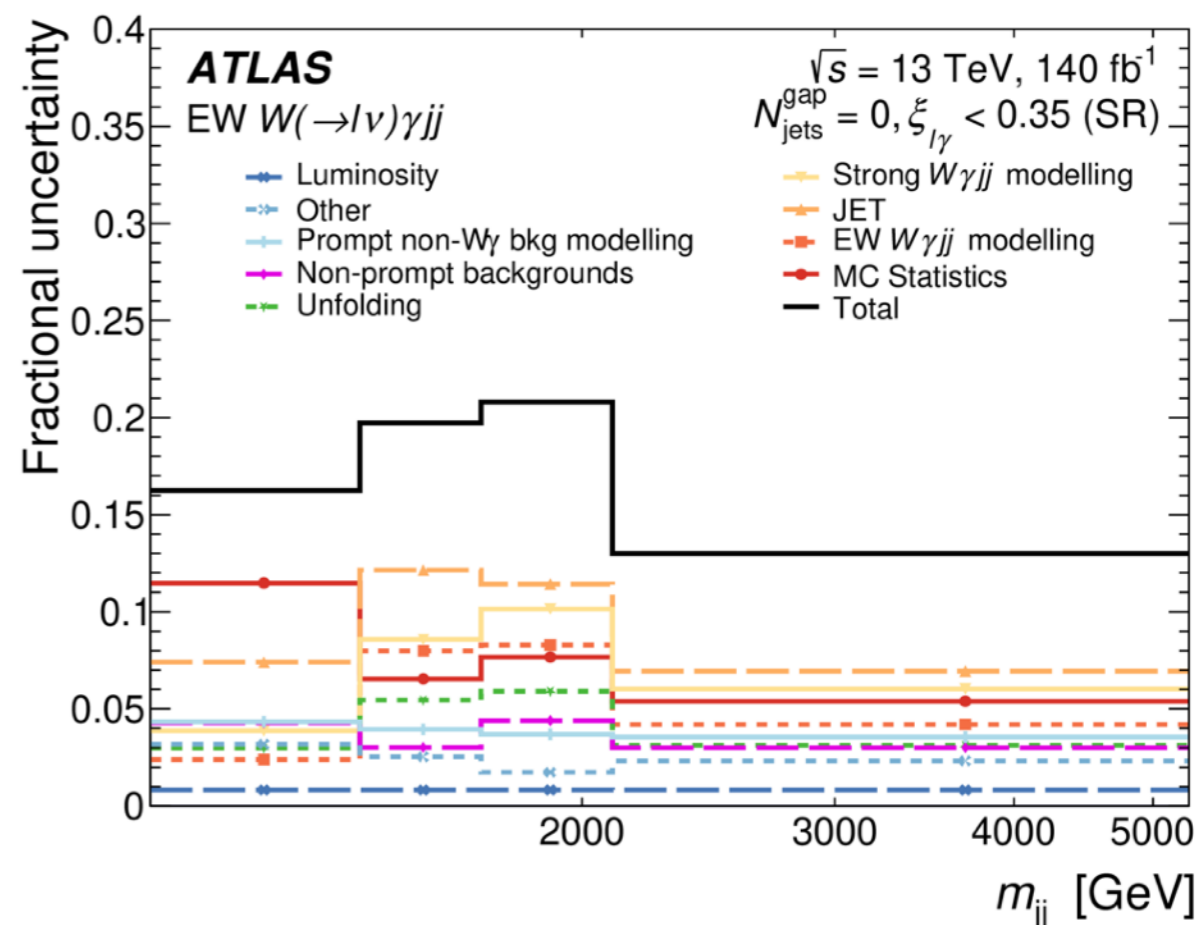
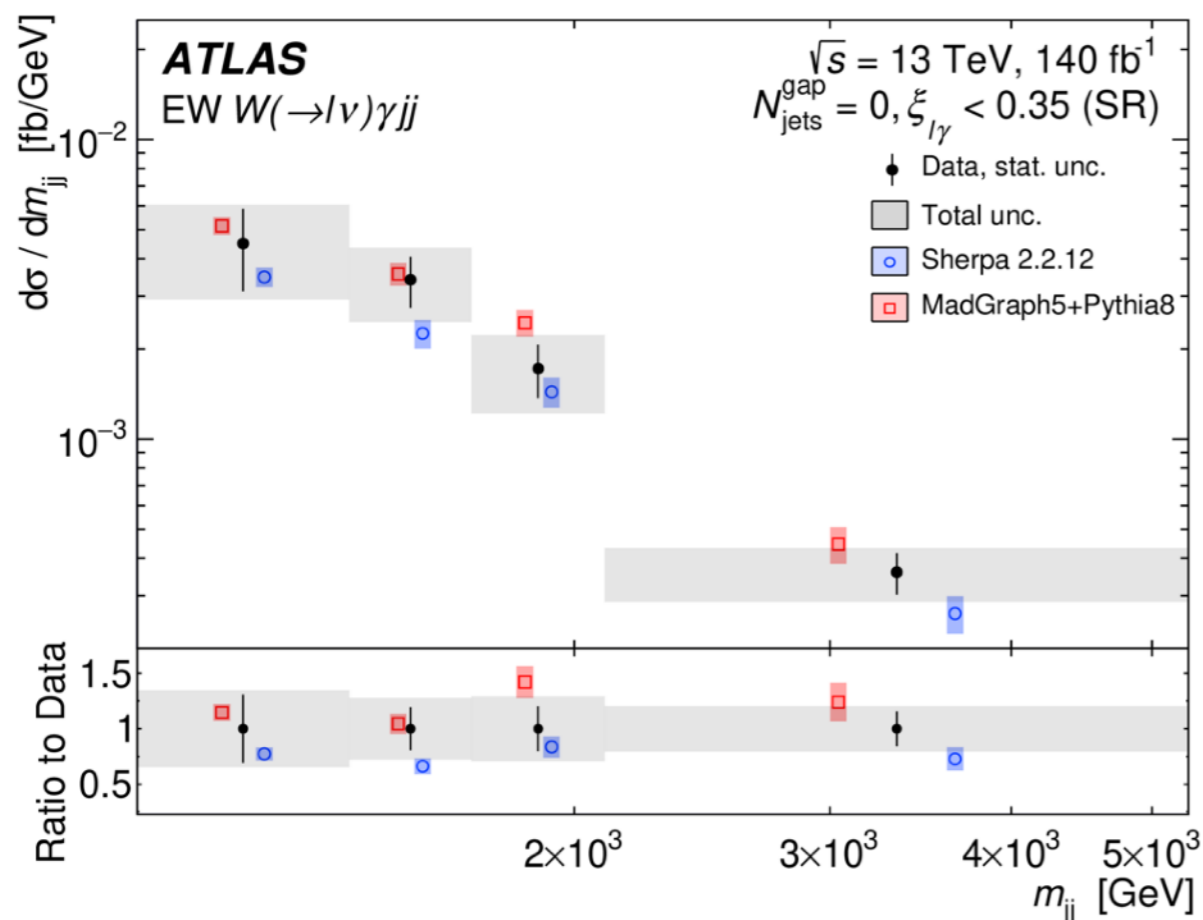
▶ the C-factor estimated from Sherpa EWK $W\gamma+jj$ sample

$$\sigma_{EW W\gamma jj}^{fid} = \frac{N_{EW W\gamma jj}}{L \cdot C_{EW W\gamma jj}}$$

- **Unfolding using iterative Bayesian procedure**

▶ done for several variables, binning optimised to account for data statistics

- **Modelling and jets uncertainties dominate the measurement**





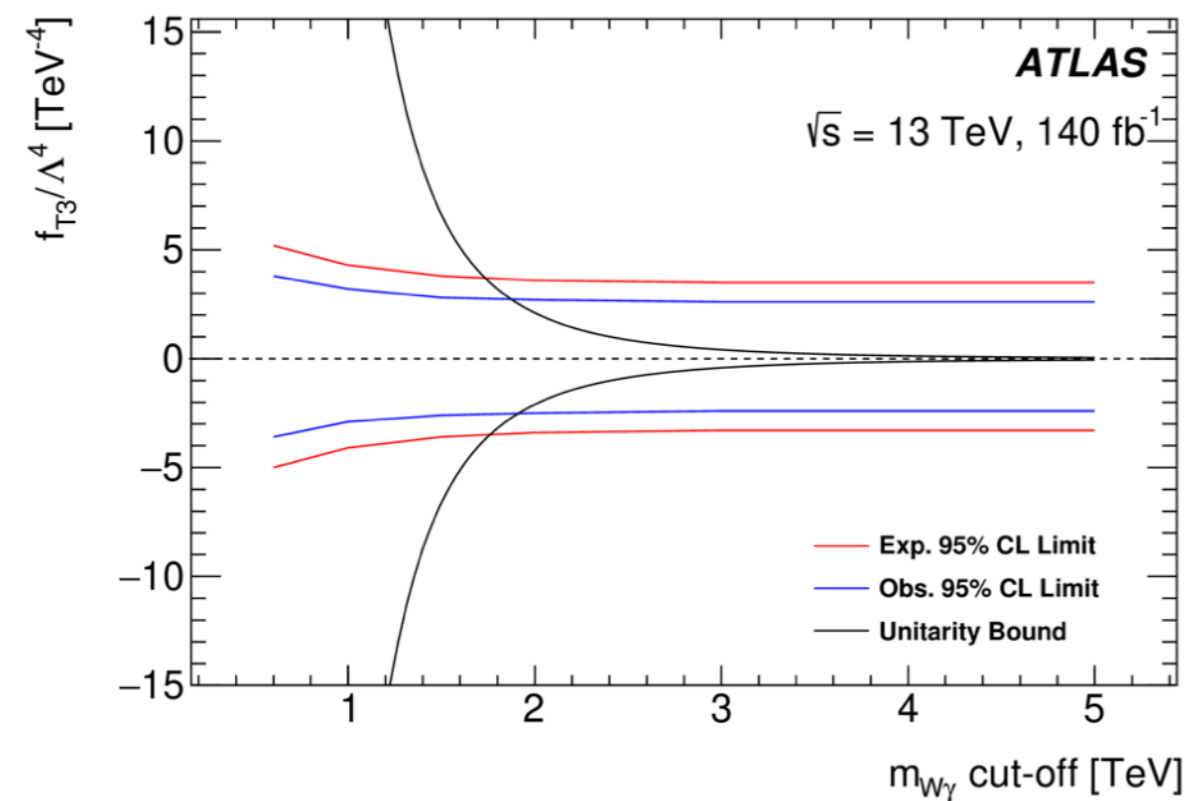
Another goal: dim-8 EFT

- The VBS component is directly sensitive to New Physics via a large variety of **dim-8 Effective Field Theory (EFT) operators** (Eboli model)

- ▶ LO MG+Pythia8 predictions
- ▶ constraint using p_T^l or p_T^{jj}

$$\mathcal{L}_{\text{eff}} = \mathcal{L}_{\text{SM}} + \sum_j \frac{f_j^{(8)}}{\Lambda^4} \mathcal{O}_j^{(8)}$$

- Clipping scan compared with the unitarity bound**



Coefficients [TeV ⁻⁴]	Observable	Expected [TeV ⁻⁴]	Observed [TeV ⁻⁴]
f_{T0}/Λ^4	p_T^{jj}	[-2.4, 2.4]	[-1.8, 1.8]
f_{T1}/Λ^4	p_T^{jj}	[-1.5, 1.6]	[-1.1, 1.2]
f_{T2}/Λ^4	p_T^{jj}	[-4.4, 4.7]	[-3.1, 3.5]
f_{T3}/Λ^4	p_T^{jj}	[-3.3, 3.5]	[-2.4, 2.6]
f_{T4}/Λ^4	p_T^{jj}	[-3.0, 3.0]	[-2.2, 2.2]
f_{T5}/Λ^4	p_T^{jj}	[-1.7, 1.7]	[-1.2, 1.3]
f_{T6}/Λ^4	p_T^{jj}	[-1.5, 1.5]	[-1.0, 1.1]
f_{T7}/Λ^4	p_T^{jj}	[-3.8, 3.9]	[-2.7, 2.8]
f_{M0}/Λ^4	p_T^l	[-28, 28]	[-24, 24]
f_{M1}/Λ^4	p_T^l	[-43, 44]	[-37, 38]
f_{M2}/Λ^4	p_T^l	[-10, 10]	[-8.6, 8.5]
f_{M3}/Λ^4	p_T^l	[-16, 16]	[-13, 14]
f_{M4}/Λ^4	p_T^l	[-18, 18]	[-15, 15]
f_{M5}/Λ^4	p_T^l	[-17, 14]	[-14, 12]
f_{M7}/Λ^4	p_T^l	[-78, 77]	[-66, 65]



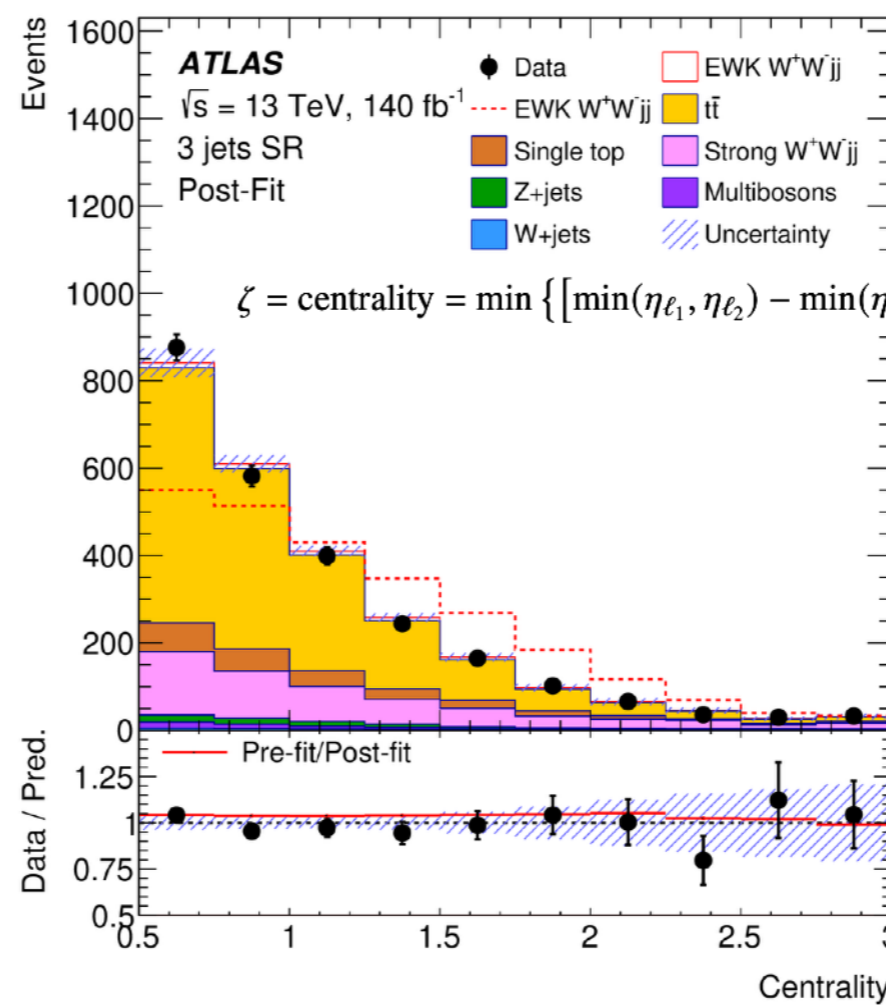
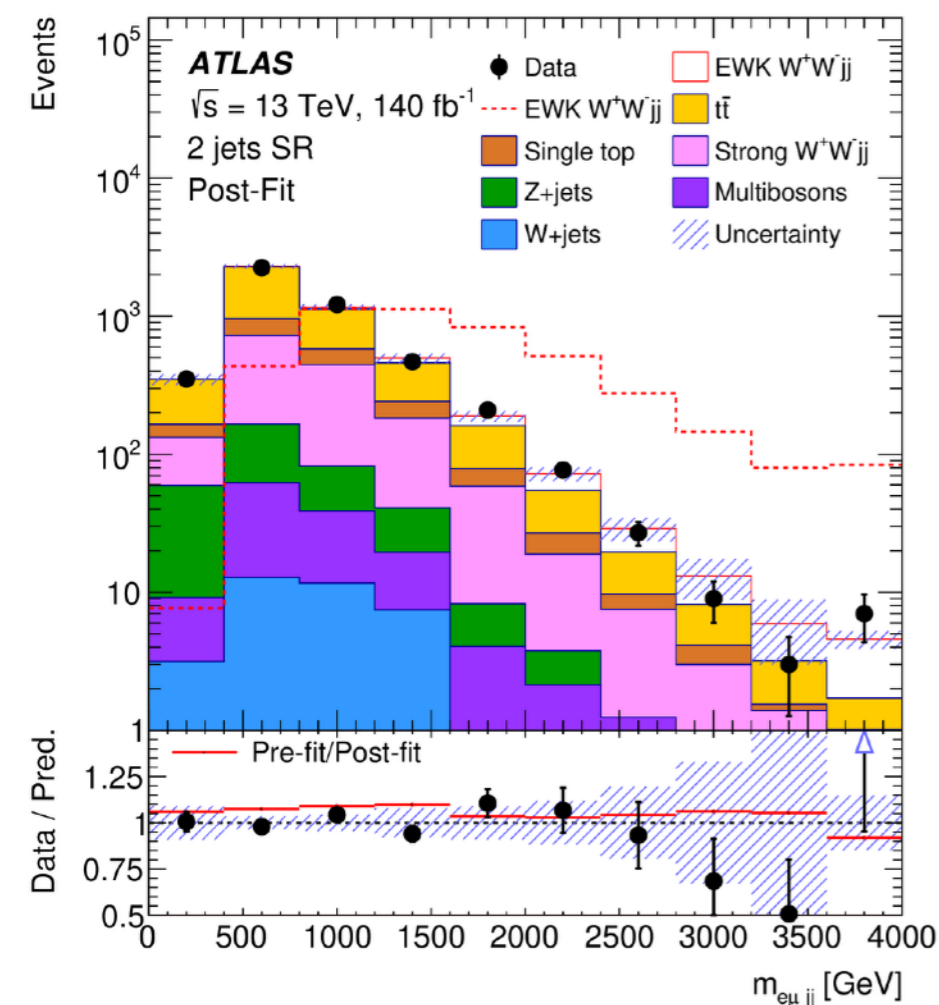
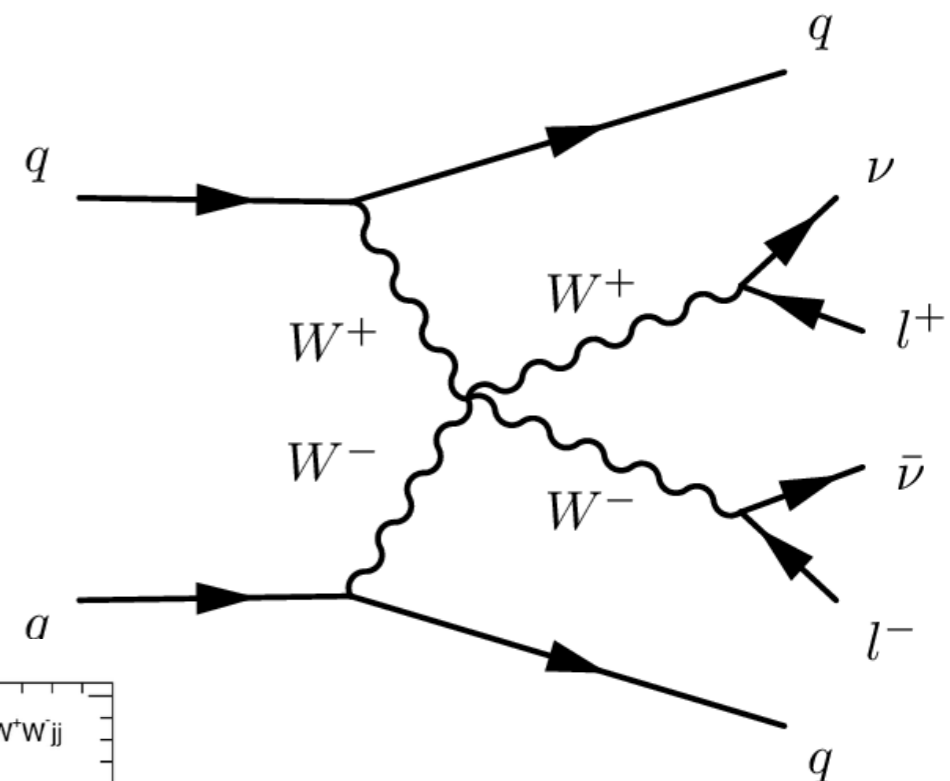
os - $WW+jj$ production

- Phase space requiring opposite sign W pair

- ▶ one electron one muon
- ▶ b-jets veto, centrality cut

- SM background processes

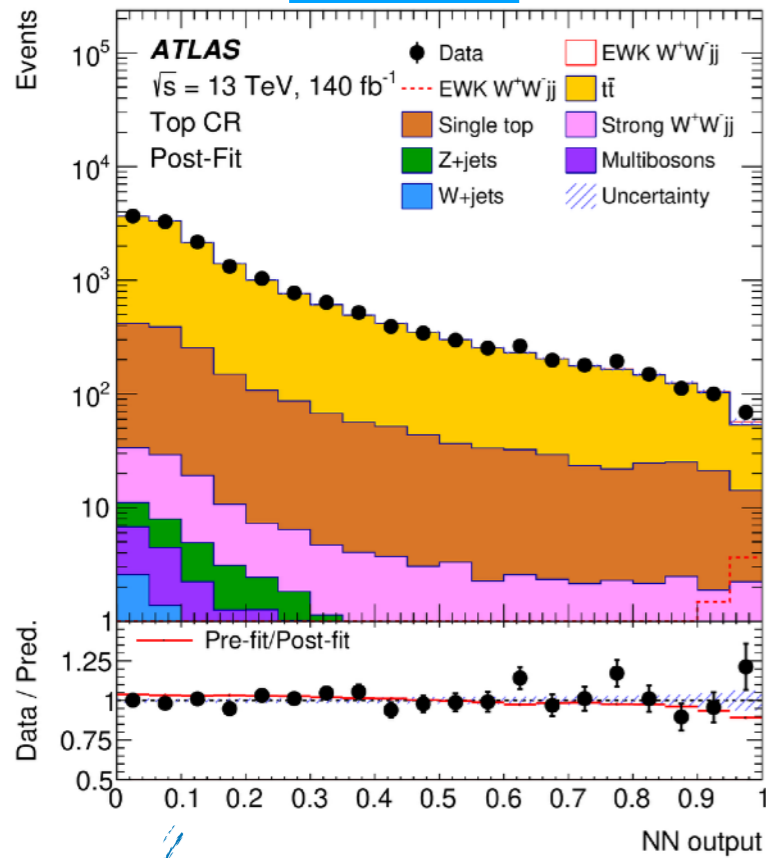
- ▶ top associated processes (dedicated CR)
- ▶ QCD $WW+jj$ production



Good modelling description of the relevant kinematic distributions in the SRs



Top-CR



Main top background constrained in CR and prediction extrapolated in the SR

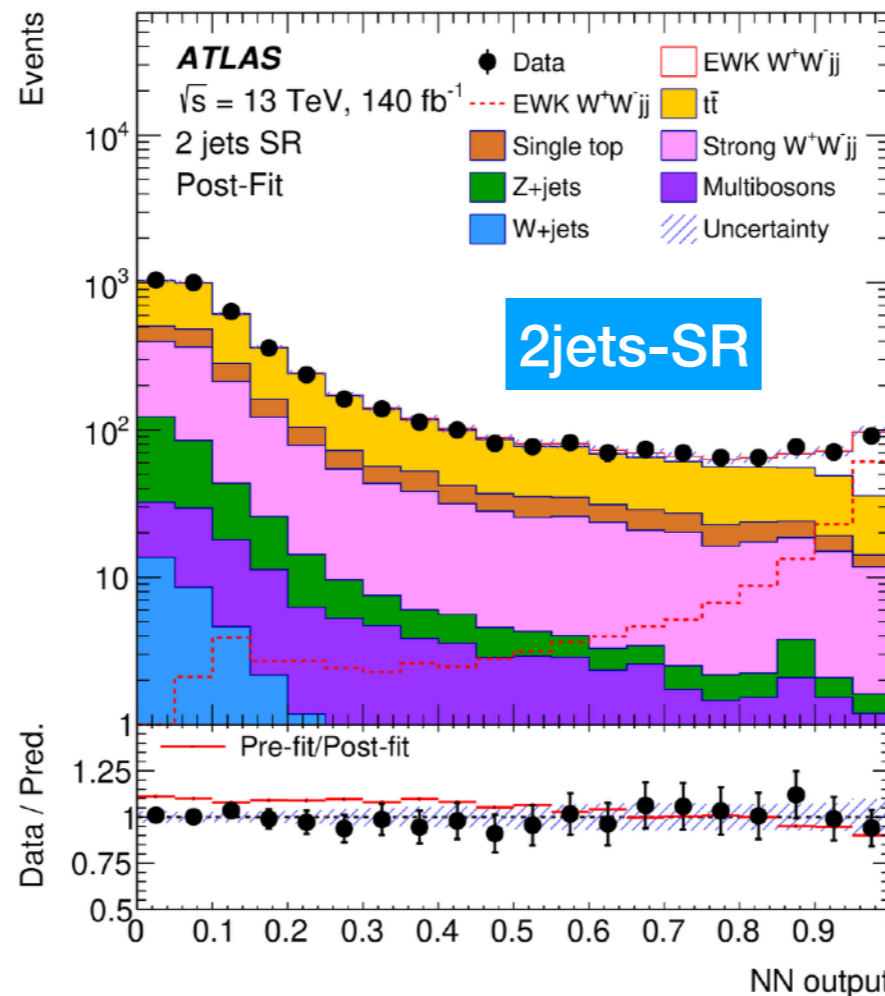
- **Signal sensitivity enhanced with defining a dedicated DNN model**

- 8 (2-jets) and 10 (3-jets) kinematic variables used as input features

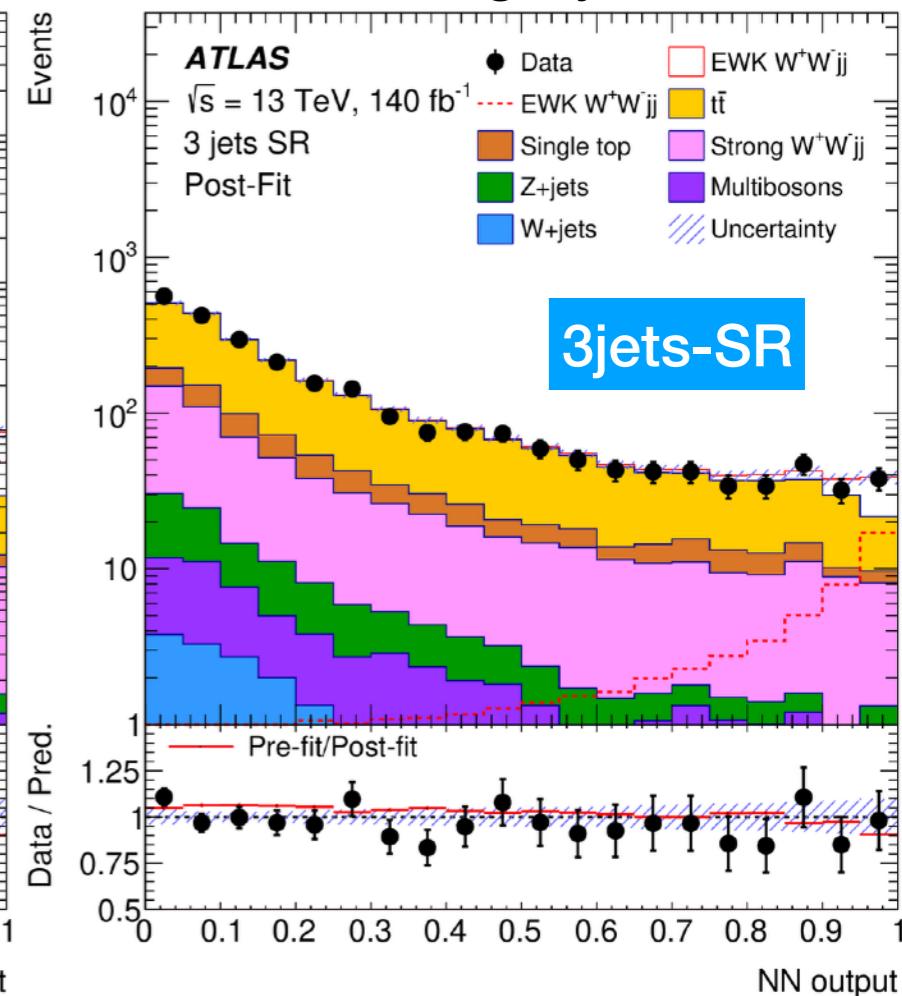
- **Dedicated models for 2-jets and 3-jets events**

- recover signal efficiency

- dedicated variables set for each category



2jets-SR



3jets-SR



- **Simultaneous CR+SRs fit to extract the signal component**

- ▶ no dedicated QCD WW+jj CR → floating

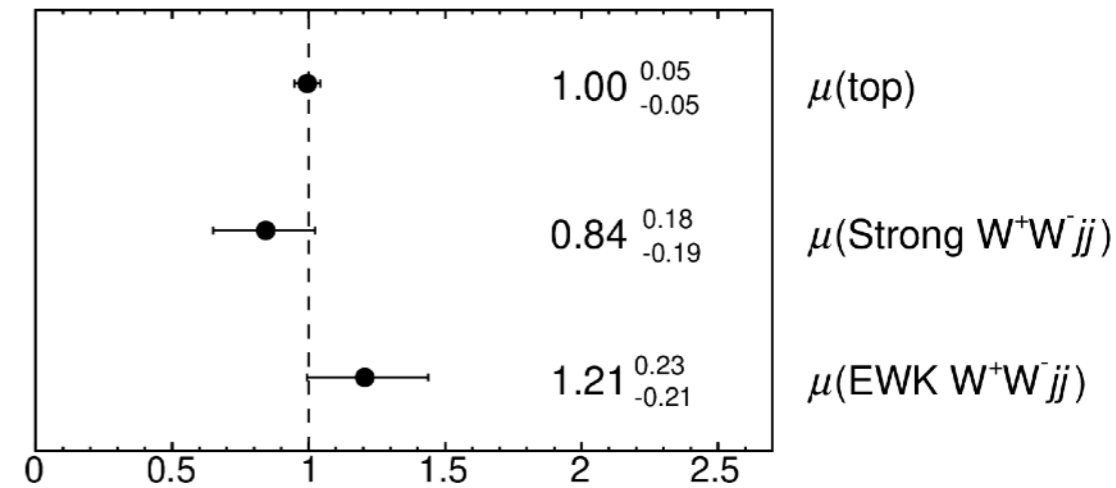
- **Main uncertainties impact**

- ▶ theory (top and EWK), MC stats, jets

Sources	$\frac{\sqrt{(\Delta\mu)^2 - (\Delta\mu')^2}}{\mu}$ [%]
MC statistical uncertainty	7.7
Top quark theoretical uncertainties	6.3
Signal theoretical uncertainties	5.8
Jet experimental uncertainties	4.9
Strong W^+W^-jj theoretical uncertainties	1.3
Luminosity	0.8
Misidentified lepton uncertainty	0.5
b -tagging	0.4
Lepton experimental uncertainties	0.1
Others	0.3
Data statistical uncertainty	12.3
Top quark normalisation uncertainty	4.9
Strong W^+W^-jj normalisation uncertainty	2.2
Total uncertainty	18.5

ATLAS

$\sqrt{s} = 13 \text{ TeV}, 140 \text{ fb}^{-1}$



- **Observation in this channel**

- ▶ 7.1 σ (observed)

- **Fiducial measurement of EWK WW+jj in VBS enhances phase space**

- ▶ remove VV contribution

- ▶ $2.65^{+0.49}_{-0.46} \text{ fb}$



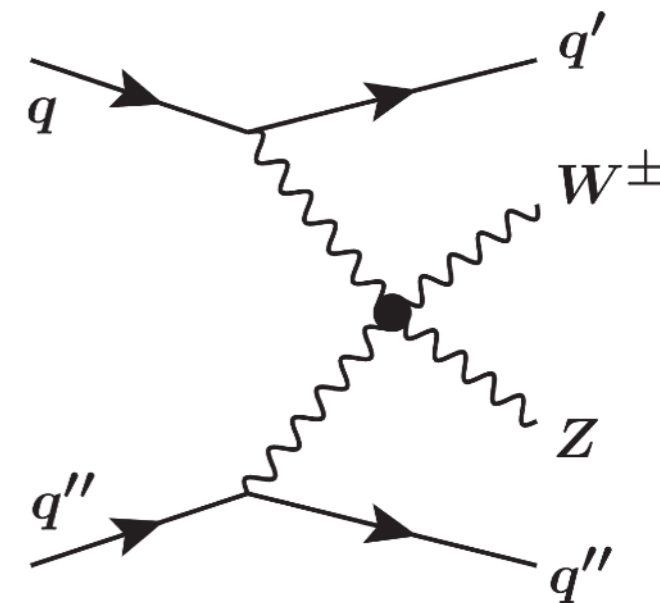
WZ + jj production

• 3 leptons, MET and additional jets final state

- ▶ additional lepton veto, loose $m_{jj} > 150$ GeV requirement
- ▶ SR events divided in $N_{\text{jets}} == 2$ and ≥ 3 categories

• Main SM backgrounds

- ▶ QCD WZ+jj production (irreducible)
- ▶ dedicated ZZ CR (additional lepton)
- ▶ b-CR to constraint tt+V process (additional b-jet)

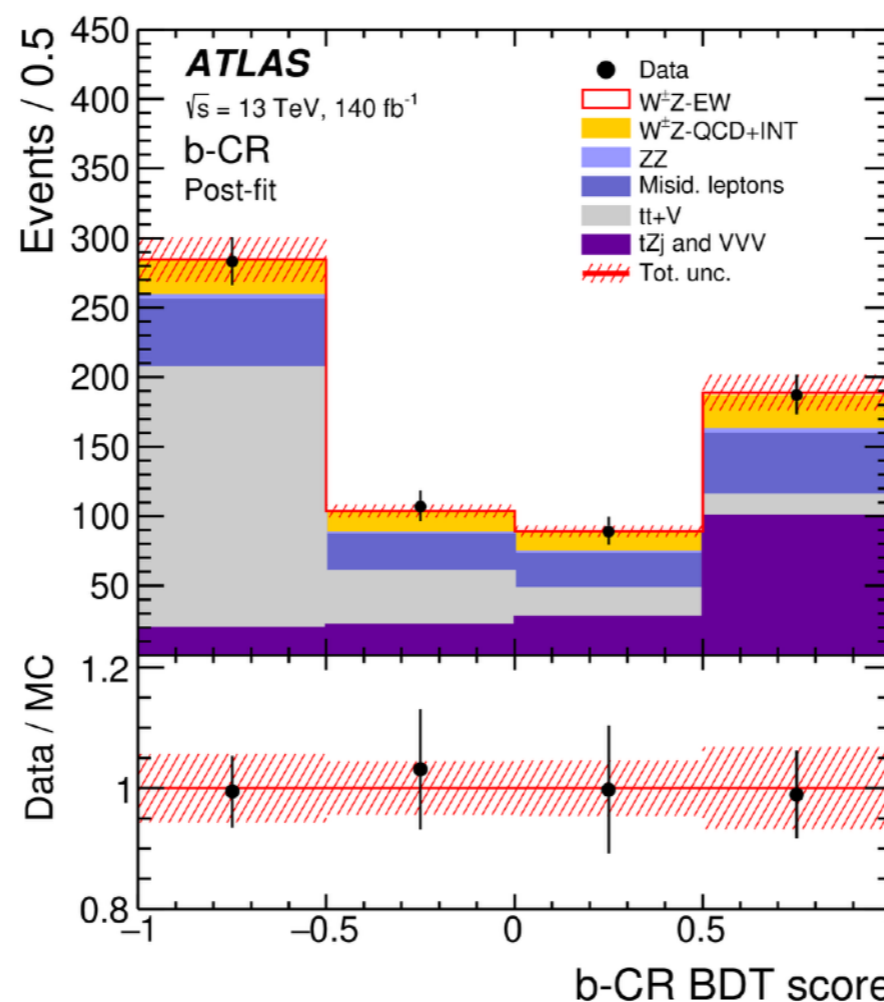
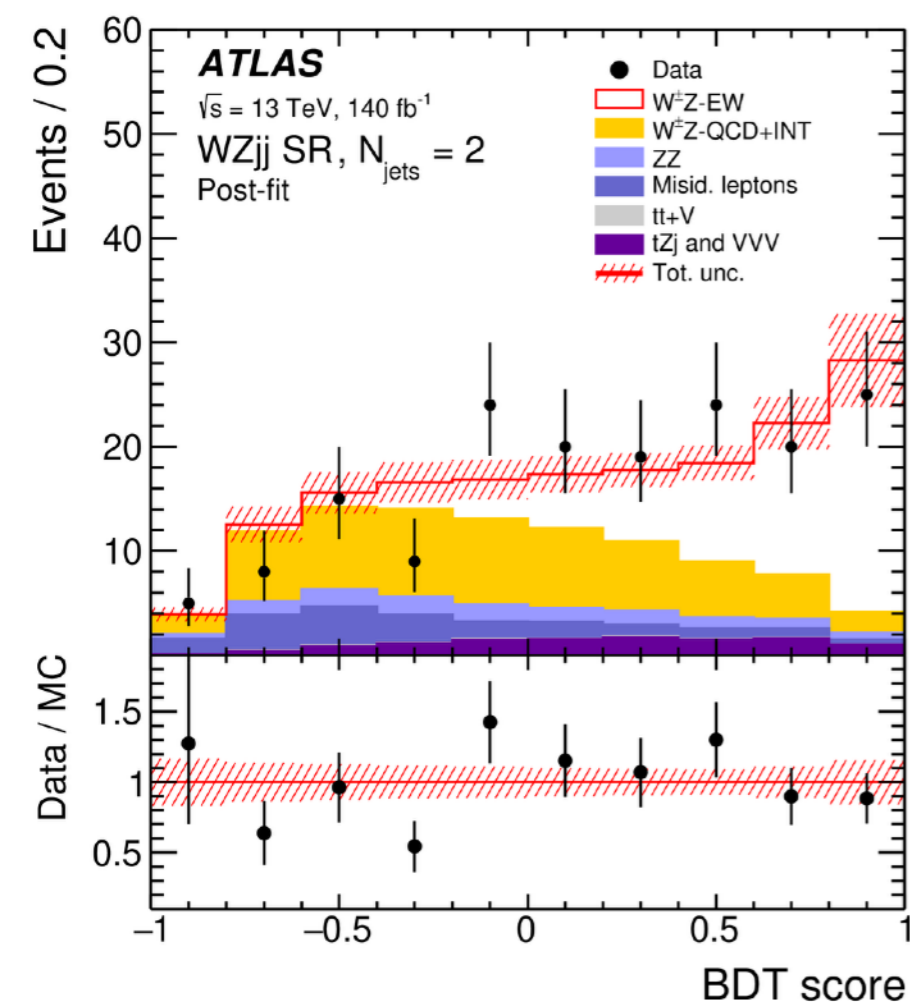


• BDT as final discriminant

- ▶ 15 inputs variables to separate EWK WZjj vs other backgrounds in SR
- ▶ 16 inputs variables to separate ttV and tZj in b-CR

• Adversarial-NN

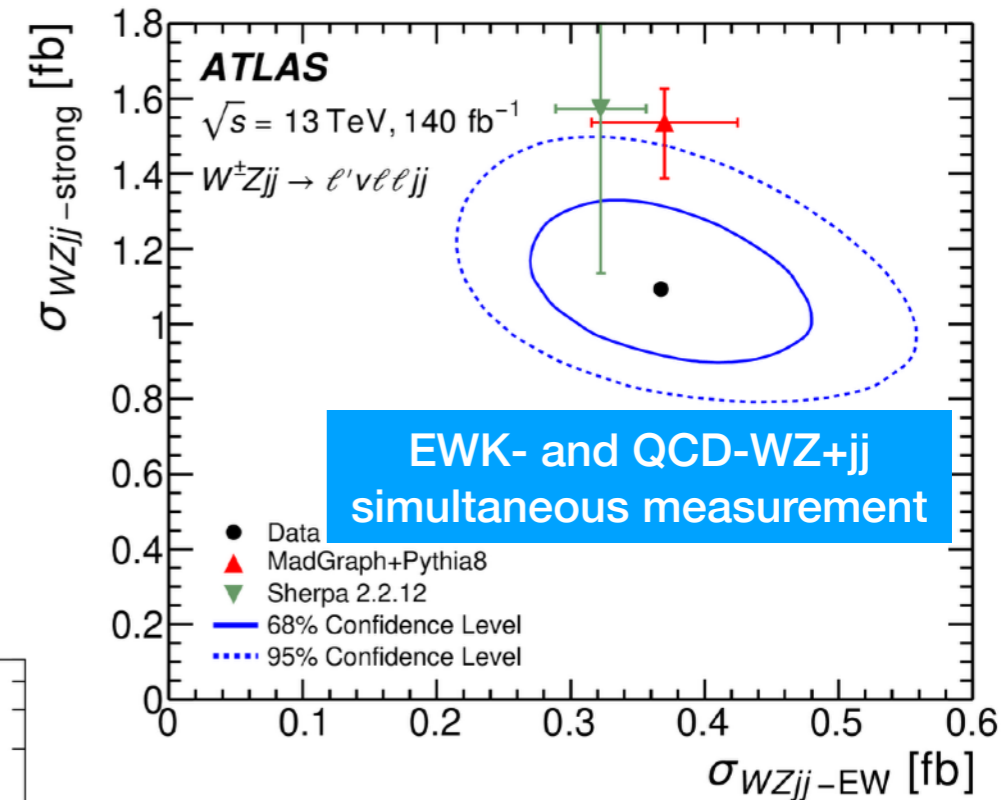
- ▶ to enhance QCD WZjj production in SR





EWK vs QCD production

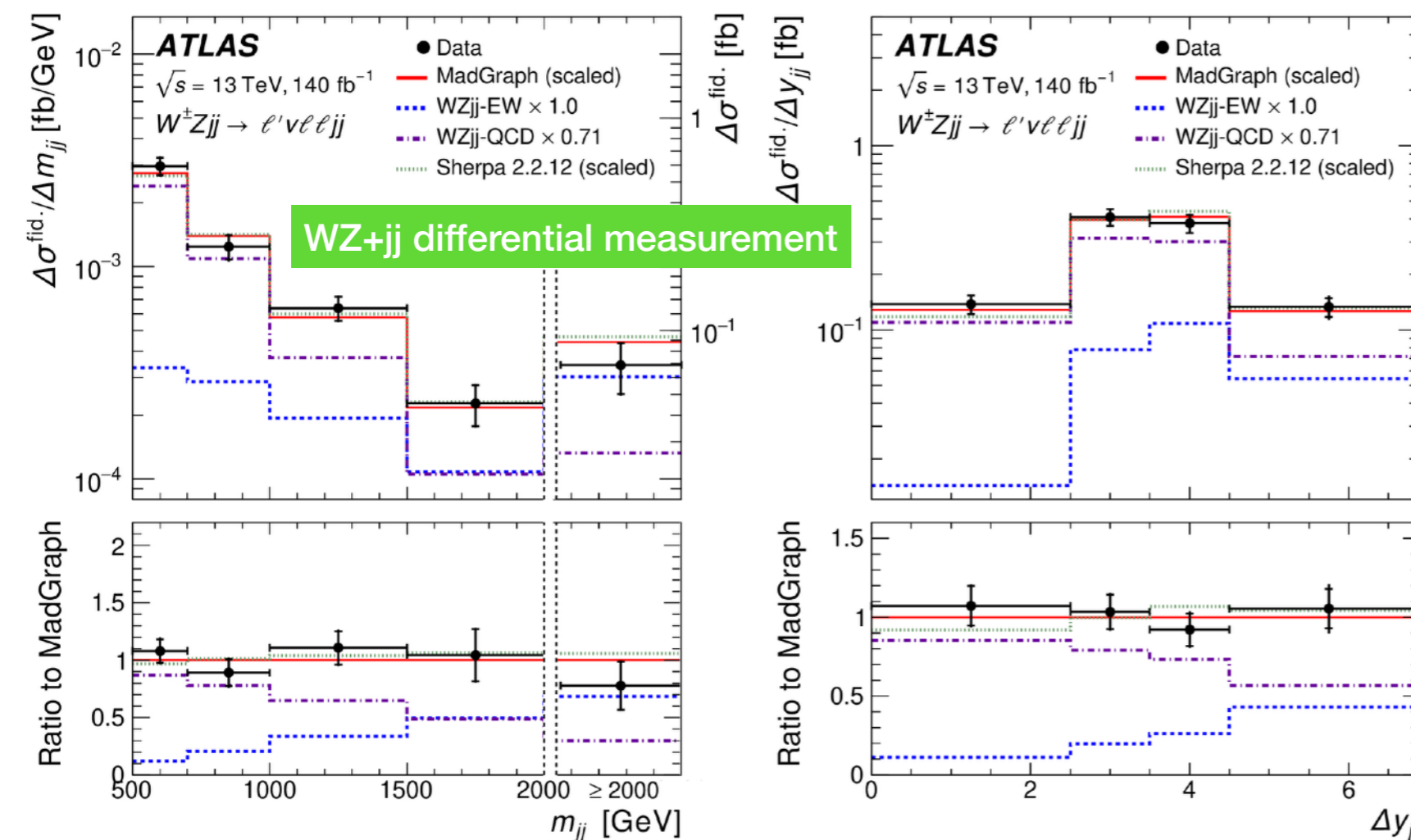
- **EWK- and QCD-WZ+*jj* production measured simultaneously; measurement in bins of:**
 - ▶ $n_{\text{Jets}} \{= 2; \geq 3\}$ bins and 3 m_{jj} bins
 - ▶ **QCD-WZ+*jj* cross section measured by factor 0.71 lower than MC prediction**
- **WZ+*jj* differential measurement**
 - ▶ SR events, predictions scaled by the integrated EWK- and QCD-WZ+*jj* measurements



- **Unfolding of several kinematics variables**

- ▶ compared with the MadGraph and Sherpa predictions
- ▶ BDT unfolded as well

- **Measurements dominated by statistical uncertainty, followed by jets experimental uncertainties**



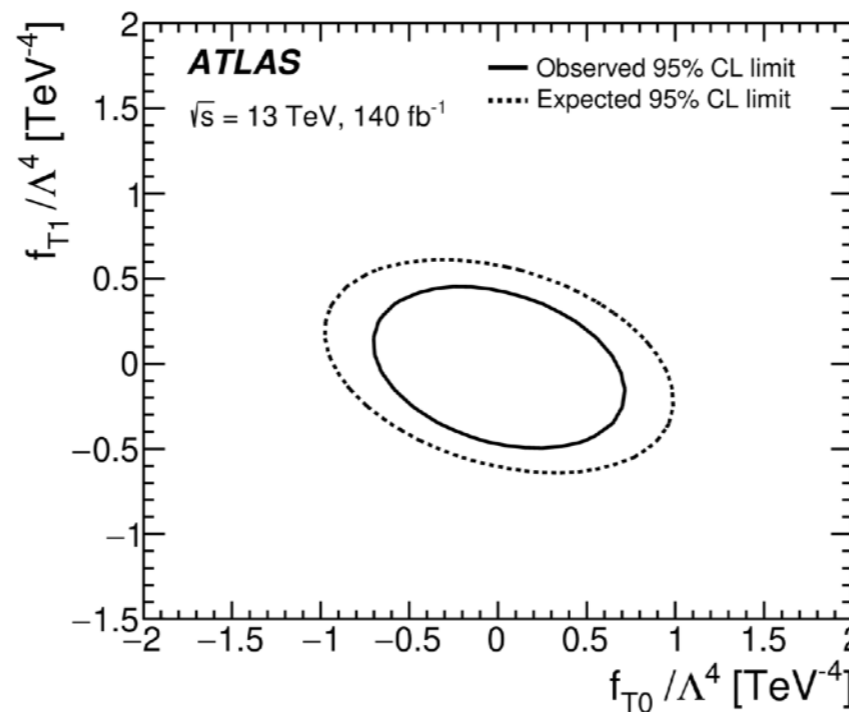
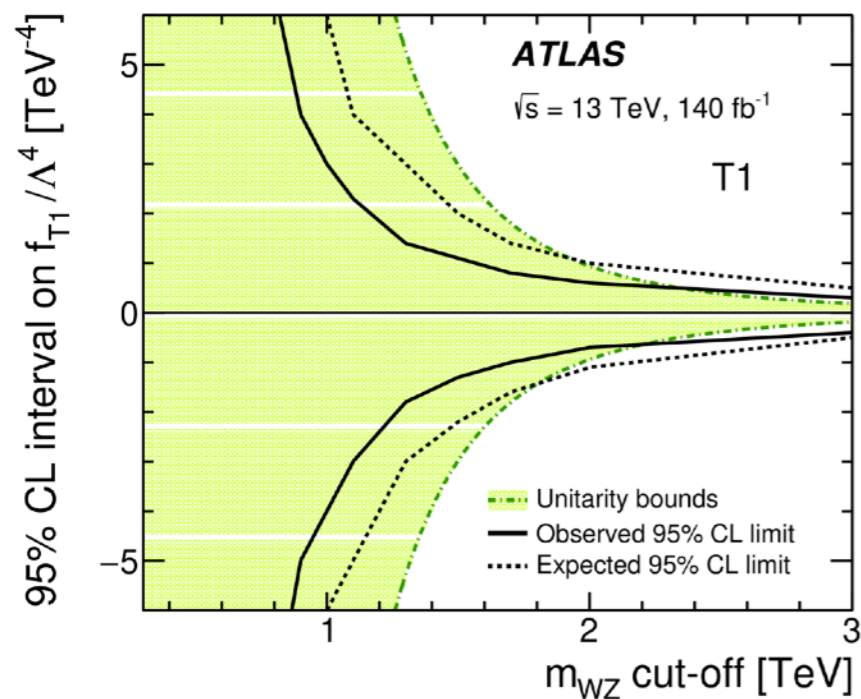
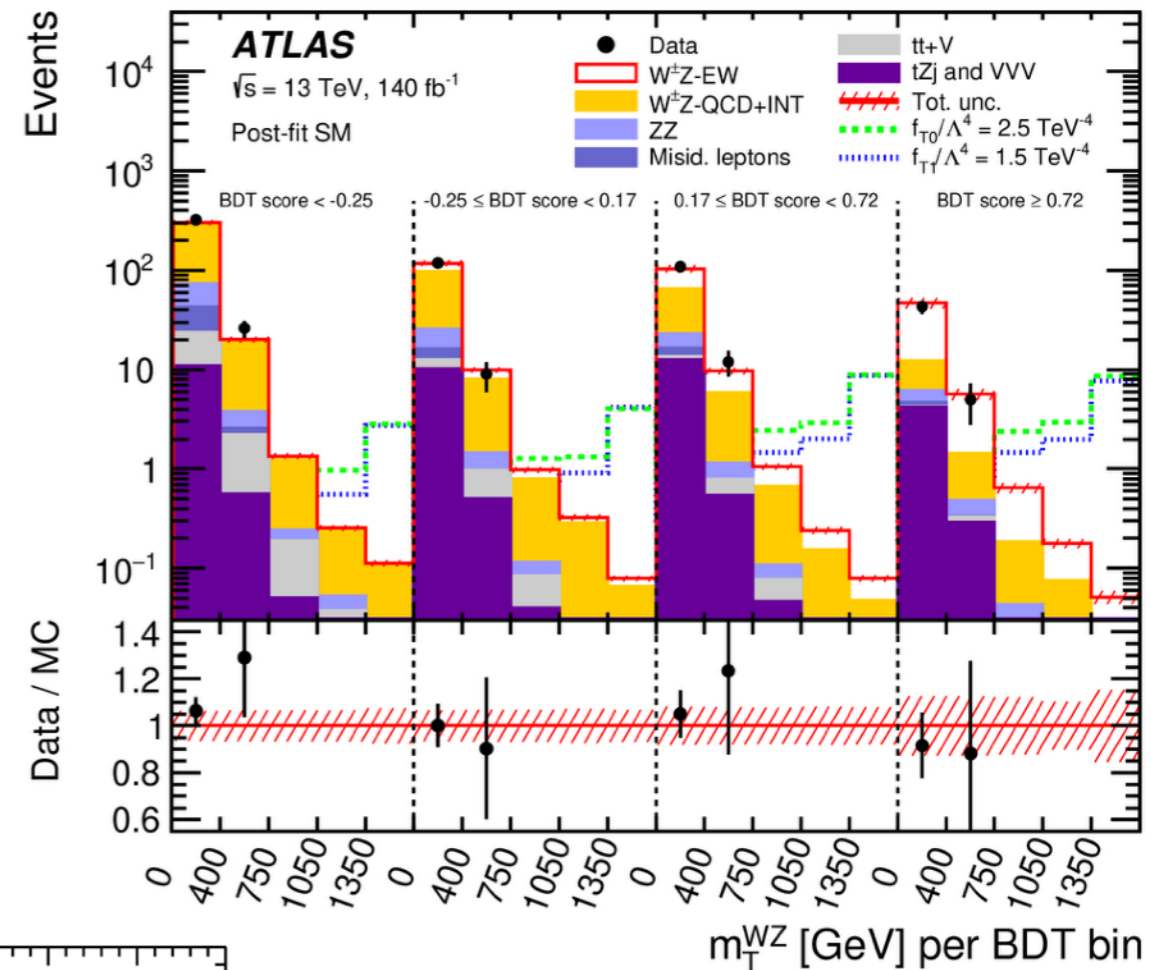


Goal: dim-8 EFT limits

Submitted to JHEP
arxiv.2403.15296

- Effects from **dim-8 EFT operators** are expected at high invariant mass for the WZ+jj production
 - ▶ constraint a set of operators sensitive to
- 2-dim fit based on the BDT and m_T^{WZ} transverse mass

Limits overall better than the $W\gamma+jj$ final state, that is actually covering complementary operators



	Expected [TeV ⁻⁴]	Observed [TeV ⁻⁴]
f_{T0}/Λ^4	[-7.0, 7.0]	[-1.5, 1.6]
f_{T1}/Λ^4	[-1.1, 1.0]	[-0.7, 0.6]
f_{T2}/Λ^4	[-12, 6]	[-2.4, 1.8]
f_{M0}/Λ^4	[-60, 60]	[-12, 12]
f_{M1}/Λ^4	[-32, 32]	[-15, 15]
f_{M7}/Λ^4	[-30, 30]	[-15, 15]
f_{S02}/Λ^4	[-41, 41]	[-18, 18]
f_{S1}/Λ^4	—	—



Summary

- **Measurements of Vector Boson Scattering with the ATLAS experiment**
- Measurement of EWK diboson + jj production in VBS-enhanced phase space quite interesting
 - ▶ crucial test of the EWK-sector of the SM
 - ▶ challenges from theory/experimental side that push us to new strategies
- Additional and new final states covered along the years
 - ▶ new measurements released
 - ▶ all diboson final states have been observed by ATLAS
 - ▶ EFT interpretations performed in this sector
- **Stay tuned for new ATLAS results with Run-2 and Run-3 datasets!!!**

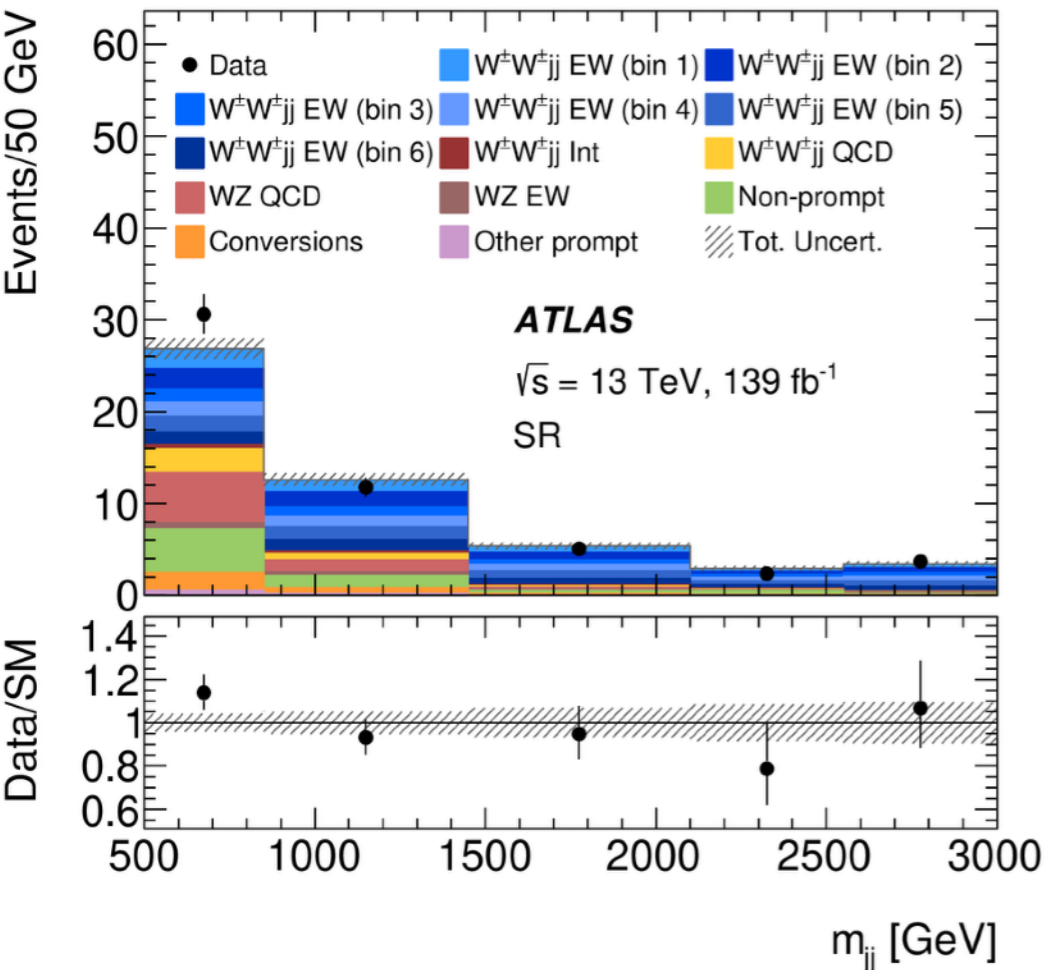
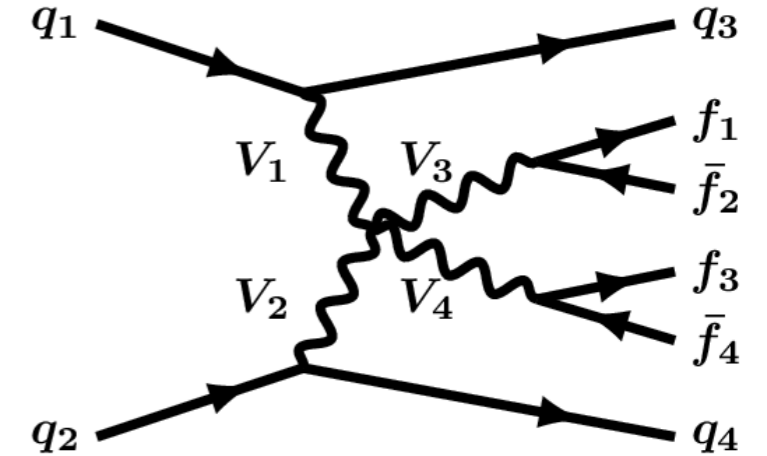


backup



$ss-WW+jj$ production

- Final state with the largest ratio (~ 5) for EWK/QCD $WW+jj$ production
 - qg and gg initiated diagrams not allowed at LO
 - $qq/q\text{-anti-}q$ suppressed at LO
- Usual VBS selection; same-sign electrons/muons pair
 - veto on additional leptons veto and b-jets
- QCD $WZ+jj$ estimated via MC + data-driven corrections
 - large source of fakes/non-prompts estimated via data-driven



Summary of MC samples for signal and background processes

Process, short description	ME Generator + parton shower	Order	Tune	PDF set in ME
EW, Int, QCD W^+W^+jj , nominal signal	MADGRAPH5_AMC@NLO2.6.7 + HERWIG7.2	LO	HERWIG	NNPDF3.0NLO
EW, Int, QCD W^+W^+jj , alternative shower	MADGRAPH5_AMC@NLO2.6.7 + PYTHIA8.244	LO	A14	NNPDF3.0NLO
EW W^+W^+jj , NLO pQCD approx.	SHERPA2.2.11 & SHERPA2.2.2(WWW) & POWHEG BOX2+PYTHIA8.235 (WH)	+0,1j@LO NLO	SHERPA A14	NNPDF3.0NNLO
EW W^+W^+jj , NLO pQCD approx.	POWHEG BOXV2 + PYTHIA8.230	NLO (VBS approx.)	AZNLO	NNPDF3.0NLO
QCD W^+W^+jj , NLO pQCD approx.	SHERPA2.2.2	+0,1j@LO	SHERPA	NNPDF3.0NNLO
QCD $VVjj$	SHERPA2.2.2	+0,1j@NLO; +2,3j@LO	SHERPA	NNPDF3.0NNLO
EW W^+Z/γ^*jj	MADGRAPH5_AMC@NLO2.6.2+PYTHIA8.235	LO	A14	NNPDF3.0NLO
EW $Z/\gamma^*Z/\gamma^*jj$	SHERPA2.2.2	LO	SHERPA	NNPDF3.0NNLO
QCD $V\gamma jj$	SHERPA2.2.11	+0,1j@NLO; +2,3j@LO	A14	NNPDF3.0NNLO
EW $V\gamma jj$	MADGRAPH5_AMC@NLO2.6.5+PYTHIA8.240	LO	A14	NNPDF3.0NLO
VVV	SHERPA2.2.1 (leptonic) & SHERPA2.2.2 (one $V \rightarrow jj$)	+0,1j@LO	SHERPA	NNPDF3.0NNLO
$t\bar{t}V$	MADGRAPH5_AMC@NLO2.3.3.p0 + PYTHIA8.210	NLO	A14	NNPDF3.0NLO
tZq	MADGRAPH5_AMC@NLO2.3.3.p1 + PYTHIA8.212	LO	A14	NNPDF2.3LO
W^+W^+jj EFT	MADGRAPH5_AMC@NLO2.6.5 + PYTHIA8.235	LO	A14	NNPDF3.0NLO
H_5^\pm	MADGRAPH5_AMC@NLO2.9.5 + PYTHIA8.245	LO	A14	NNPDF3.0NLO

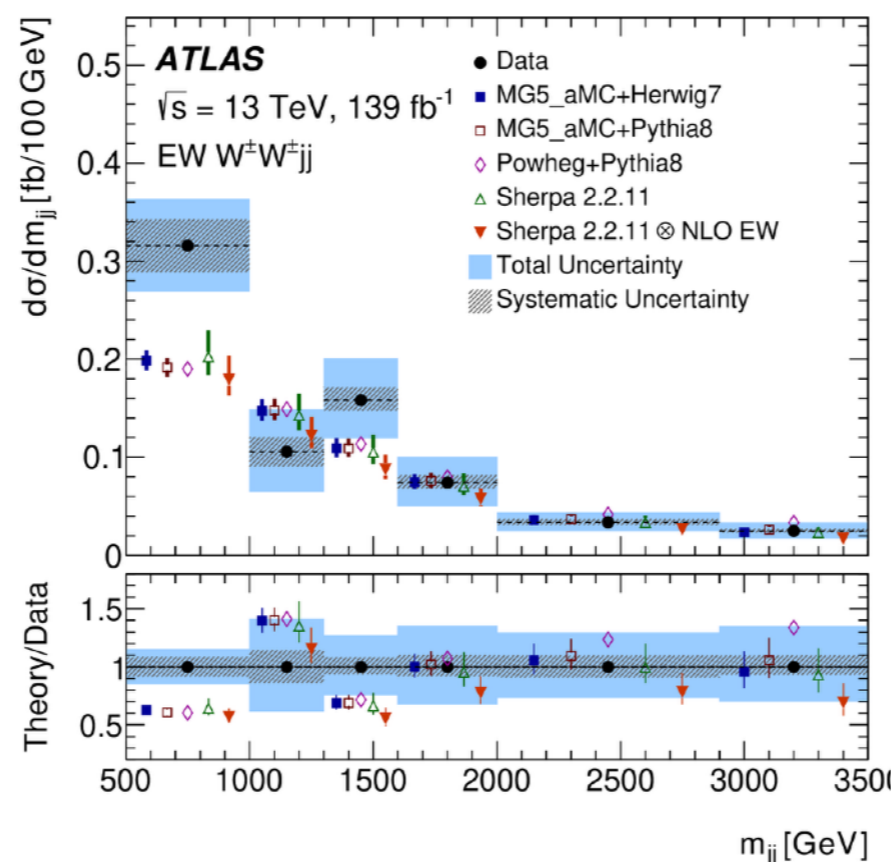
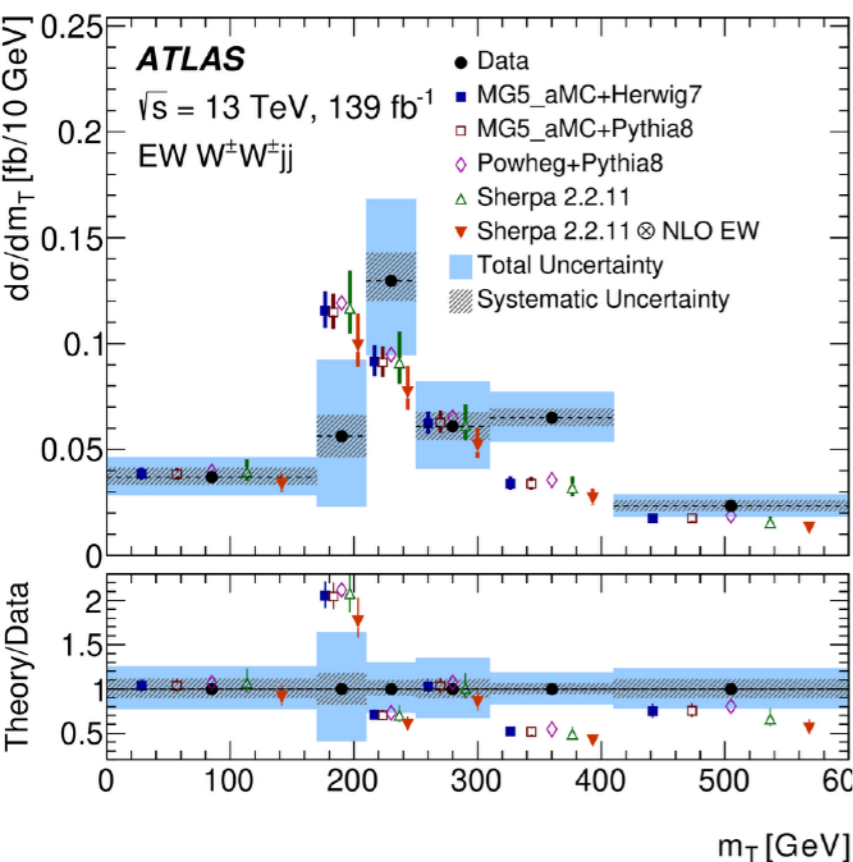


Differential measurement

Submitted to JHEP
arxiv.2312.00420

- SRs based on the lepton flavour (ee, eμ, μe, μμ)
 - ▶ same for the low-m_{jj} CR, one-bin for the WZ-CR
- m_{jj} used to enhance the signal sensitivity in each bin of the measured variables
 - ▶ m_{ll} is instead used to measure the cross section as function of the m_{jj}
- $\mu^{\text{EW}} = 1.15 \pm 0.09$ (stat.) ± 0.05 (mod. syst.) ± 0.05 (exp. syst.) ± 0.02 (lumi.)

Source	Impact [%]
Experimental	4.6
Electron calibration	0.4
Muon calibration	0.5
Jet energy scale and resolution	1.9
E_T^{miss} scale and resolution	0.2
<i>b</i> -tagging inefficiency	0.7
Background, misid. leptons	3.4
Background, charge misrec.	1.0
Pile-up modelling	0.1
Luminosity	1.9
Modelling	4.5
EW W^+W^+jj , shower, scale, PDF & α_s	0.7
EW W^+W^+jj , QCD corrections	1.9
EW W^+W^+jj , EW corrections	0.9
Int W^+W^+jj shower scale, PDF & α_s	0.6
QCD W^+W^+jj , shower, scale, PDF & α_s	2.6
QCD W^+W^+jj , QCD corrections	0.8
Background, WZ scale, PDF & α_s	0.3
Background, WZ reweighting	1.5
Background, other	1.3
Model statistical	1.8
Experimental and modelling	6.4
Data statistical	7.4
Total	9.8

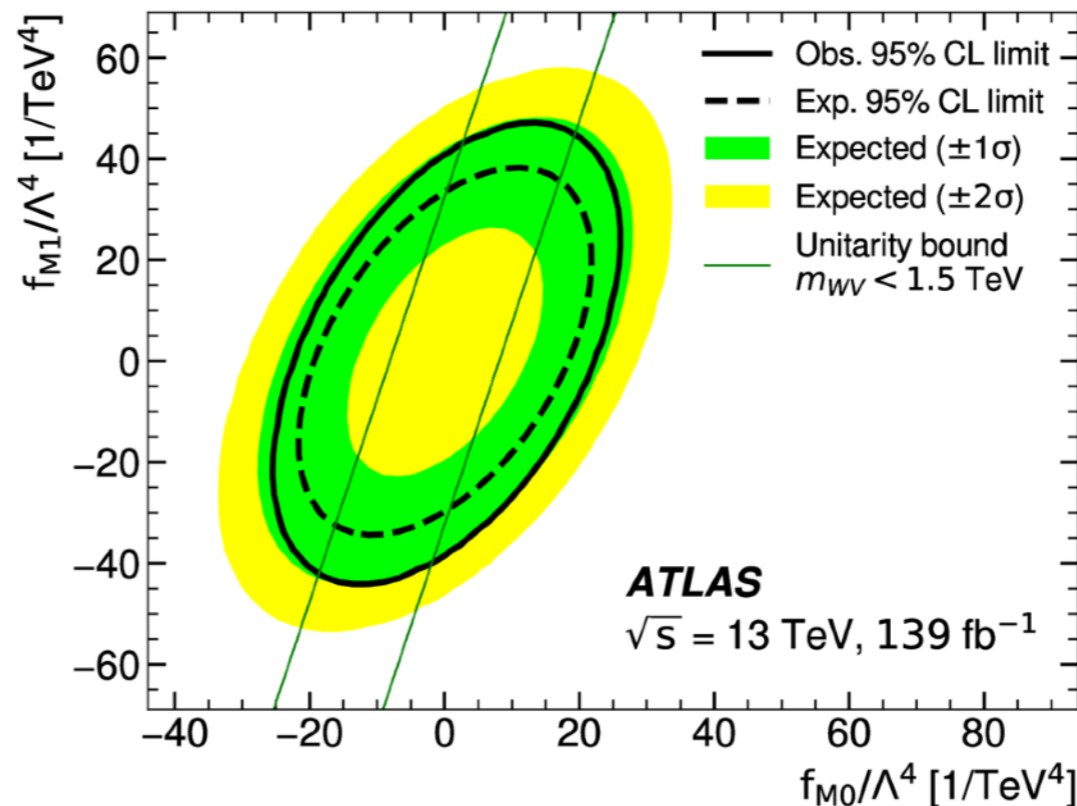
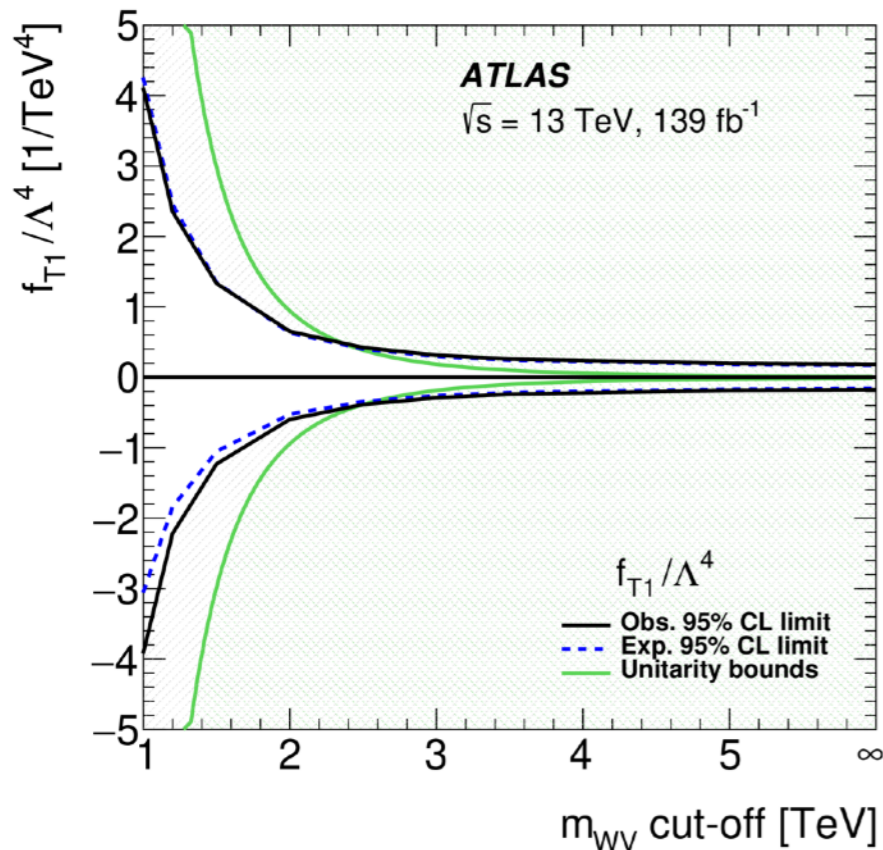
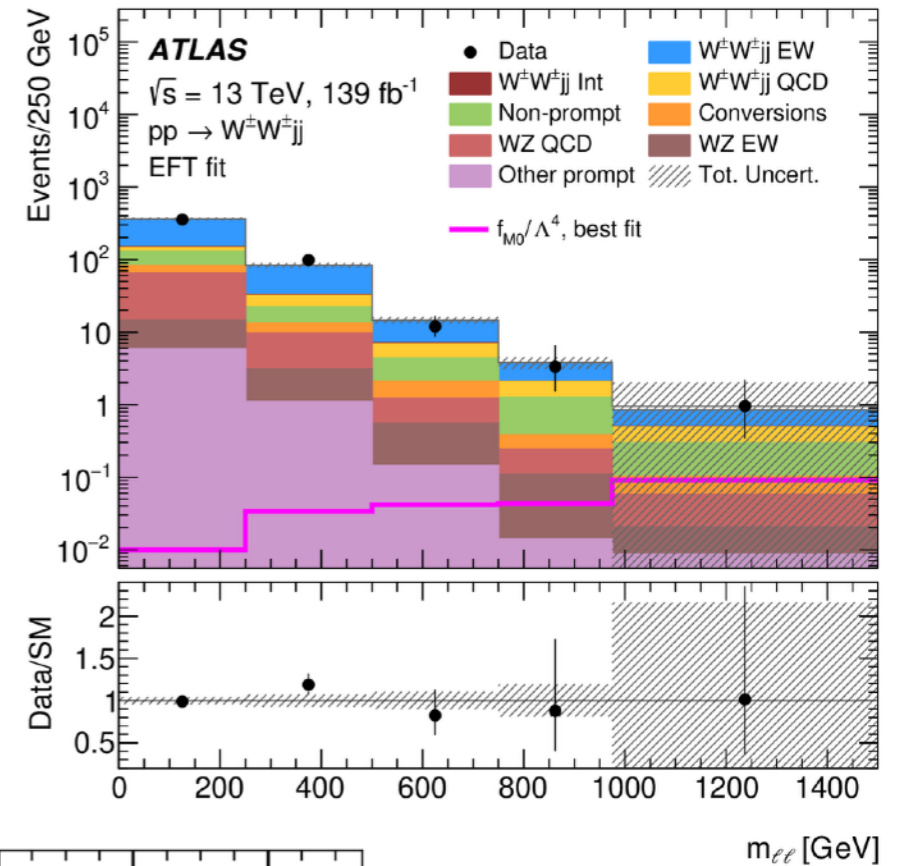


Description	$\sigma_{\text{fid}}^{\text{EW}}$ [fb]
Measured cross section	2.92 ± 0.22 (stat.) ± 0.19 (syst.)
MG5_AMC+HERWIG7	2.53 ± 0.04 (PDF) $^{+0.22}_{-0.19}$ (scale)
MG5_AMC+PYTHIA8	2.53 ± 0.04 (PDF) $^{+0.22}_{-0.19}$ (scale)
SHERPA	2.48 ± 0.04 (PDF) $^{+0.40}_{-0.27}$ (scale)
SHERPA ⊗ NLO EW	2.10 ± 0.03 (PDF) $^{+0.34}_{-0.23}$ (scale)
POWHEG BOX+PYTHIA	2.64



dim-8 EFT constraints

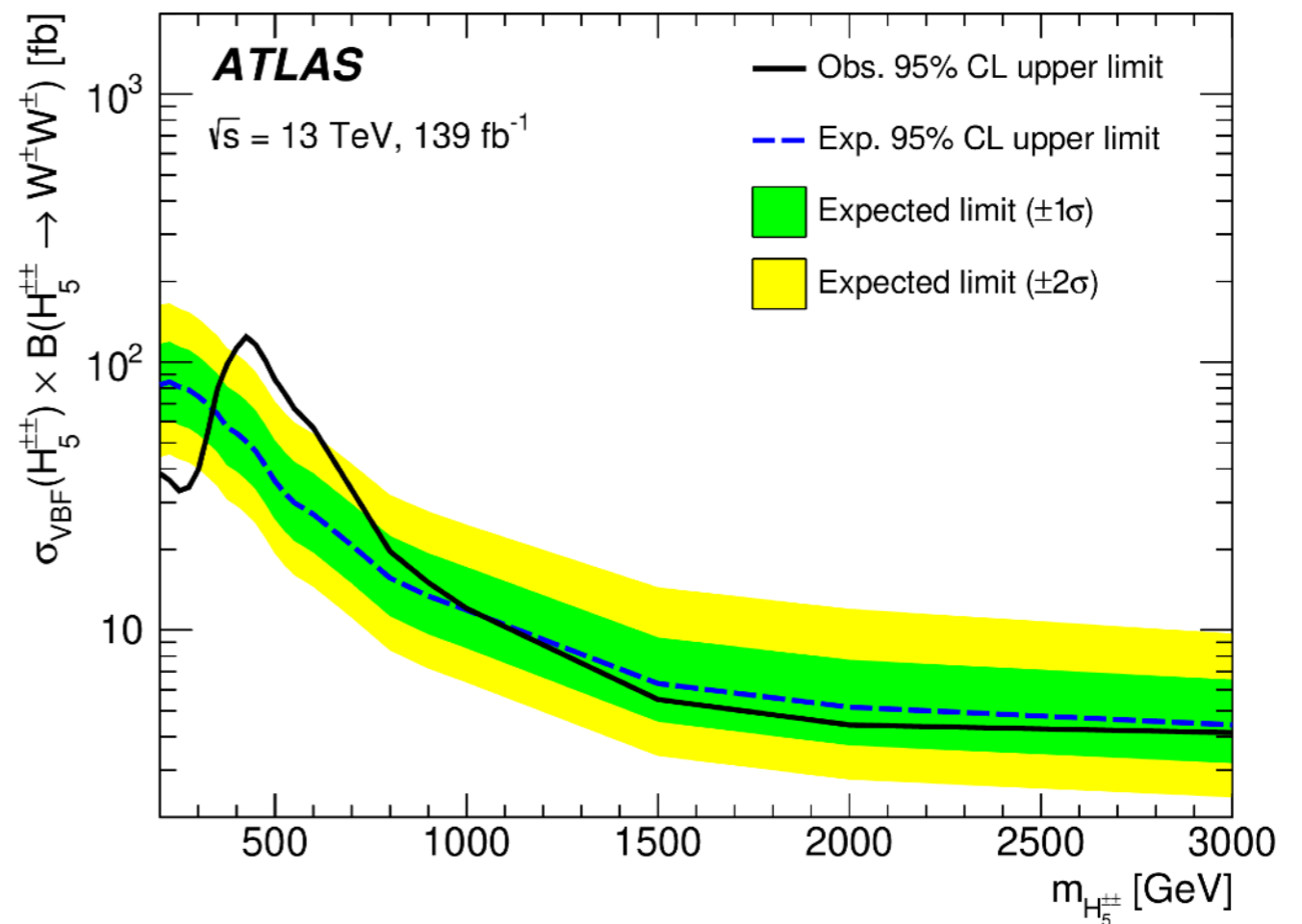
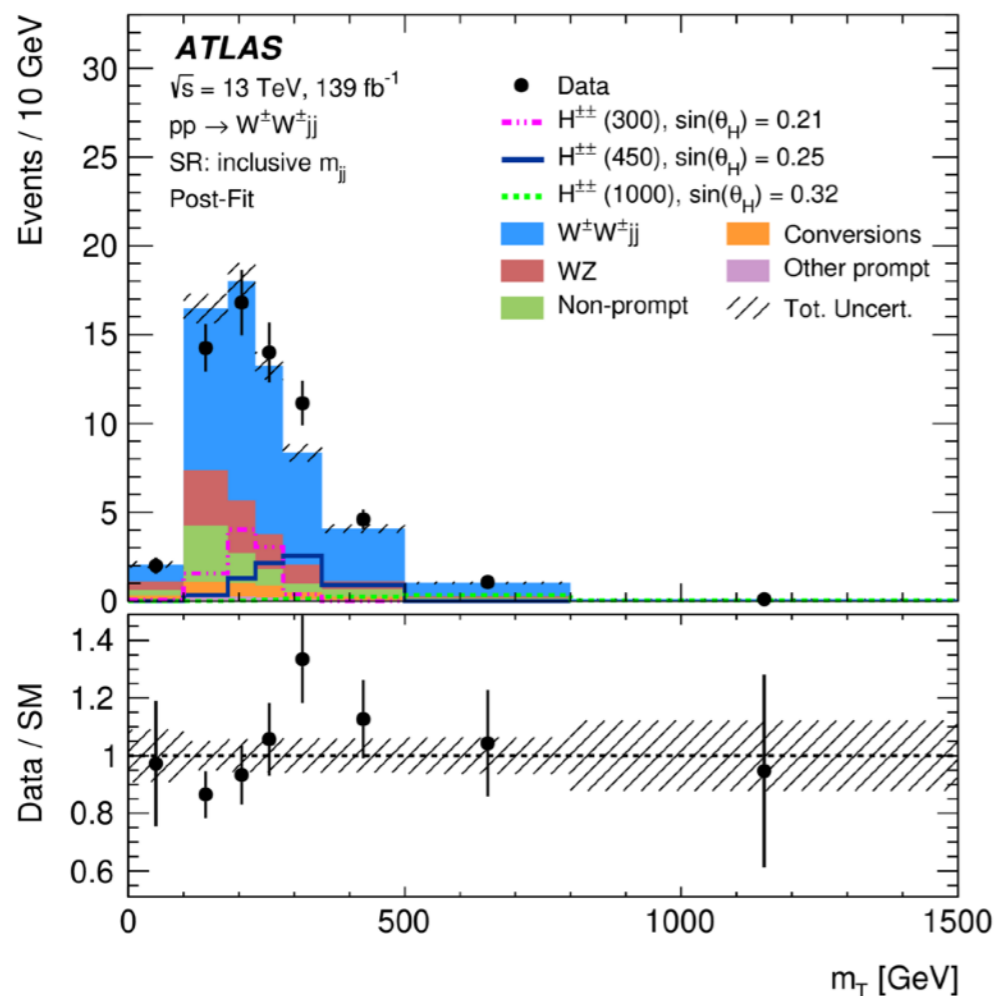
- Phase space sensitive to a variety of dim-8 EFT operators
- 95% exclusion limits as a function of the clipping cut-off
 - ▶ tighter limit on T1 excluding up to 2.4 - 2.5 TeV
- 2-dimensional limits derived w/ a 1.5 TeV unitarisation cut-off and w/o it
 - ▶ interesting positive/negative correlation among the operators



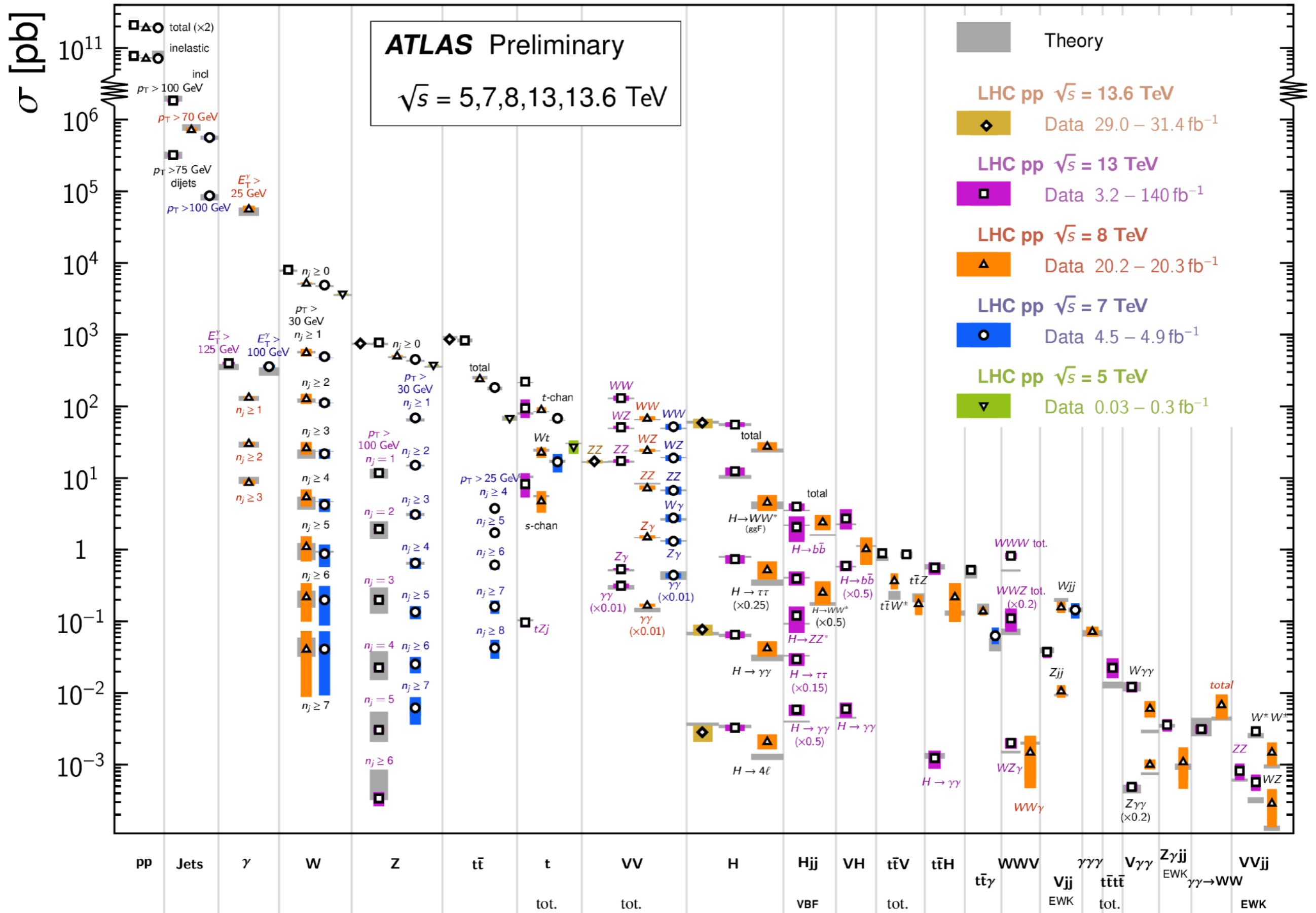
VBS: more than a measurement

- Limits on the production of doubly charged H^{++} via Vector Boson Fusion (VBF)
 - ▶ Georgi-Machacek model ([Nucl. Phys. B 262 \(1985\) 463](#)) foresees the presence of an additional quintuplet ($H^{\pm\pm}$, H^\pm , H^0) that couples to SM W/Z bosons
- Similar analysis strategy, 2-dim fit on m_{jj} and m_T variables
- Excess around 450 GeV: local 3.3, global 2.5

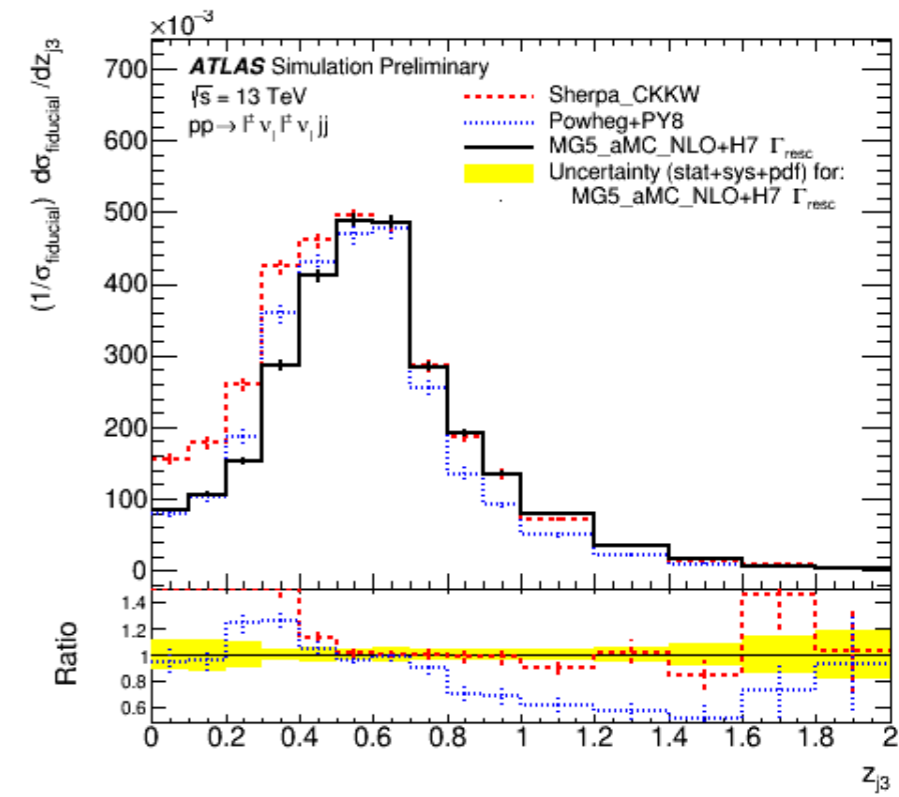
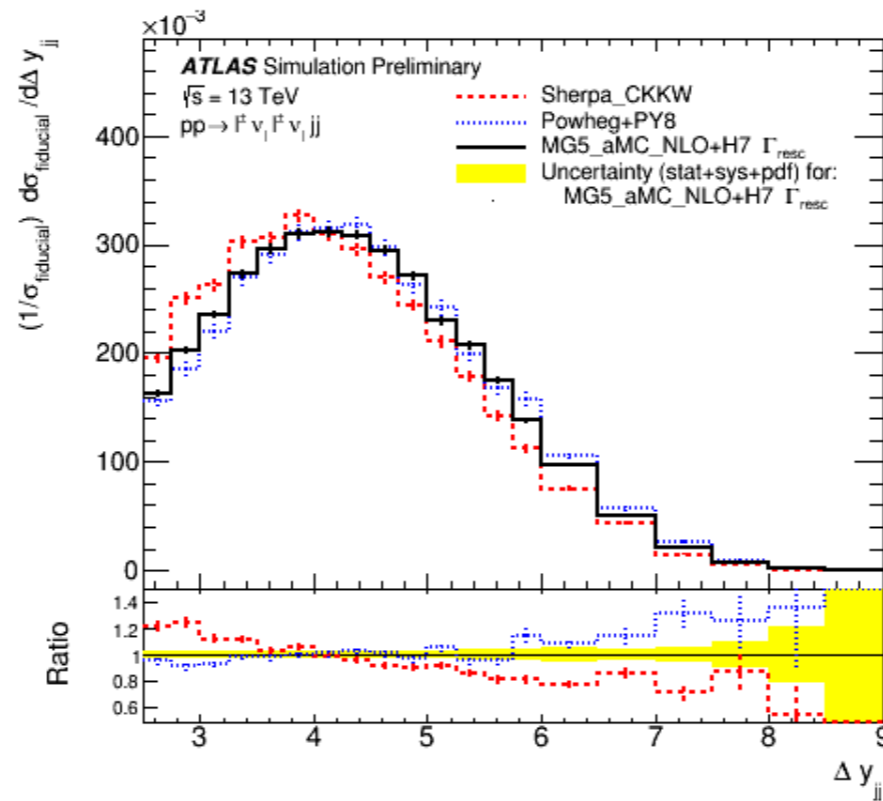
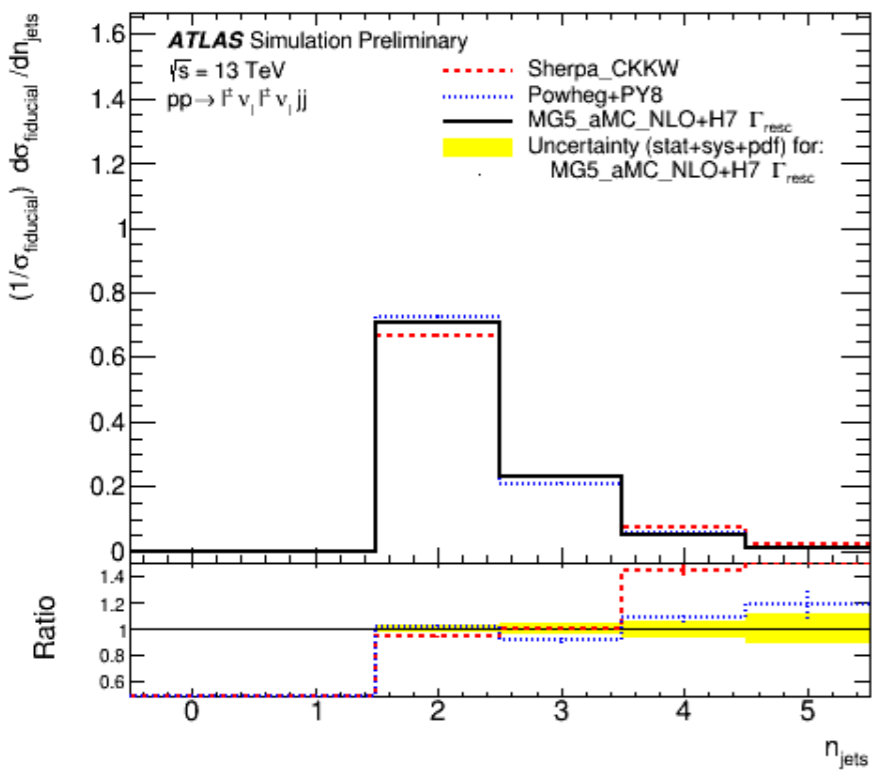
Submitted to JHEP
[arxiv.2312.00420](#)



Standard Model Production Cross Section Measurements



More MC generator comparisons



$W\gamma jj$: diagrams

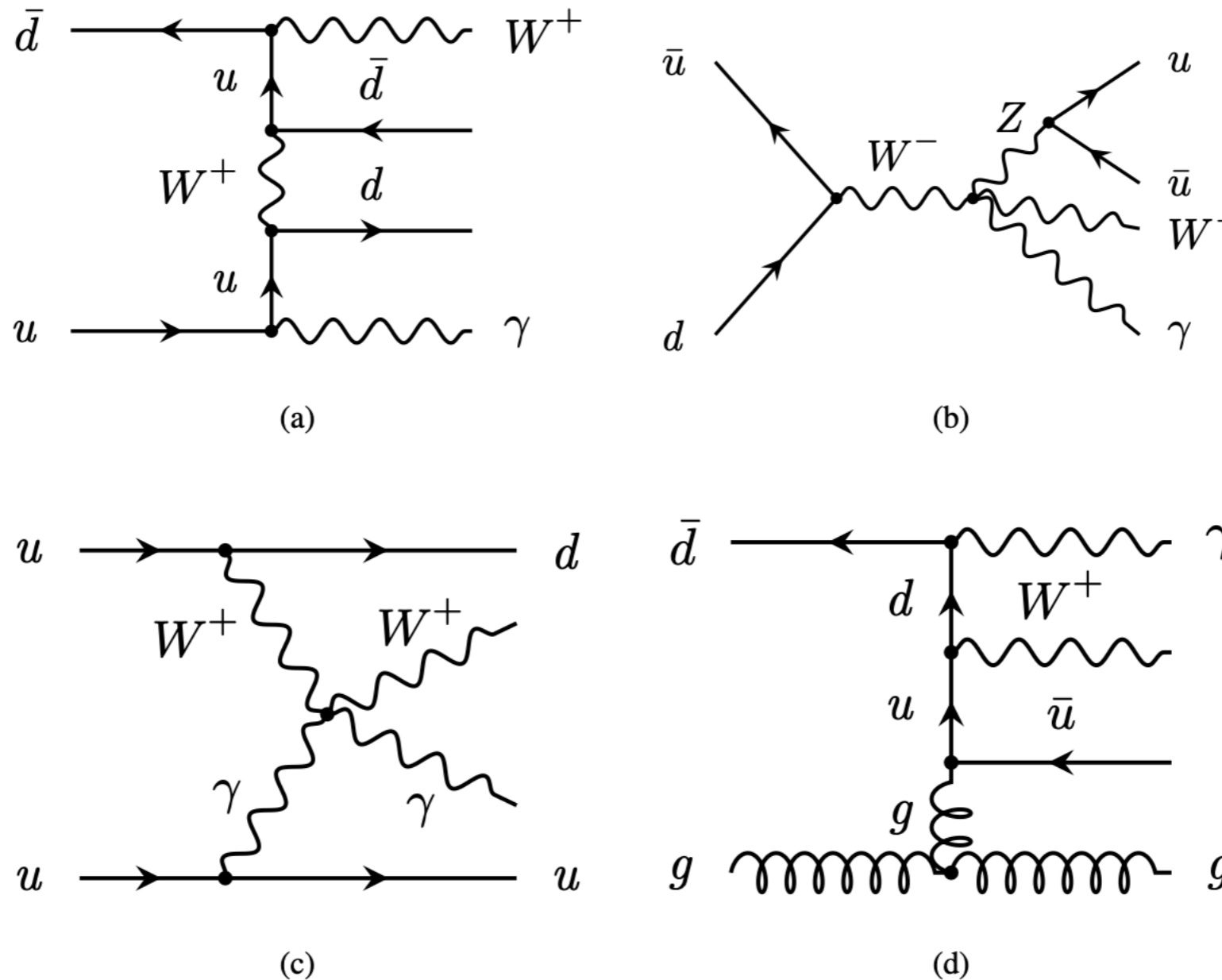


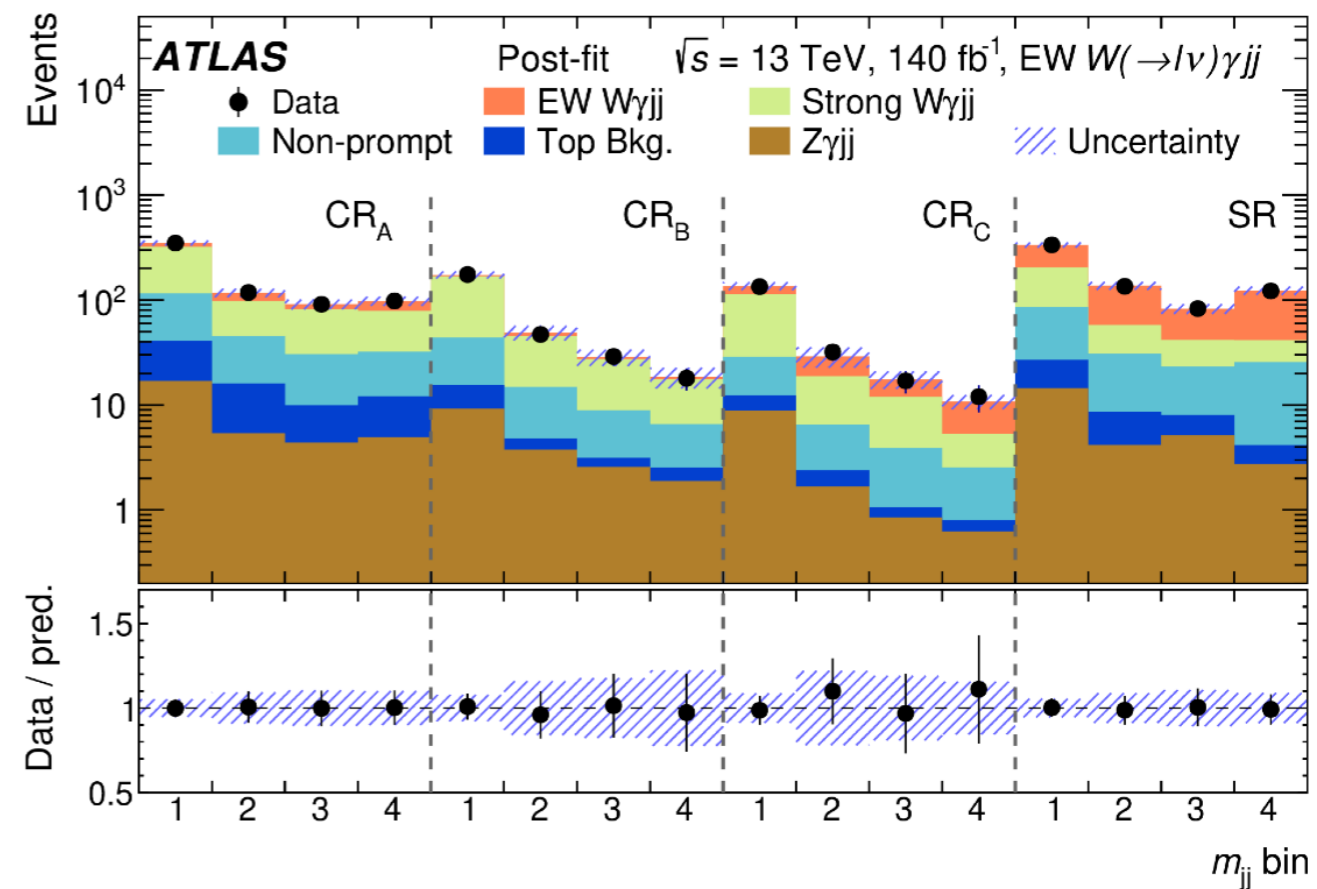
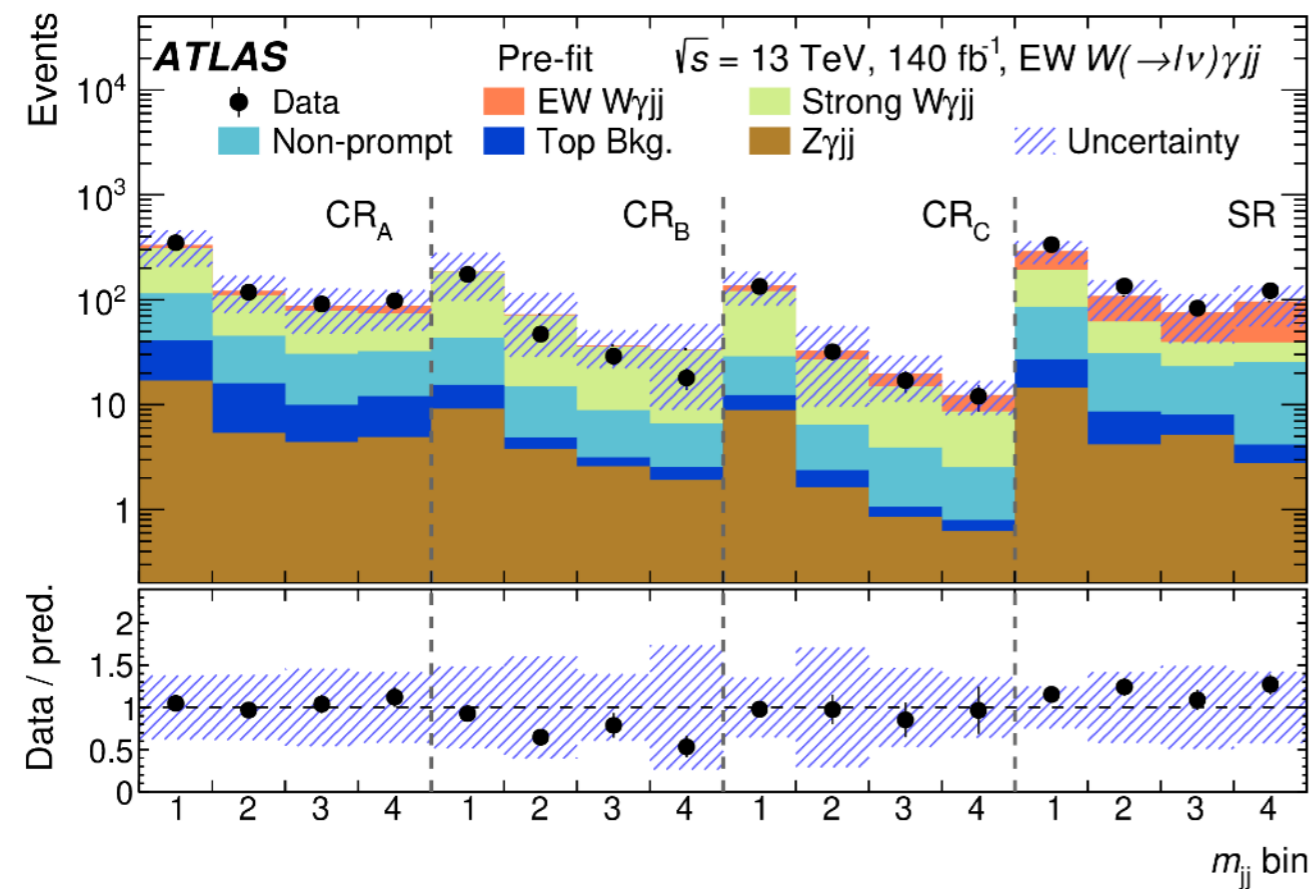
Figure 1: Representative Feynman diagrams for the $W\gamma jj$ final state: (a) EW $W\gamma jj$ production involving no gauge boson self-interactions, (b) bremsstrahlung EW $W\gamma jj$ non-VBS production involving quartic gauge boson interactions, (c) $W\gamma$ VBS involving quartic gauge boson interactions, and (d) Strong $W\gamma jj$ production.

$W\gamma+j\bar{j}$: event selection

Object	Selection requirements
Dressed muons	$p_T > 30$ GeV and $ \eta < 2.5$
Dressed electrons	$p_T > 30$ GeV and $ \eta < 2.47$ (excluding $1.37 < \eta < 1.52$)
Isolated photons	$E_T^\gamma > 22$ GeV and $ \eta < 2.37$ (excluding $1.37 < \eta < 1.52$) and $E_T^{\text{iso}} < 0.2E_T^\gamma$
Jets	At least two jets with $p_T > 50$ GeV and $ y < 4.4$, b -jet veto
Missing transverse momentum	$E_T^{\text{miss}} > 30$ GeV and $m_T^W > 30$ GeV
VBS topology	$N_\ell = 1, N_\gamma \geq 1, m_{\ell\gamma} - m_Z > 10$ GeV $\Delta R_{\min}(\ell, j) > 0.4, \Delta R_{\min}(\gamma, j) > 0.4, \Delta R_{\min}(\ell, \gamma) > 0.4$ $\Delta R_{\min}(j_1, j_2) > 0.4, \Delta\phi_{\min}(E_T^{\text{miss}}, j) > 0.4$ $N_{\text{jets}} \geq 2, p_T^{j_1}, p_T^{j_2} > 50$ GeV $m_{jj} > 500$ GeV, $ \Delta y_{jj} > 2$
Fiducial measurement	VBS topology
Differential measurement	VBS topology \oplus ($m_{jj} > 1000$ GeV, $N_{\text{jets}}^{\text{gap}} = 0$, and $\xi_{W\gamma} < 0.35$)

	SR ^{fid} ($N_{\text{jets}}^{\text{gap}} = 0$)	CR ^{fid} ($N_{\text{jets}}^{\text{gap}} > 0$)
EW $W\gamma jj$	520 ± 141	120 ± 49
Strong $W\gamma jj$	1550 ± 830	1970 ± 950
Non-prompt	692 ± 57	698 ± 58
Top quark processes	109 ± 18	183 ± 37
EW + strong $Z\gamma jj$	128 ± 34	163 ± 77
Total	3000 ± 830	3140 ± 960
Data	3341	3143

$W\gamma+j\bar{j}$: pre- vs post-fit



Wγjj: re-parameterisation

The fitted number of events in region r and bin i is expressed as

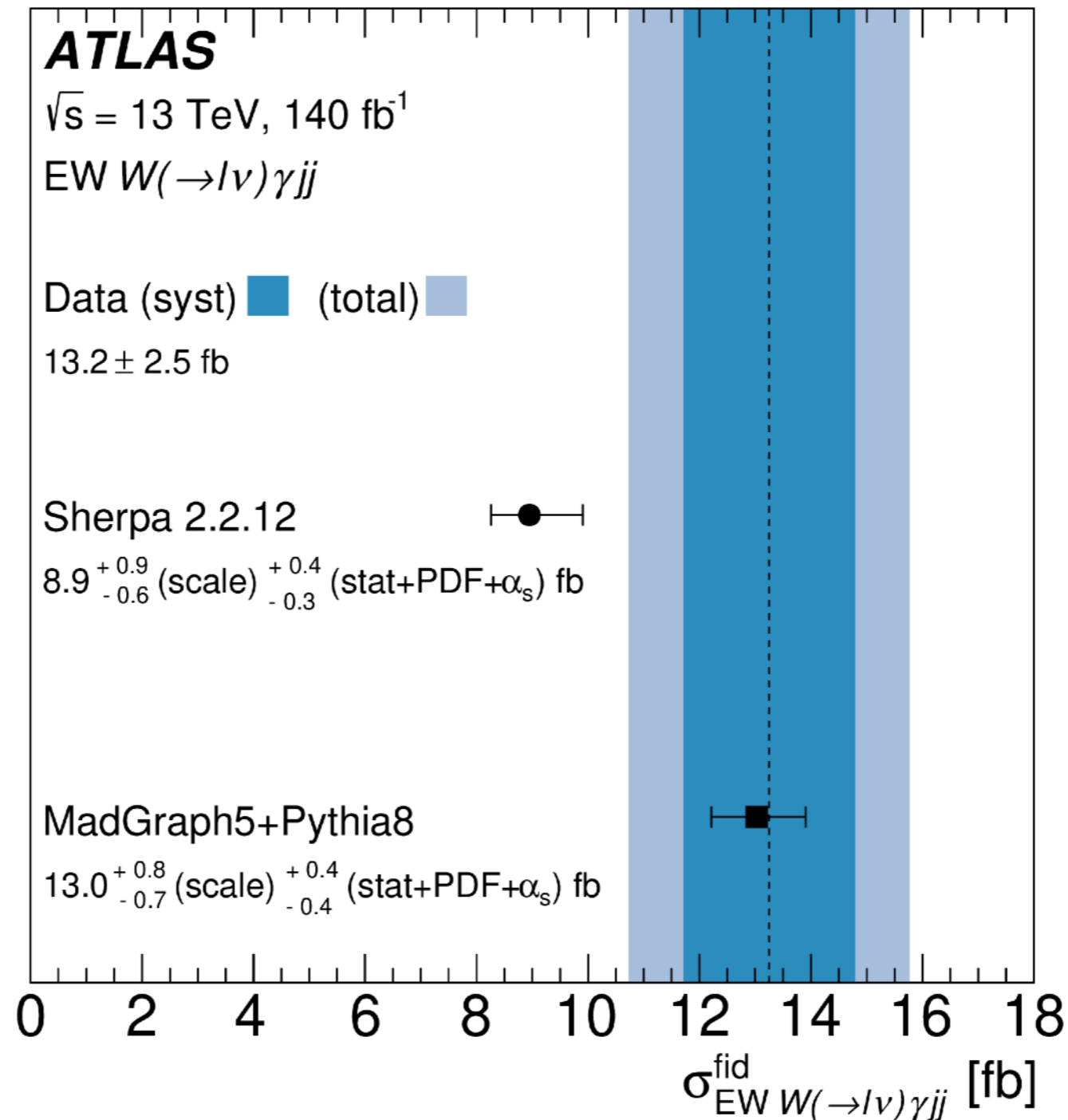
$$\nu_{ri} = \mu_{EW,i} \nu_{ri}^{EW,MC} + \nu_{ri}^{strong} + \nu_{ri}^{other,bkg}, \quad (2)$$

where $\mu_{EW,i}$ is the signal strength of EW $W\gamma jj$ in bin i , and $\nu_{ri}^{EW,MC}$ and $\nu_{ri}^{other,bkg}$ correspond to the EW $W\gamma jj$ prediction and contributions from reducible background processes, respectively. The strong $W\gamma jj$ prediction is constrained using the signal-suppressed control regions based on the following four relations:

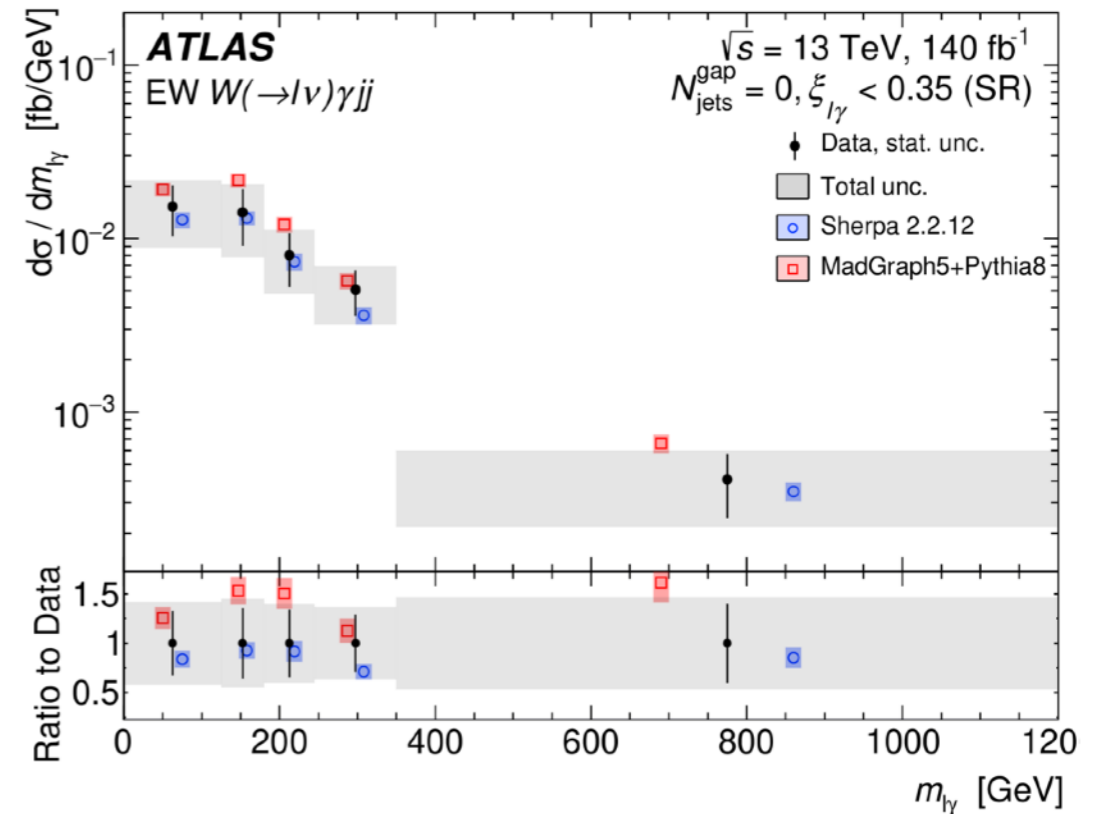
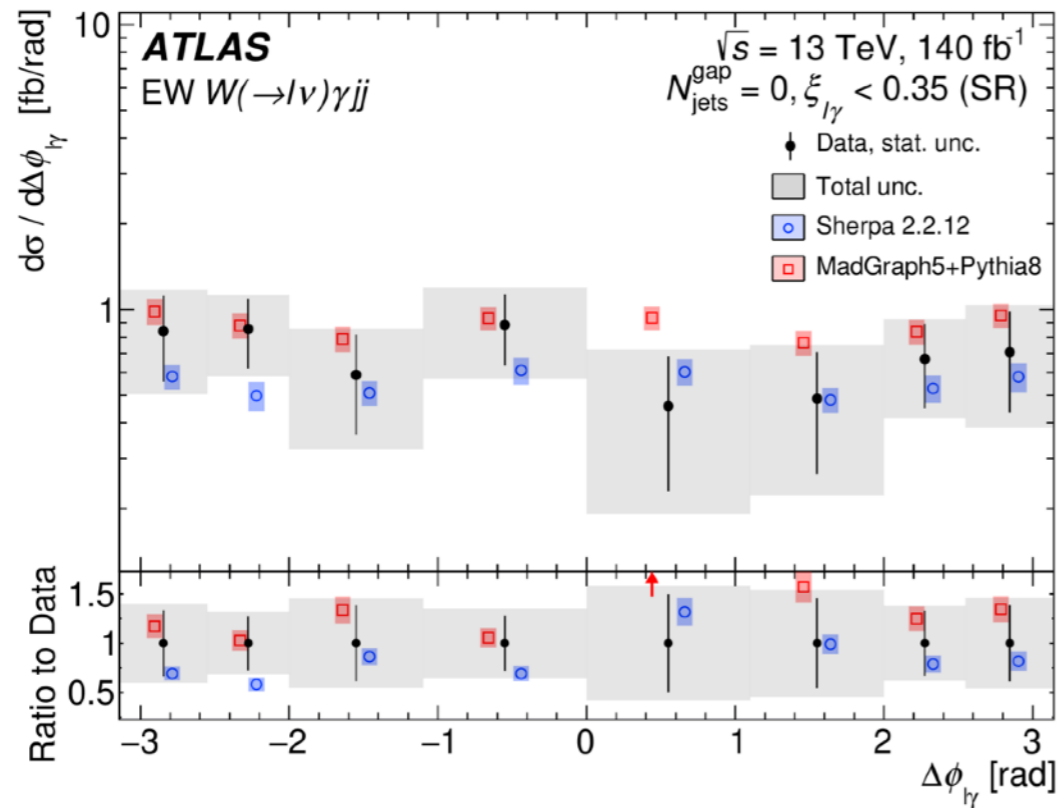
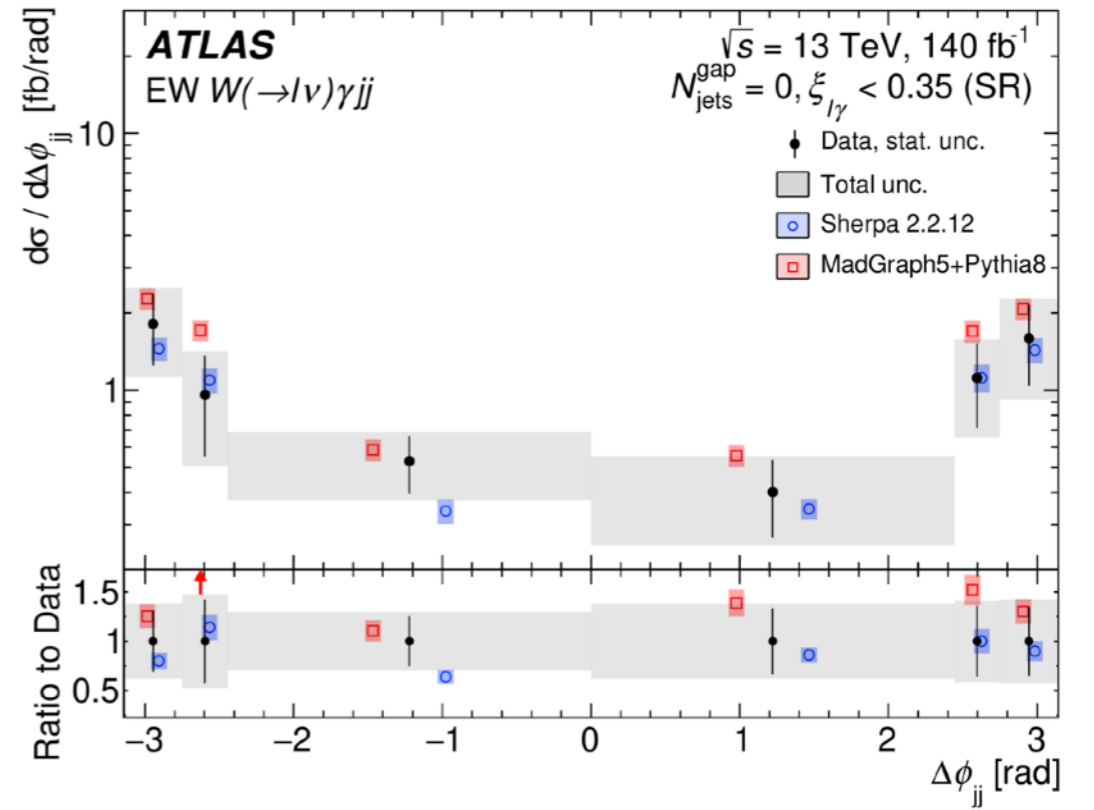
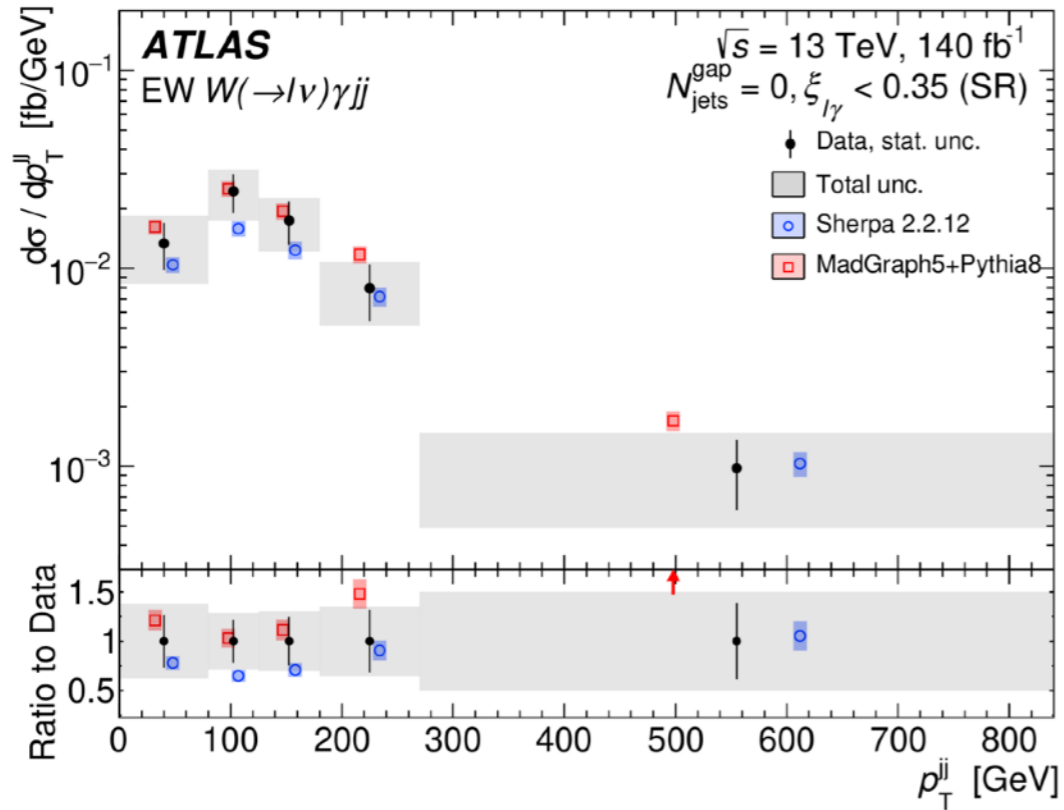
$$\begin{aligned} \nu_{CR_A,i}^{strong} &= b_{L,i} \nu_{CR_A,i}^{strong,MC}, & \nu_{CR_B,i}^{strong} &= b_{H,i} \nu_{CR_B,i}^{strong,MC}, \\ \nu_{SR,i}^{strong} &= b_{L,i} c \nu_{SR,i}^{strong,MC}, \text{ and} & \nu_{CR_C,i}^{strong} &= b_{H,i} c \nu_{CR_C,i}^{strong,MC}. \end{aligned} \quad (3)$$

The parameters $b_{L,i}$ and $b_{H,i}$ are sets of bin-dependent free parameters that correspond to the $\xi_{l\gamma} < 0.35$ and $\xi_{l\gamma} > 0.35$ regions, respectively. The low- $\xi_{l\gamma}$ parameter, $b_{L,i}$, is primarily constrained by CR_A , while $b_{H,i}$ is primarily constrained by CR_B . These two sets of parameters introduce additional degrees of freedom to the predicted strong $W\gamma jj$ event yield to allow the fitted number of strong $W\gamma jj$ events to be more consistent with the observed data. A floating parameter c is used to provide a residual correction that can account for any mismodelling across N_{jets}^{gap} . This configuration is found to be more robust against

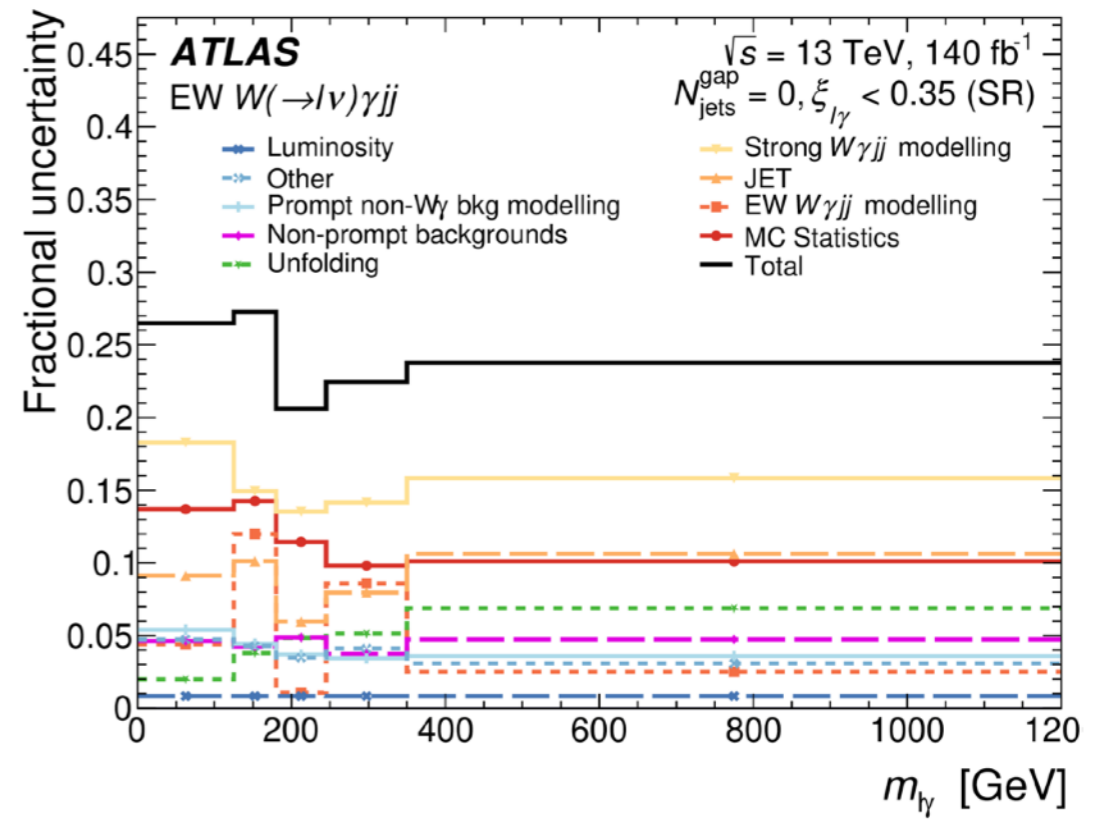
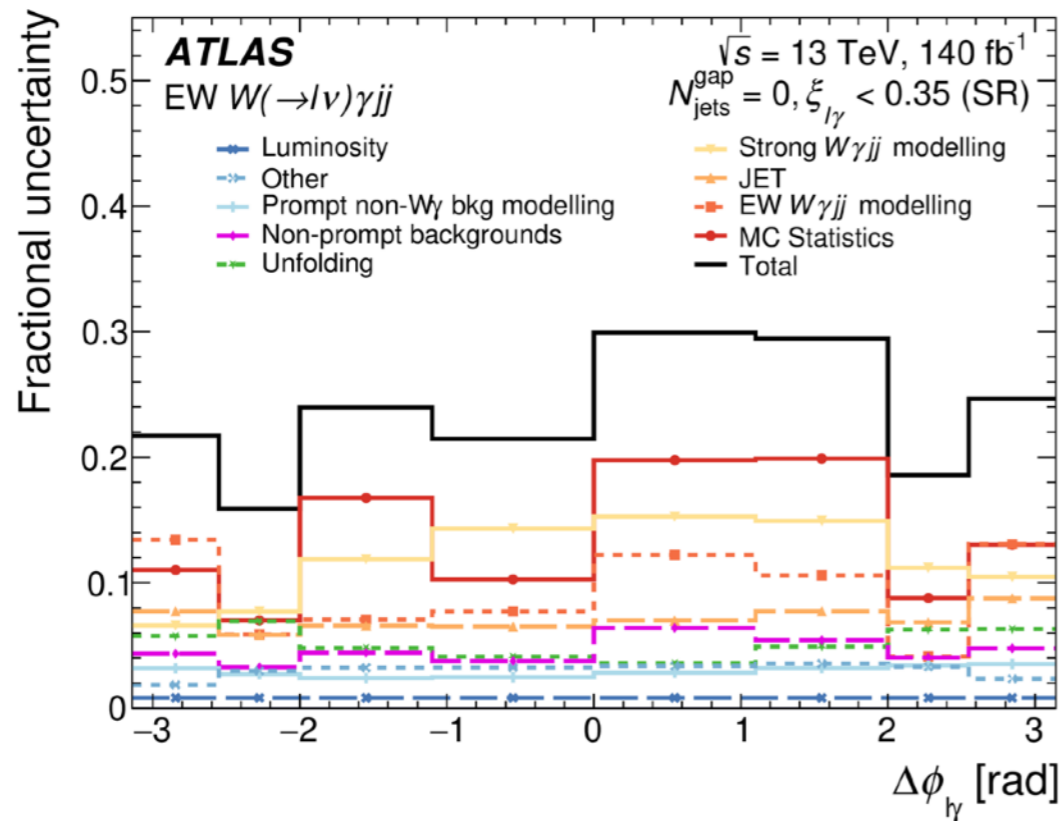
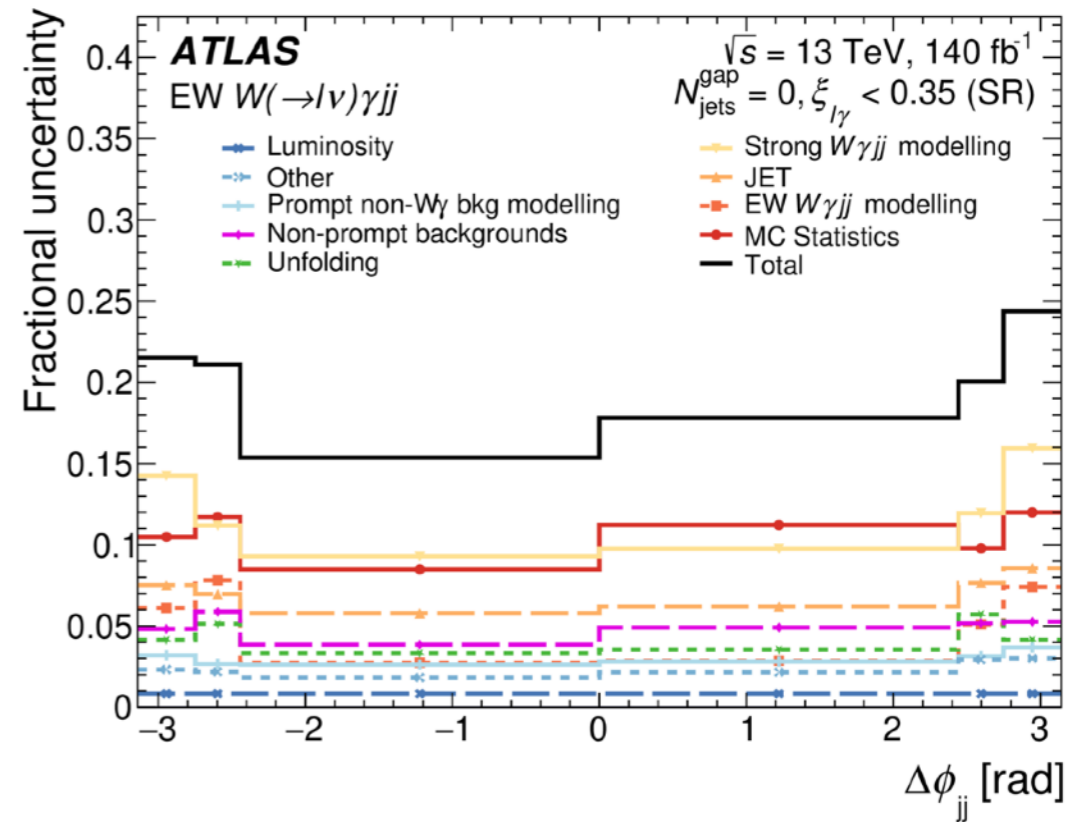
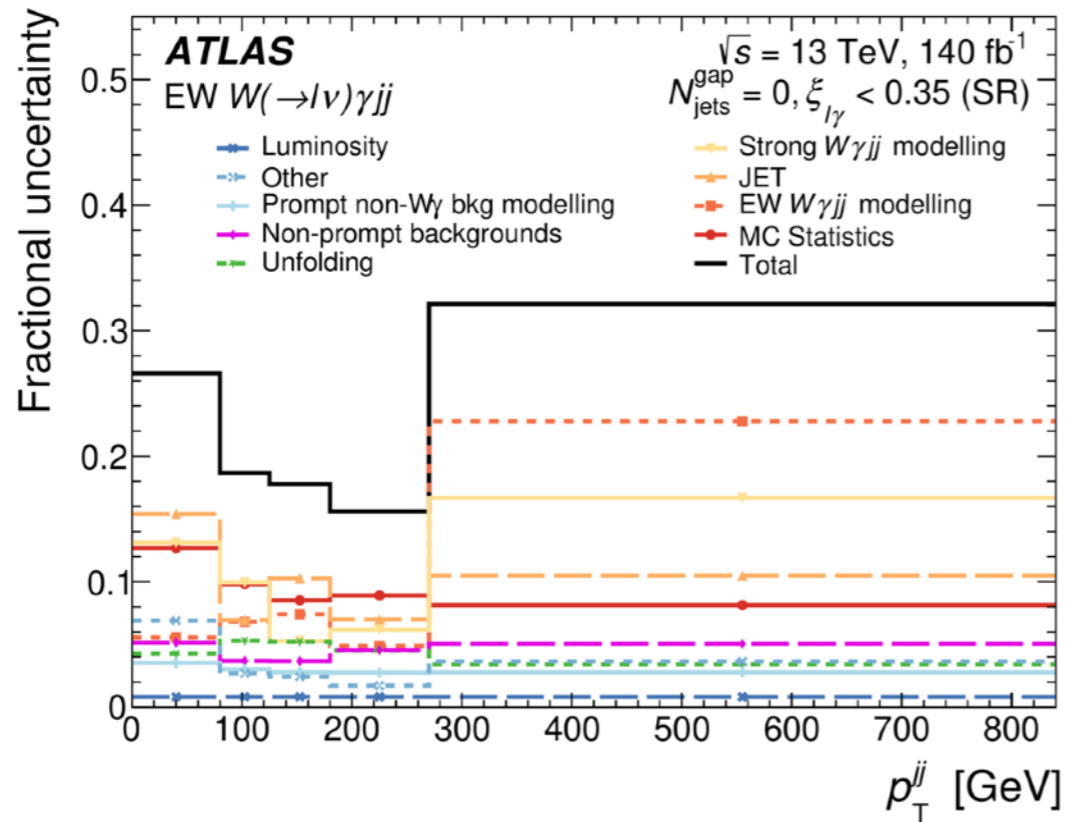
$W\gamma+j\bar{j}$: inclusive xsection



$W\gamma+j\bar{j}$: more differential plots



$W\gamma+j\bar{j}$: more differential plots



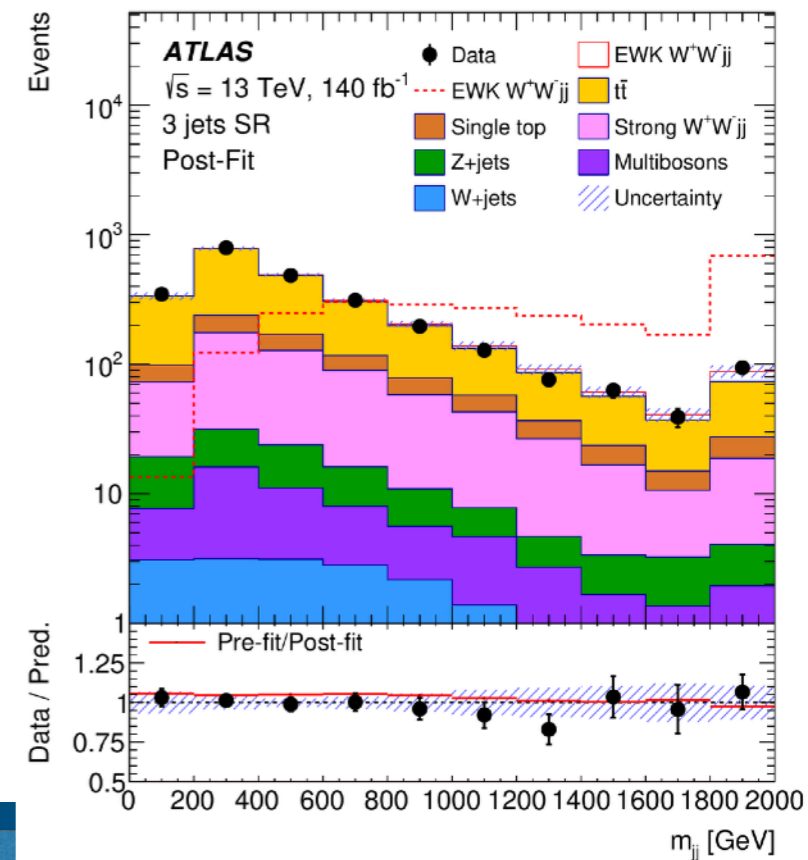
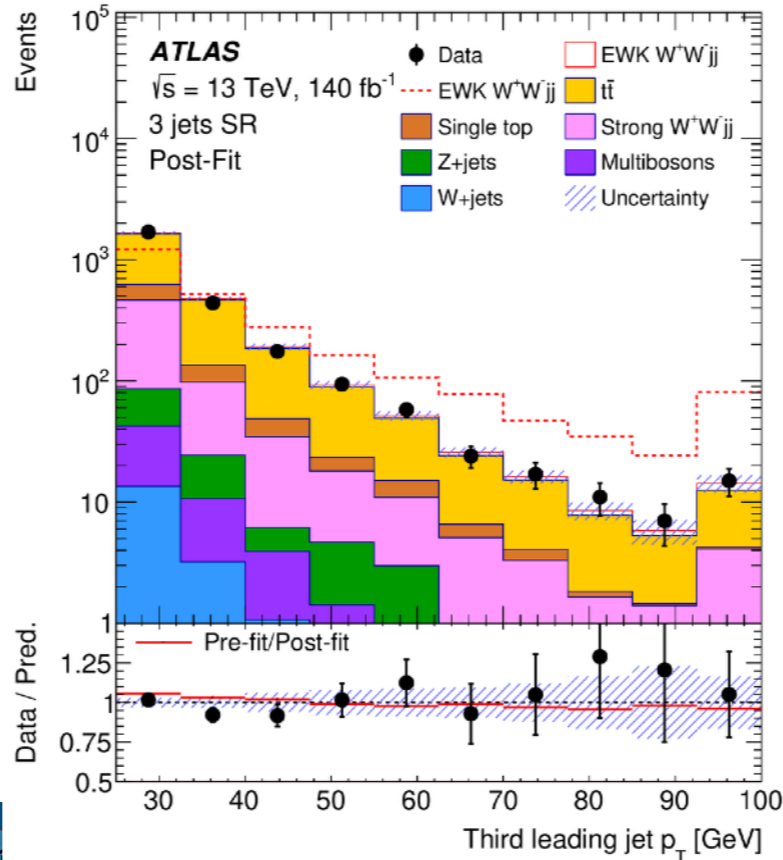
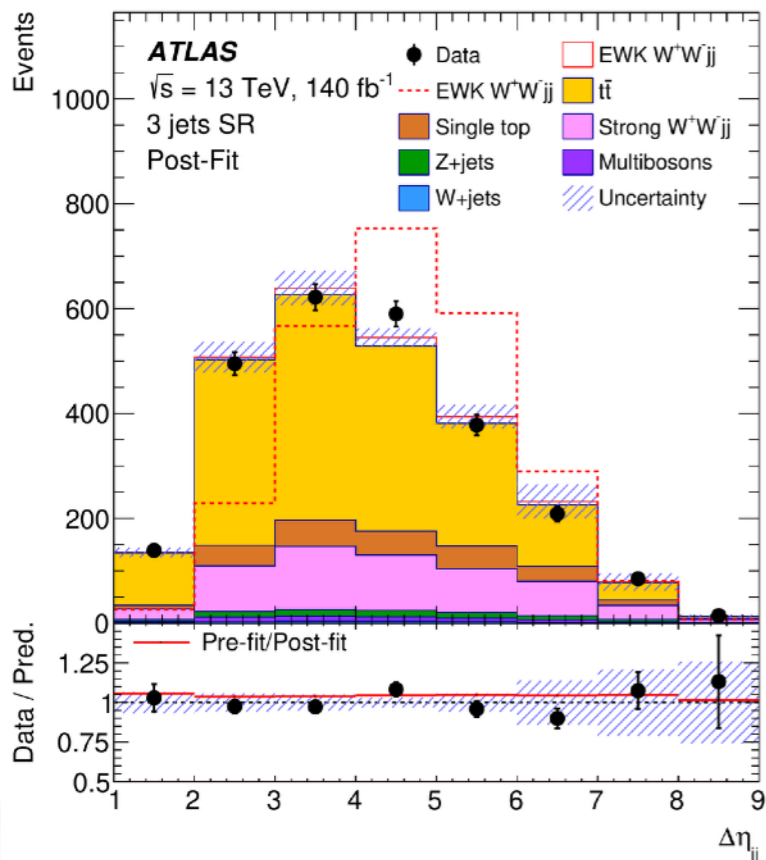
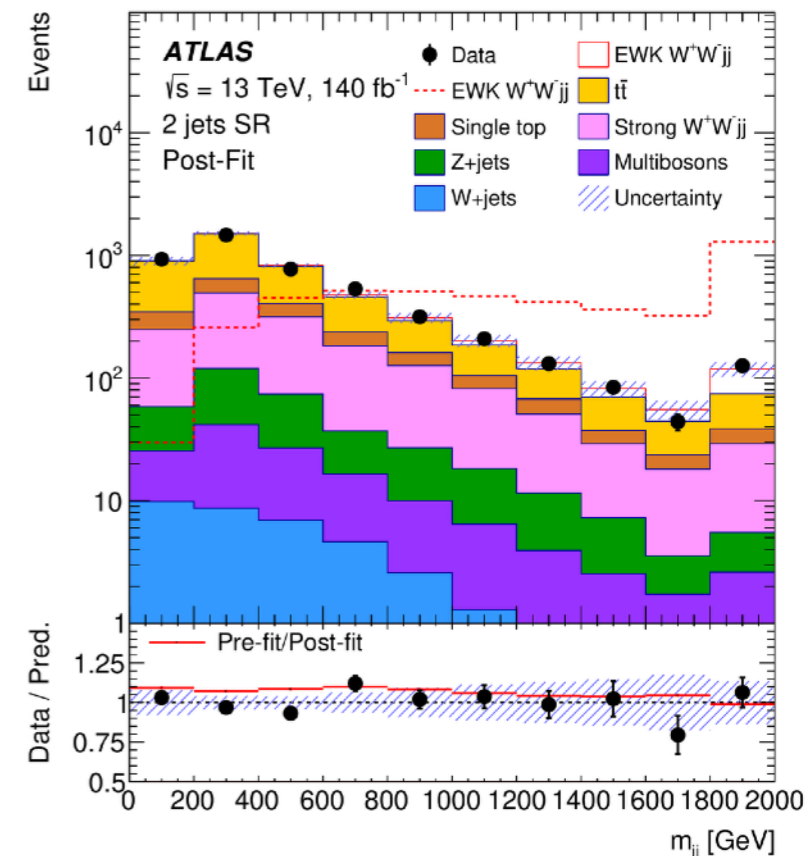
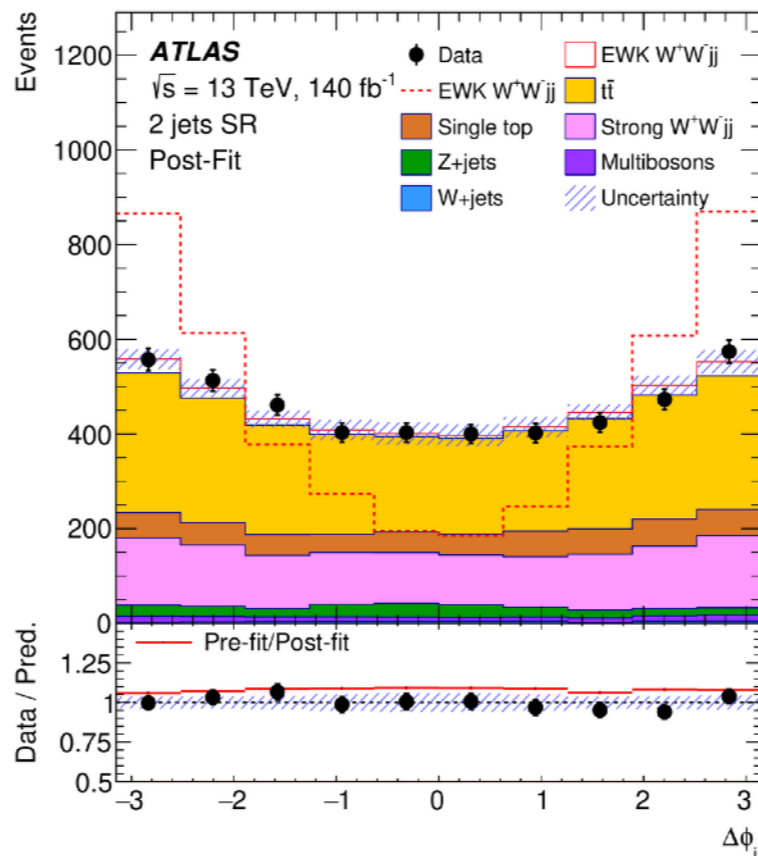
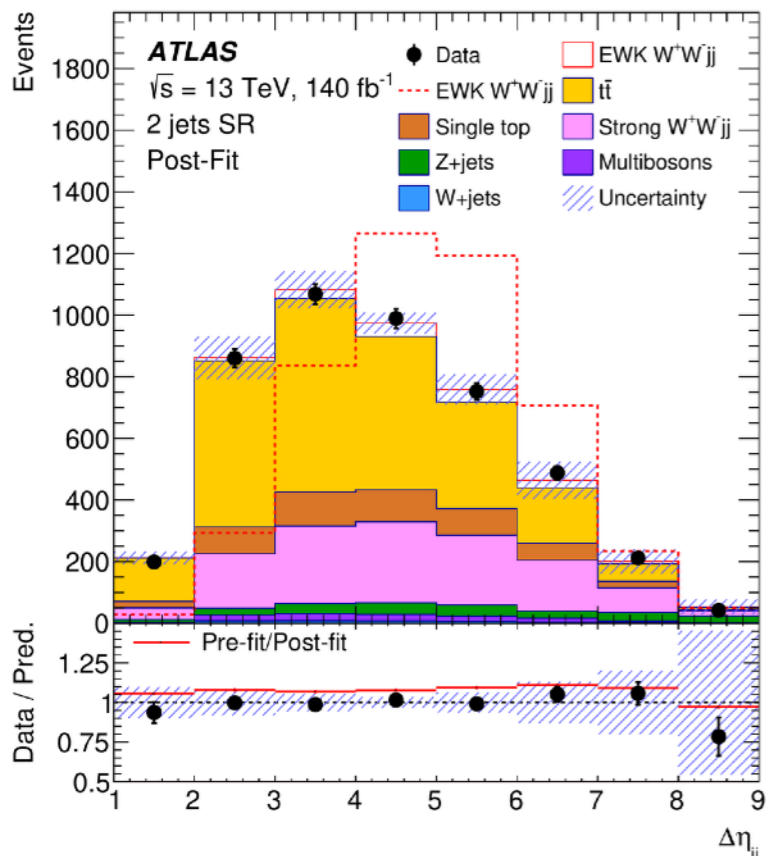
$\sigma_{\gamma-WW+jj}$: event selection

Category	Requirements
Leptons	$p_T > 27$ GeV $ \eta < 2.47$ excluding $1.37 < \eta < 1.52$ (electrons) $ \eta < 2.5$ (muons) Identification: Tight Isolation: Gradient (electrons), Tight_FixedRad (muons) $ d_0/\sigma_{d_0} < 5$ (electrons), $ d_0/\sigma_{d_0} < 3$ (muons) $ z_0 \sin \theta < 0.5$ mm
b -jets	$p_T > 20$ GeV and $ \eta < 2.5$ (DL1r b -tagging with 85% efficiency)
Jets	$p_T > 25$ GeV and $ \eta < 4.5$
Events	One electron and one muon with opposite electric charges No additional lepton with $p_T > 10$ GeV, Loose isolation, Tight/Medium (electrons) and Loose (muons) identification $m_{e\mu} > 80$ GeV $E_T^{\text{miss}} > 15$ GeV No b -jet Two or three jets $\zeta > 0.5$

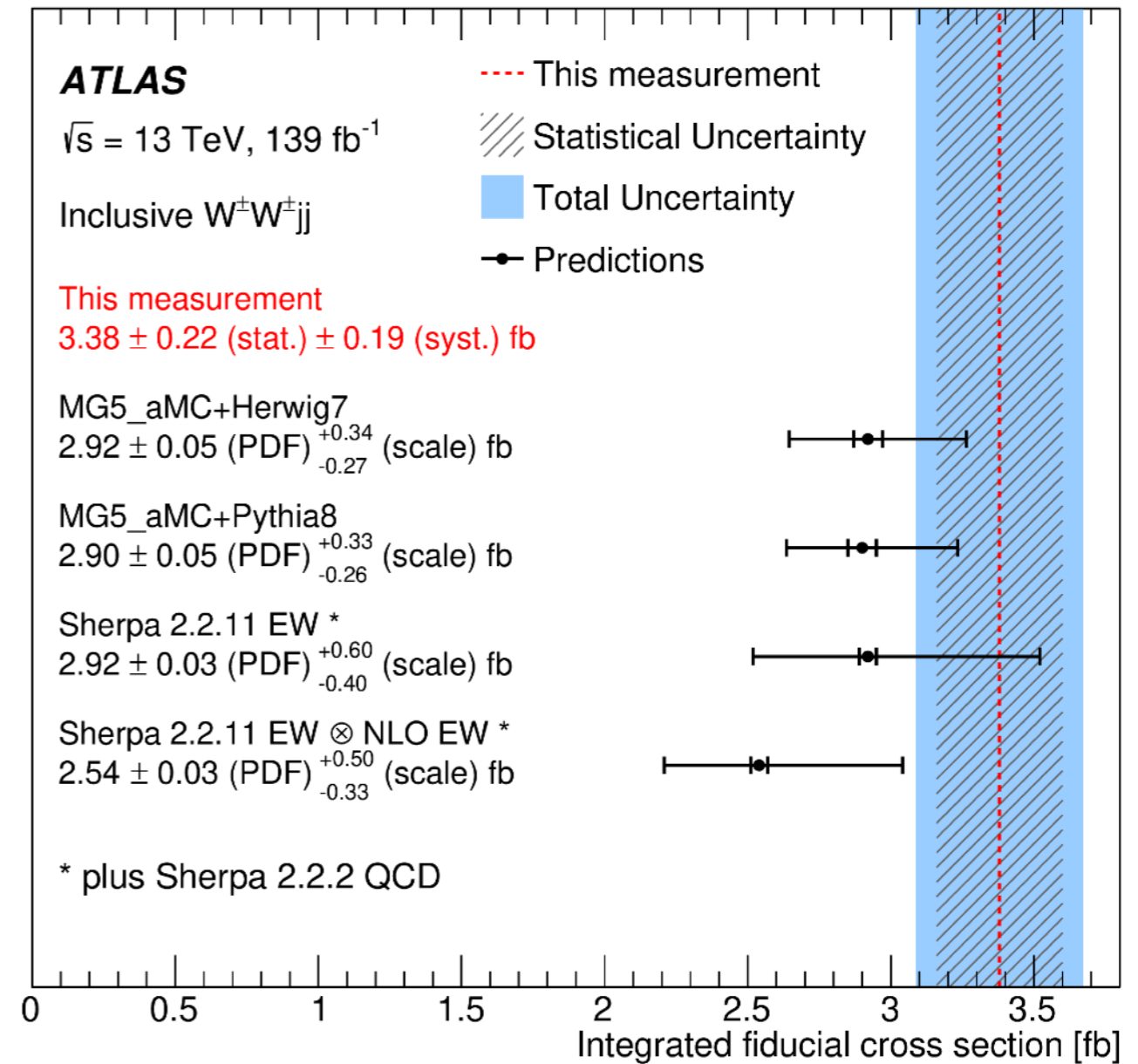
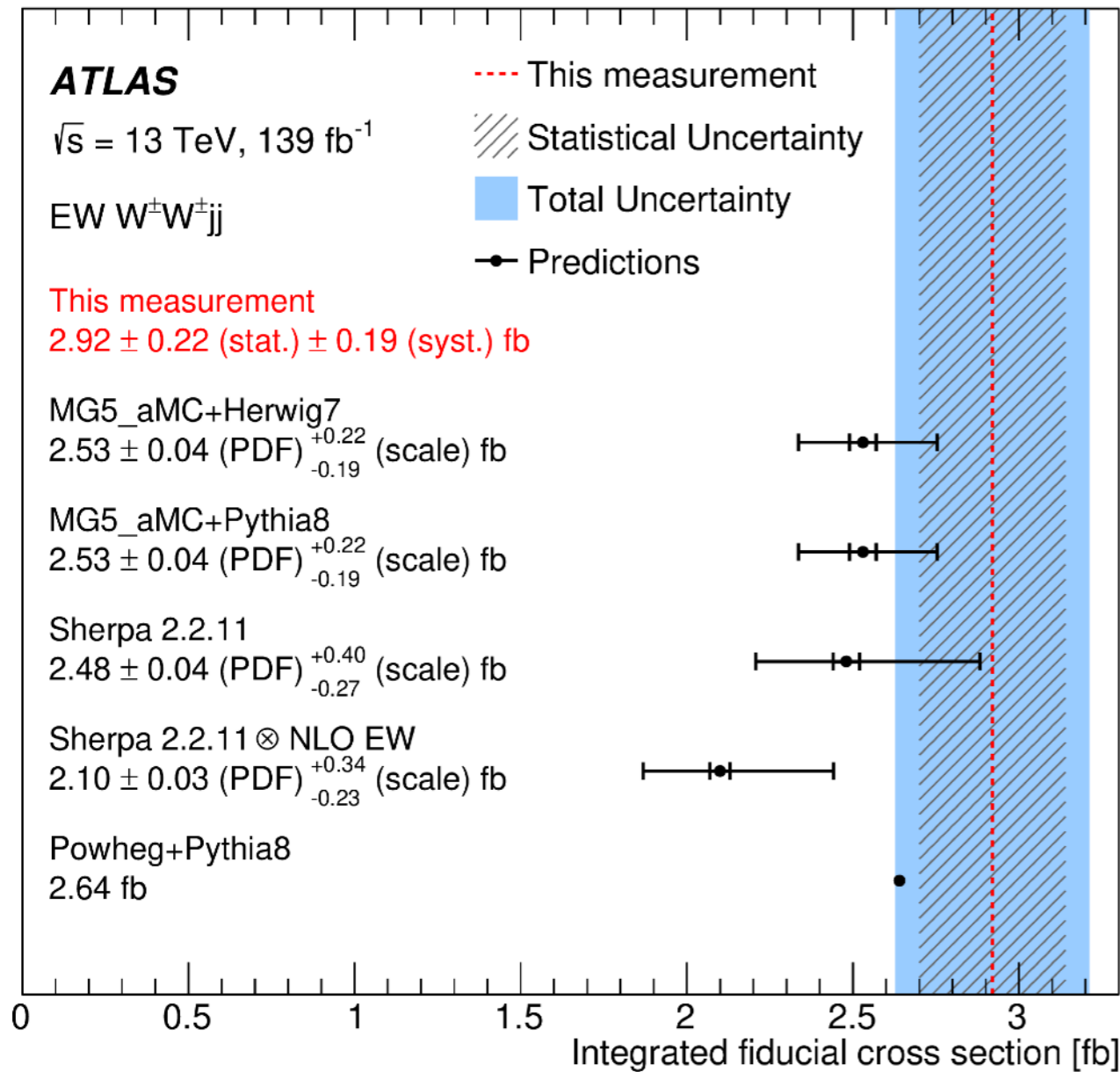
Process	Event yields	
	$n_{\text{jets}} = 2$	$n_{\text{jets}} = 3$
EWK W^+W^-jj	158 ± 27	54 ± 13
$t\bar{t}$	2394 ± 194	1625 ± 125
Single top	491 ± 34	225 ± 21
Strong W^+W^-jj	1214 ± 256	514 ± 121
W +jets	37 ± 97	19 ± 48
Z +jets	216 ± 62	65 ± 25
Multiboson	101 ± 5	42 ± 3
SM prediction	4610 ± 77	2546 ± 48
Data	4610	2533

Sources	$\frac{\sqrt{(\Delta\mu)^2 - (\Delta\mu')^2}}{\mu}$ [%]
MC statistical uncertainty	7.7
Top quark theoretical uncertainties	6.3
Signal theoretical uncertainties	5.8
Jet experimental uncertainties	4.9
Strong W^+W^-jj theoretical uncertainties	1.3
Luminosity	0.8
Misidentified lepton uncertainty	0.5
b -tagging	0.4
Lepton experimental uncertainties	0.1
Others	0.3
Data statistical uncertainty	12.3
Top quark normalisation uncertainty	4.9
Strong W^+W^-jj normalisation uncertainty	2.2
Total uncertainty	18.5

$\sigma_{\gamma-WW+jj}$: more post-fit plots



$ssWW+jj$: inclusive xSection



WZ ll: diagrams

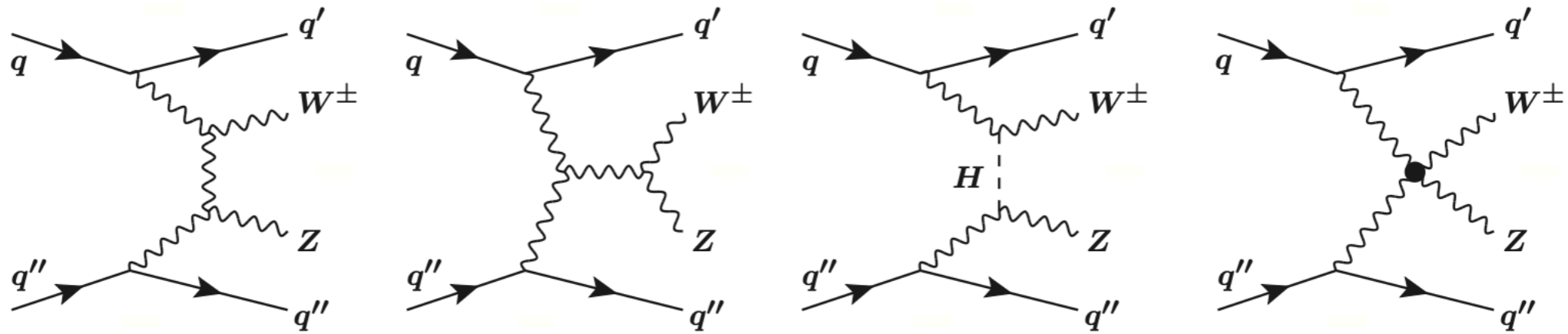


Figure 1: Representative diagrams at LO of the $WZjj$ -EW production in pp collisions.

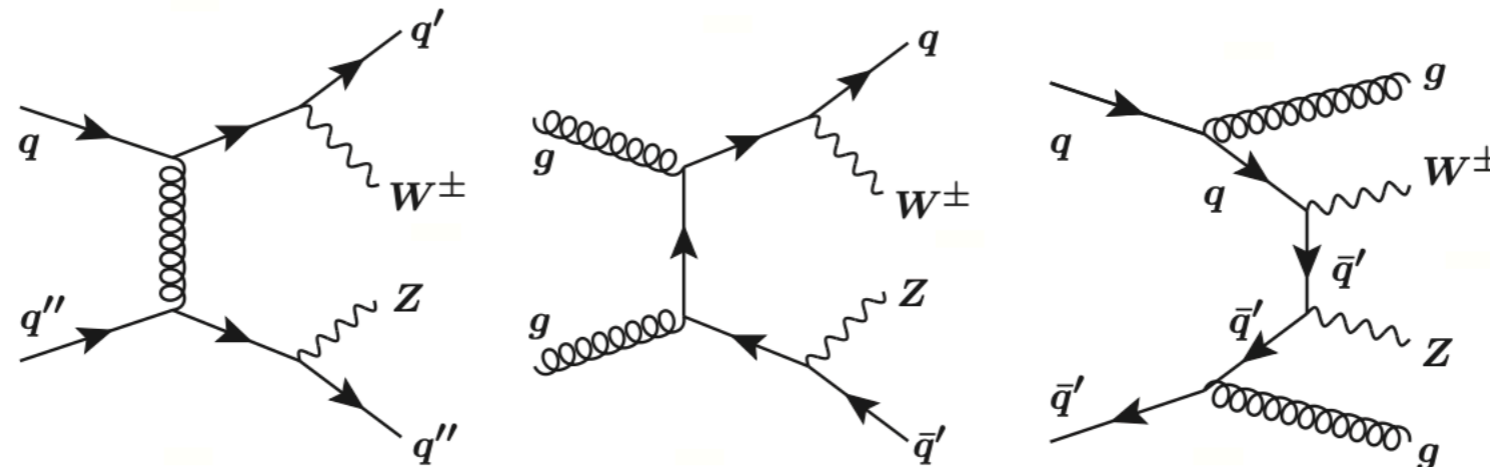


Figure 2: Representative diagrams at LO of the $WZjj$ -QCD production in pp collisions.

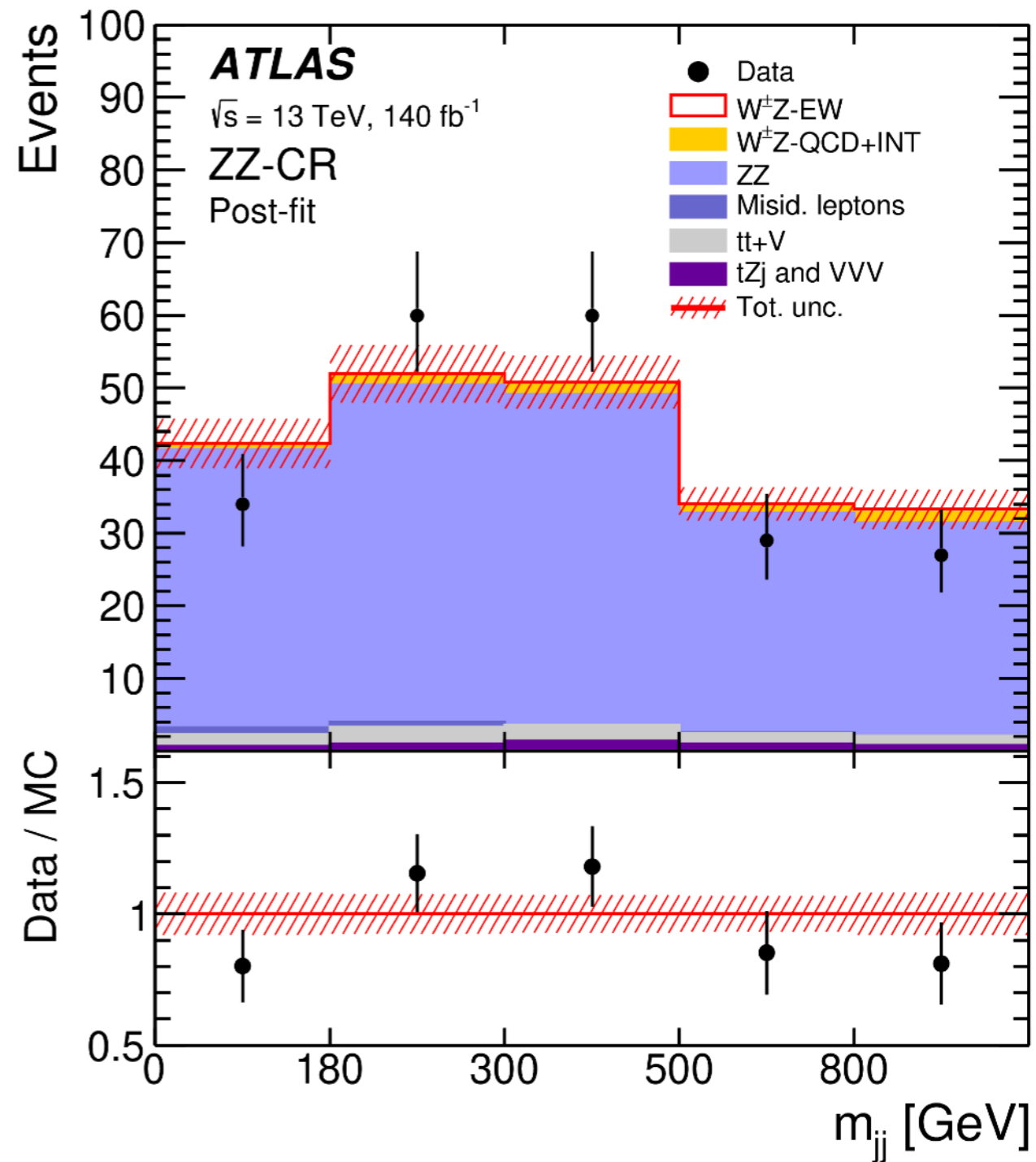
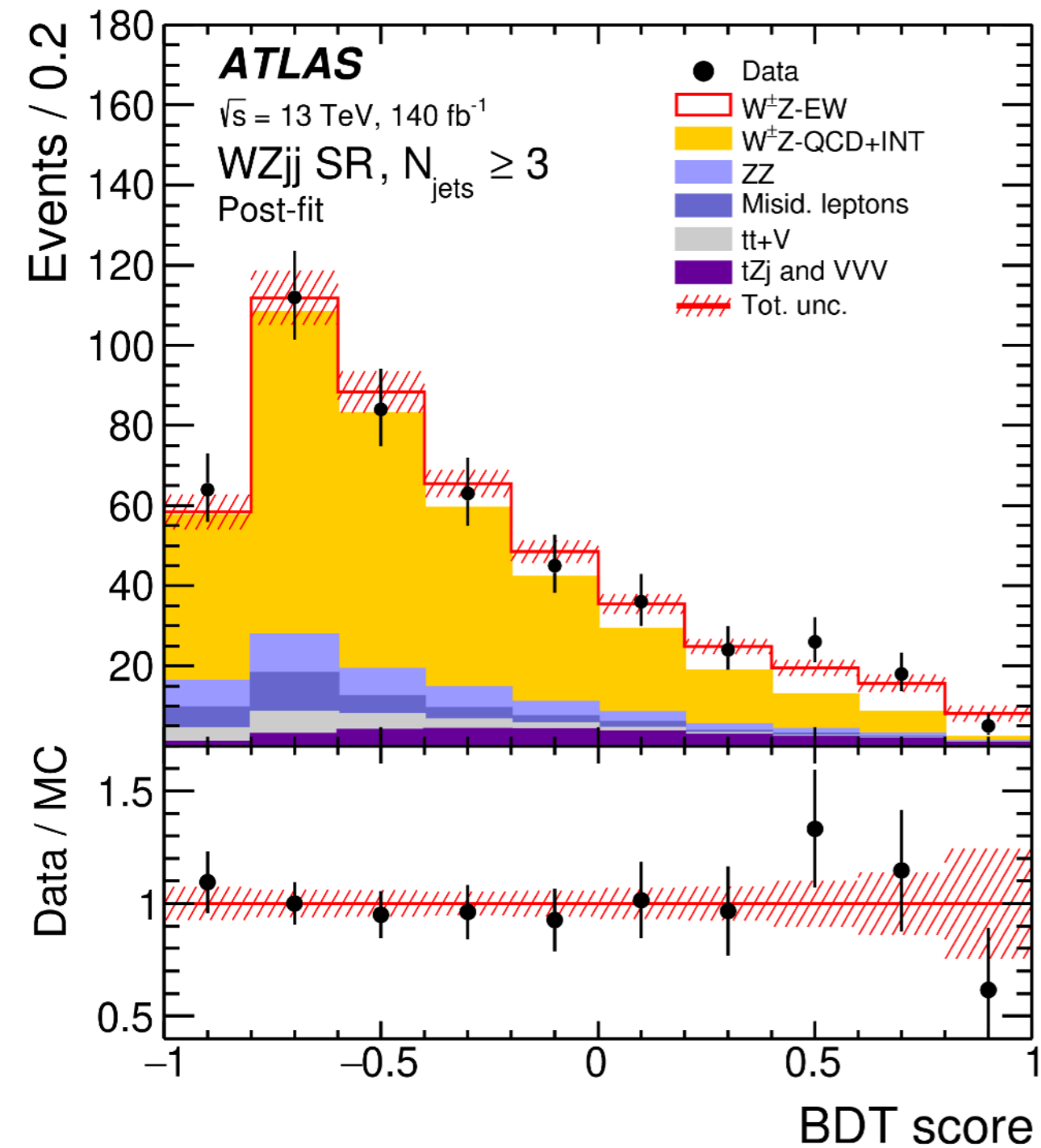


WZ *ll*: more info

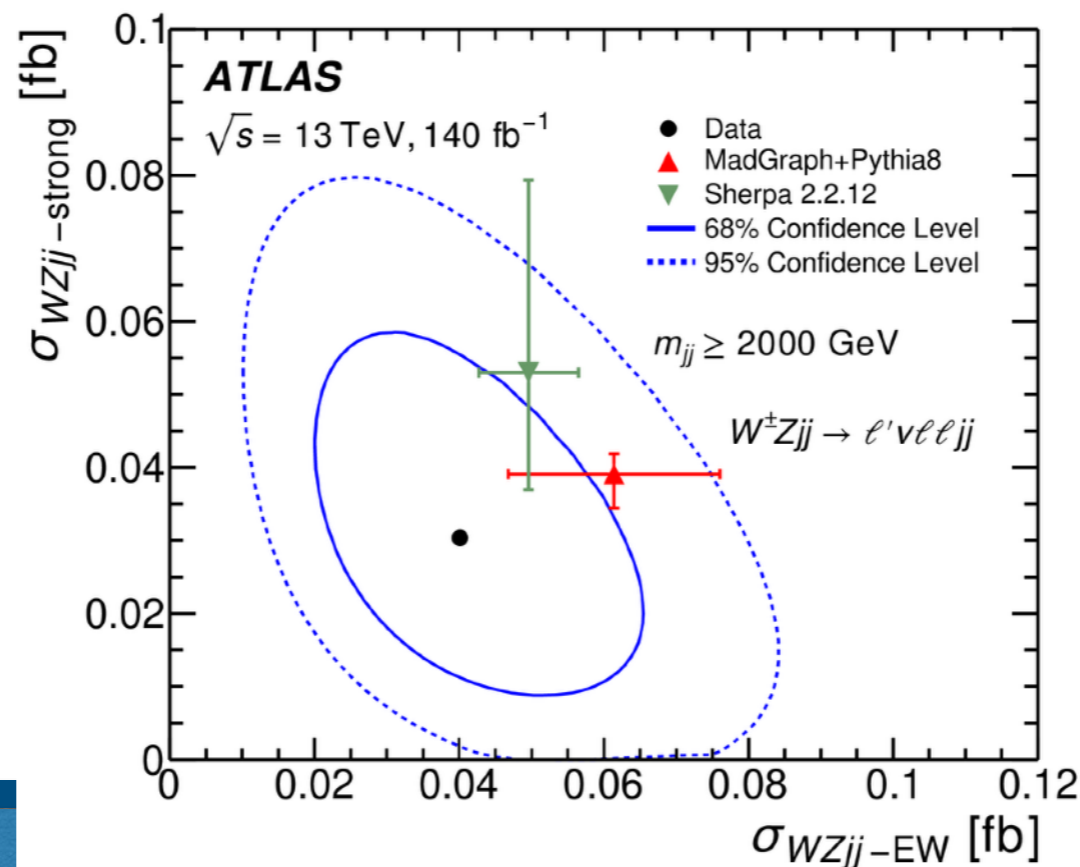
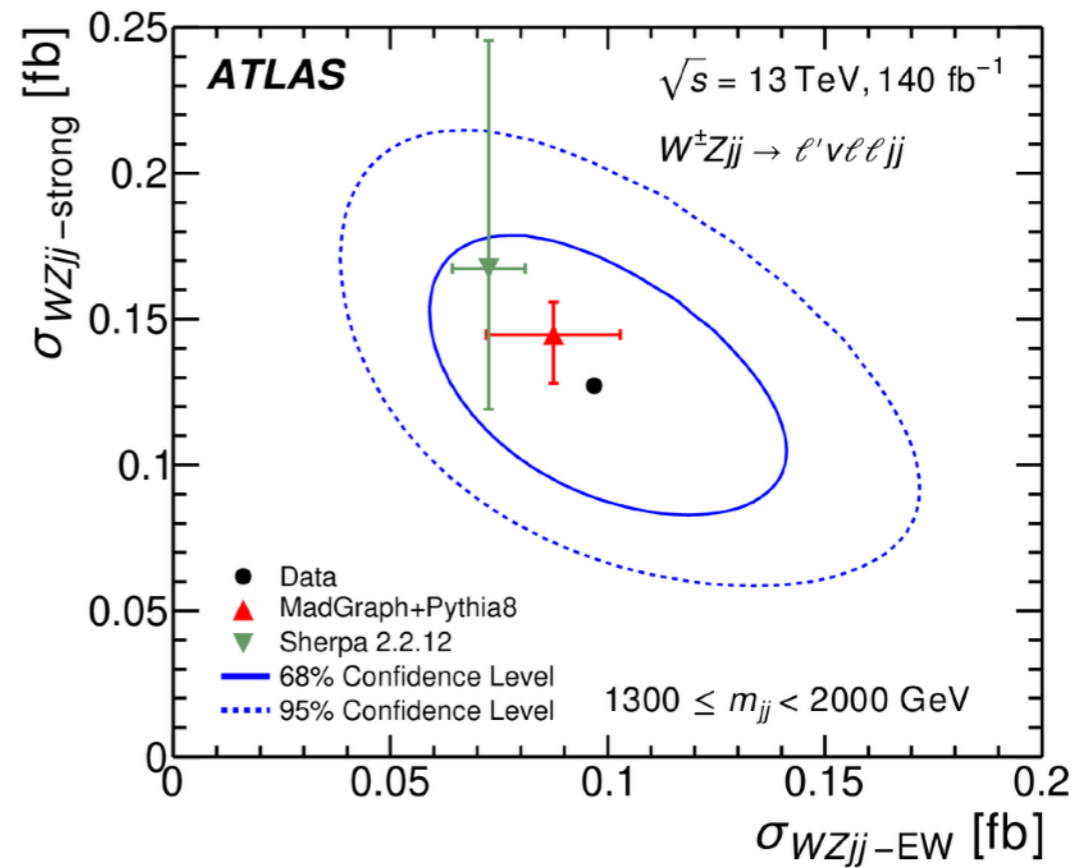
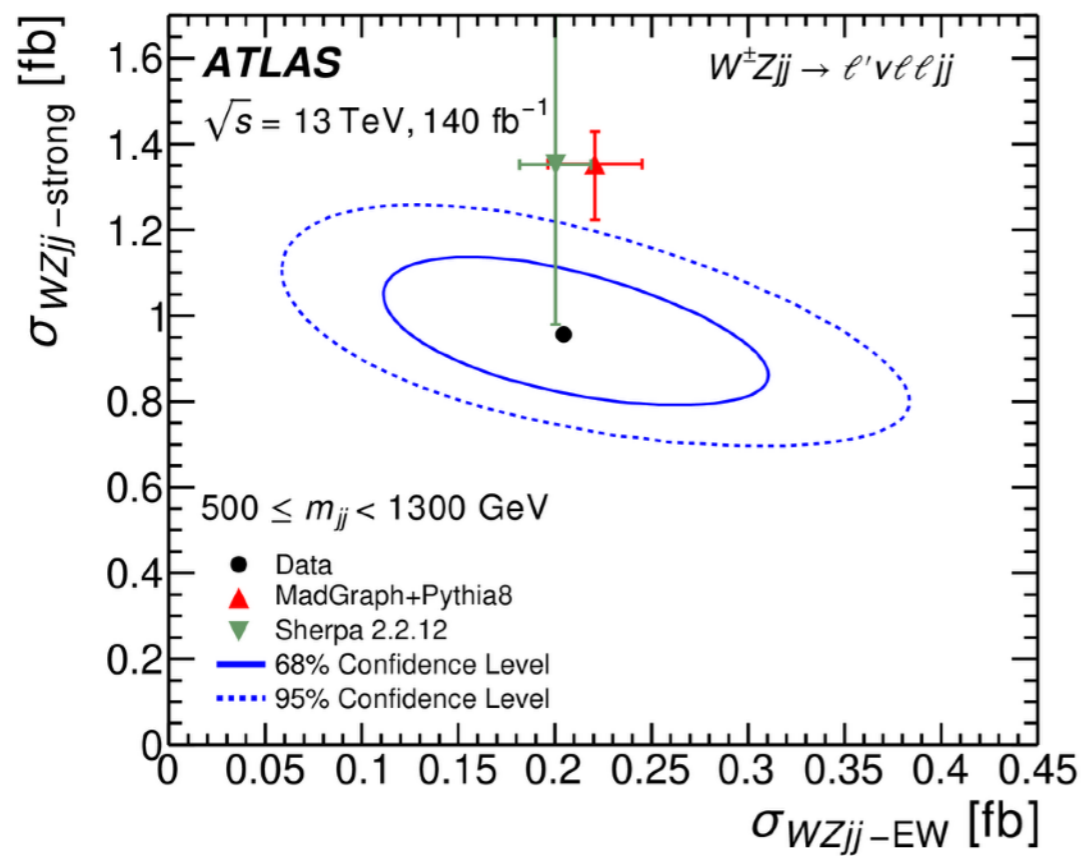
	SR, $N_{\text{jets}} = 2$		SR, $N_{\text{jets}} \geq 3$		<i>b</i> -CR		ZZ-CR	
Data	169		477		666		210	
Total pred.	231	± 12	550	± 50	660	± 40	205	± 11
<i>WZjj</i> -EW	65.0	± 3.5	60	± 6	4.82	± 0.28	0.725	± 0.014
<i>WZjj</i> -QCD	125	± 9	380	± 50	77	± 18	6.2	± 0.7
<i>WZjj</i> -INT	1.3	± 0.6	5.3	± 2.6	0.58	± 0.29	0.22	± 0.11
$t\bar{t} + V$	0.66	± 0.04	20.2	± 0.7	289	± 10	9.89	± 0.28
tZj	8.78	± 0.34	19.7	± 1.2	134	± 4	0.432	± 0.005
ZZ-QCD	9.6	± 0.4	32.0	± 2.5	10.1	± 0.6	159	± 9
ZZ-EW	2.2	± 0.6	4.4	± 1.1	0.25	± 0.06	23	± 6
VVV	0.41	± 0.10	2.0	± 0.5	0.39	± 0.10	4.1	± 1.1
Misid. leptons	18	± 4	28	± 7	150	± 40	1.7	± 0.5



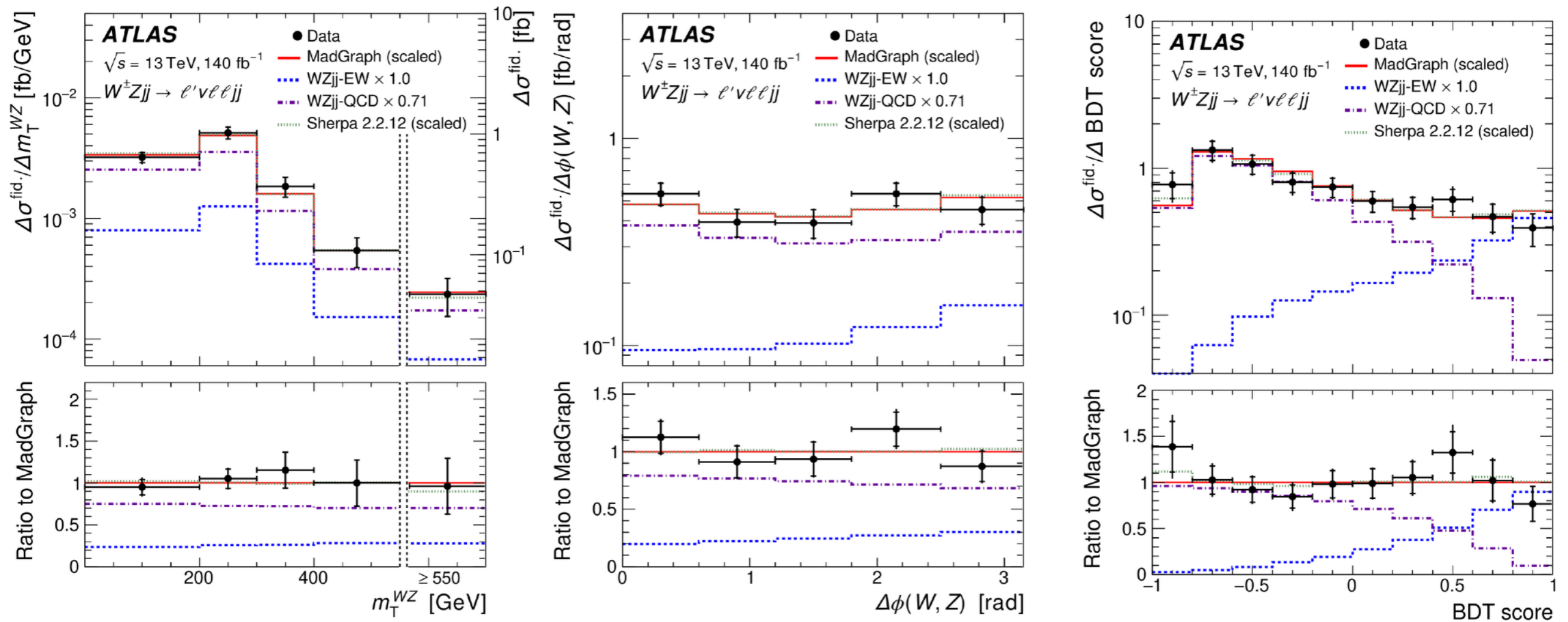
WZ ll: other post-fits



WZ ll: m_{jj} bins cross sections



WZ ll: more differential plots



WZ ll: other EFT plots

	Expected [TeV ⁻⁴]	Observed [TeV ⁻⁴]
f_{T0}/Λ^4	[-0.80, 0.80]	[-0.57, 0.56]
f_{T1}/Λ^4	[-0.52, 0.49]	[-0.39, 0.35]
f_{T2}/Λ^4	[-1.6, 1.4]	[-1.2, 1.0]
f_{M0}/Λ^4	[-8.3, 8.3]	[-5.8, 5.6]
f_{M1}/Λ^4	[-12.3, 12.2]	[-8.6, 8.5]
f_{M7}/Λ^4	[-16.2, 16.2]	[-11.3, 11.3]
f_{S02}/Λ^4	[-14.2, 14.2]	[-10.4, 10.4]
f_{S1}/Λ^4	[-42, 41]	[-30, 30]

	Expected [TeV ⁻⁴]	Observed [TeV ⁻⁴]
f_{T0}/Λ^4	[-7.0, 7.0]	[-1.5, 1.6]
f_{T1}/Λ^4	[-1.1, 1.0]	[-0.7, 0.6]
f_{T2}/Λ^4	[-12, 6]	[-2.4, 1.8]
f_{M0}/Λ^4	[-60, 60]	[-12, 12]
f_{M1}/Λ^4	[-32, 32]	[-15, 15]
f_{M7}/Λ^4	[-30, 30]	[-15, 15]
f_{S02}/Λ^4	[-41, 41]	[-18, 18]
f_{S1}/Λ^4	—	—

